Nano Research

Open Access

Review Article

Microneedle electrodes for collecting bioelectrical signals: From a materials science perspective

Xianghong Li and Tingkai Zhao

NPU-NCP Joint International Research Center on Advanced Nanomaterials & Defects Engineering, Shaanxi Engineering Laboratory for Graphene New Carbon Materials and Applications, School of Materials Science and Engineering, Northwestern Polytechnical University, Xi'an 710072, China

Cite this article: *Nano Research*, **2025**, *18*, 94907377. https://doi.org/10.26599/NR.2025.94907377

ABSTRACT: Microneedle electrodes acquire bioelectrical signals by measuring the potential difference generated through active cells. The common bioelectrical signals include electroencephalographic, electromyographic, and electrocardiographic signals, which have been extensively utilized across medical, neuroscience, and bioengineering domains. Microneedle electrodes, as invasive dry electrodes minimal penetrating the stratum corneum without reaching the dermis, effectively mitigate the impedance of the electrode-skin interface without requiring conductive gel, thus accommodating the requirements of long-term and high-precision measurements. This review provides a comprehensive summary of the electrode materials, fabrication methods, performance evaluation, and applications of microneedle electrodes for bioelectrical signal acquisition. Special emphasis is placed on the development of materials used in the fabrication of microneedle electrodes. Additionally, we discuss the challenges related to material selection and performance testing, offering insights into future trends in this field.

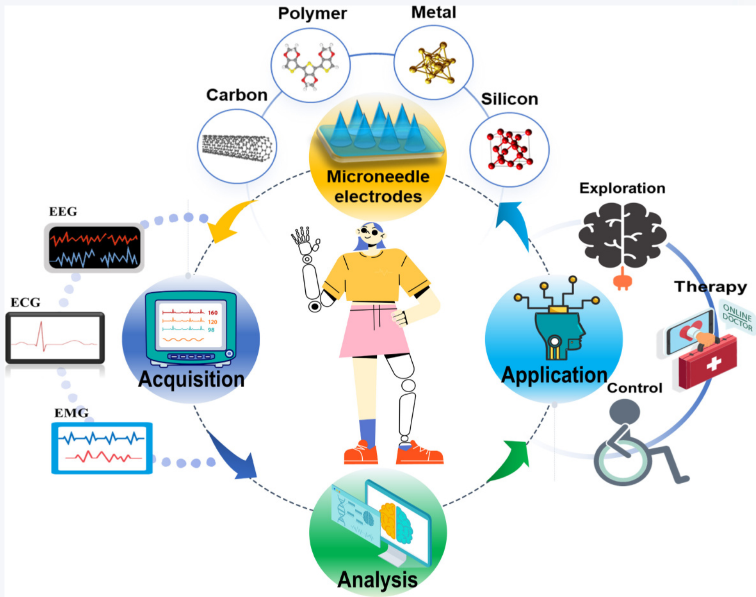

KEYWORDS: microneedle electrodes, bioelectrical signals, human–machine interface, material development

1 Introduction

1.1 Background on bioelectrical signals and their importance in biological research

Living cells in humans and animals generate consistent electrical signals in both resting and active states, known as bioelectrical signals [1]. Typically, these signals have low amplitudes, generally under 5 mV, and are characterized by their instability and randomness. Despite these challenges, bioelectrical signals are essential to numerous physiological processes, such as muscle contraction, nerve transmission, and brain activity. Abnormalities in these signals are closely linked to various diseases and disorders, including neurological conditions, cardiac abnormalities, and developmental issues. Furthermore, bioelectrical signals are increasingly harnessed for therapeutic and diagnostic purposes. For instance, deep brain stimulation [2] is employed to alleviate Alzheimer's dementia, while transcutaneous electrical nerve stimulation helps in pain management [3]. Electroencephalogram (EEG) electrodes, placed on the scalp, detect weak electrical signals generated by neuronal discharges in the cerebral cortex (5–300 μV, 0.5–100 Hz) [4]. EEG is invaluable for diagnosing and monitoring neurological conditions such as epilepsy, sleep disorders, and dementia [5]. Additionally, EEG plays a crucial role in brain-computer interfaces, enabling individuals with physical disabilities or limited mobility to communicate and control external devices,

Received: December 20, 2024; **Revised:** February 22, 2025
Accepted: March 17, 2025

Address correspondence to ztk-xjtu@163.com

thereby improving their quality of life [6]. Similarly, electrocardiogram (ECG) records the electrical activity of heart contractions and relaxations (10 μV–4 mV, 0.05–100 Hz) through electrodes placed near the heart [7]. ECG is essential for diagnosing acute myocardial ischemia, identifying arrhythmia pathways, evaluating therapeutic options for heart failure, and assessing patients with genetic predispositions to arrhythmias [8]. Electromyography (EMG), with a broader bandwidth of 0–500 Hz and signal amplitude of 0–1.5 mV, detects and analyzes the electrical activity of contracting muscles [9].

Advances in research have also facilitated the growing use of bioelectrical signals like electroretinogram and electrooculogram for specialized diagnostic purposes [10]. The accurate study and application of these signals depend fundamentally on the initial step: effective and precise signal collection. Electrodes are typically positioned on the skin's corresponding areas or implanted directly to establish contact with cells or nerves for bioelectrical signal measurement [11]. Common electrode types include surface electrodes, capacitive electrodes, wet electrodes, microneedle electrodes, and implantable electrodes. Among these, microneedle electrodes stand out as minimally invasive electrodes, occupying an intermediary position between non-invasive [12] and invasive electrodes [13]. Microneedle electrodes generally consist of an array of microneedles with variable numbers, and their needle lengths range from tens to thousands of microns [14]. These needle-like structures are specifically designed to penetrate the stratum corneum, reaching the subcutaneous tissue. This penetration bypasses the high impedance introduced by the stratum corneum, significantly enhancing the quality and accuracy of bioelectrical signal recordings.

This review article offers a concise overview of the categorization, fabrication techniques, and performance characteristics of microneedle electrodes used for bioelectrical signal measurement. It highlights recent applications and anticipates the future potential of microneedle electrodes in portable health monitoring, disease detection, and a wide range of applications, including wearable devices and human-computer interfaces. The multifunctional capabilities of microneedle electrodes promote cross-disciplinary integration across life sciences, materials science, electronics, artificial neural networks, deep learning, and brain-computer interfaces, strategically positioning them to meet evolving practical demands.

1.2 Brief overview of current methods for measuring bioelectrical signals

Electrodes used for bioelectrical signal measurement are categorized into non-invasive, minimally invasive, and invasive types based on their measurement principles, as illustrated in Fig. 1. These electrodes function as transducers, converting ionic currents in the human body into electronic currents . The selection of an electrode type is determined by the specific application and the required spatial resolution.

Non-invasive electrodes, which are placed on the surface of the skin, include surface electrodes, capacitive electrodes, and conventional silver/silver chloride (Ag/AgCl) wet electrodes. Surface electrodes are the most commonly used non-invasive type due to their ease of use and lack of need for skin preparation [25]. These electrodes can capture bioelectrical signals without damaging skin tissues, ensuring minimal discomfort to the user [26]. Various surface electrode types have been developed, including micro/nanostructured electrodes, flat film electrodes, textile electrodes, and tattoo electrodes. Micro/nanostructured electrodes employ finely tailored micro- or nanoscale surface architectures to enhance sensitivity, selectivity, and the signal-to-noise ratio [27–29]. Flat film electrodes [16, 30, 31] provide a planar design that simplifies fabrication and integration. Textile electrodes offer unique advantages in terms of conformability, comfort, and compatibility with wearable and flexible electronics [32–38]. Tattoo electrodes, a recent innovation, are notable for their ability to conform seamlessly to the skin's contours, ensuring optimal skin contact while minimizing motion artifacts [39]. Despite the convenience of surface electrodes, they have limitations, such as relatively high skin-electrode impedance and low signal-to-noise ratios. Capacitive electrodes measure bioelectrical signals through capacitive coupling between the electrode and the skin [40, 41]. These electrodes are popular in long-term ECG monitoring because they can operate without direct skin contact or complex clinical procedures [42]. They are typically made from metals [43, 44] or conductive polymers [45–47]. While metallic materials provide excellent conductivity, their rigidity can lead to motion artifacts and reduced signal quality. In contrast, conductive polymers are flexible and conform well to the skin, with adjustable conductivity to suit specific needs. However, capacitive electrodes are prone to ambient interference and high-impedance issues, which, along with their sensitivity to motion artifacts and low signal amplitudes, limit their effectiveness [48, 49]. Ag/AgCl wet electrodes are the most widely used electrodes in clinical settings for bioelectrical signal measurement [50, 51]. These electrodes use a conductive gel to reduce skin-electrode impedance, making them the gold standard for recording brain potentials [52]. However, their long-term use is limited due to skin irritation and reduced conductivity as the gel dries [53, 54]. Additionally, hair at electrode placement sites can complicate preparation and inconvenience users during diagnostic tests.

Invasive electrodes, as the name implies, penetrate biological tissues or are implanted into living organisms. They can be categorized into microneedle electrodes and implantable electrodes [55]. Implantable electrodes are widely used for recording and stimulating bioelectrical signals due to their ability to obtain high-quality signals with high spatial and temporal resolution [56]. However, they still face challenges such as a high risk of infection and the long-term stability of the device after implantation [57].

Minimally invasive electrodes are a type of electrode that falls between non-invasive and invasive electrodes. They avoid the high impedance associated with non-invasive electrodes while also mitigating the high risks of invasive electrodes. Microneedle electrodes are a typical representative of minimally invasive electrodes. Microneedle electrodes, although placed on the skin's surface, have microneedles that penetrate the stratum corneum. Classified as minimally invasive, they avoid the complex surgical procedures required for implantable electrodes and mitigate the high impedance and low signal-to-noise ratio issues of non-invasive electrodes. Therefore, microneedle electrodes are expected to measure bioelectrical signals more accurately and conveniently [58]. As a relatively new technology, microneedle electrodes offer several advantages: They provide high spatial resolution, reduce impedance by penetrating the stratum corneum [59], minimize motion artifacts, and accurately record bio-signals without requiring skin preparation or electrolytic gels, all with minimal invasiveness [60]. Additionally, they are suitable for long-term EEG monitoring

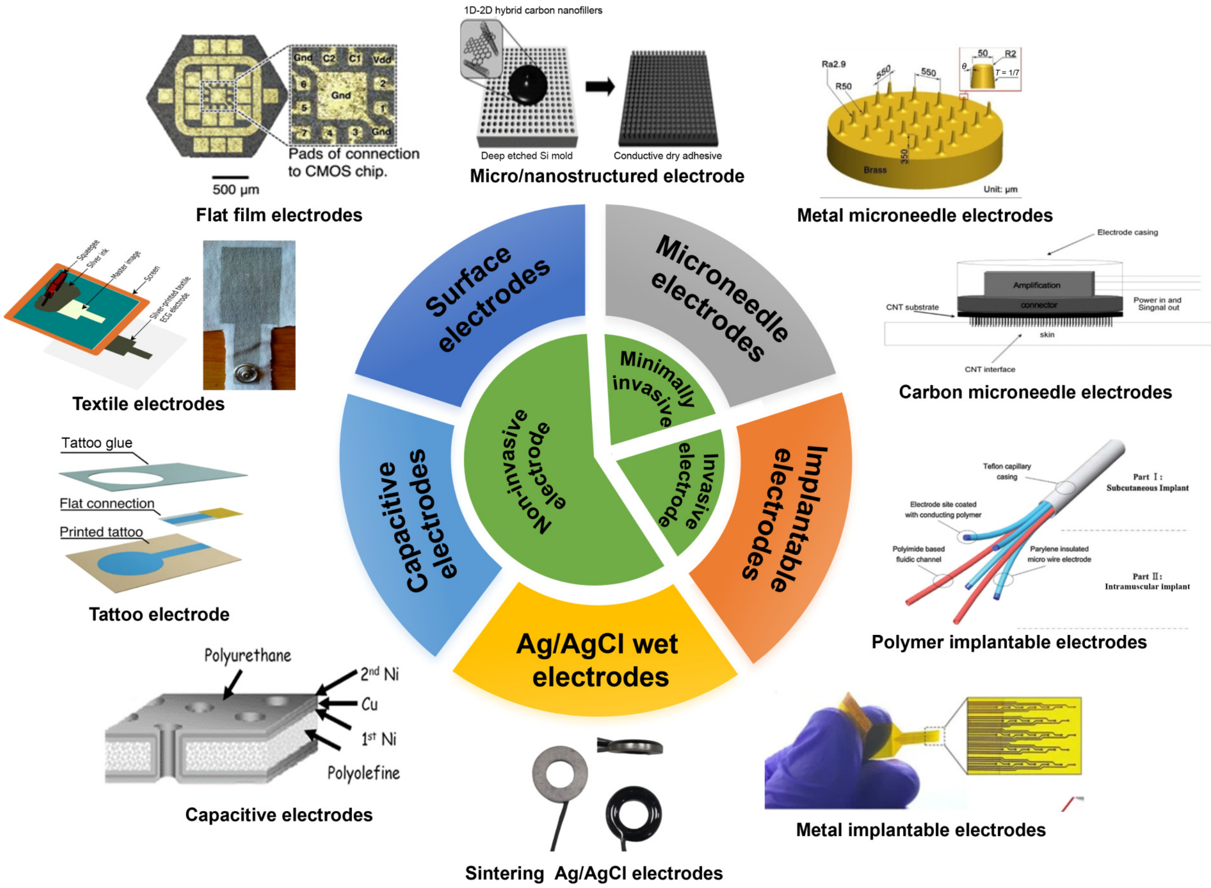

Figure 1 Classification of electrodes for measuring bioelectrical signals. Non-invasive electrodes: surface electrodes, micro/nanostructured electrode, flat film electrodes, textile electrodes, tattoo electrode, conductive polymer electrodes, sintering Ag/AgCl wet electrodes. Reproduced with permission from Ref. [15], © American Chemical Society 2016; Ref. [16], © The Japan Society of Applied Physics 2023; Ref. [17], © Nigusse, A. B. et al. Licensee MDPI, Basel, Switzerland 2020; Ref. [18], © Ferrari, L. M. et al. 2020; Ref. [19], ©IEEE 2012; Ref. [20], © Li, L. et al. Licensee MDPI, Basel, Switzerland 2021. Invasive electrode: polymer implantable electrodes, metal implantable electrodes. Reproduced with permission from Ref. [21], © The Royal Society of Chemistry 2021; Ref. [22], © Chatterjee, S. et al. under exclusive licence to Springer Science Business Media, LLC, part of Springer Nature 2022. Minimally invasive electrodes: metal microneedle electrodes, carbon microneedle electrodes. Reproduced with permission from Ref. [23], © Elsevier B.V. All rights reserved 2017; Ref. [24], © Elsevier B.V. All rights reserved 2008.

because they do not require gel application [61]. Despite their benefits, microneedle electrodes face significant challenges. Designing microneedle electrodes requires balancing rigidity for effective skin penetration with flexibility to accommodate skin stretching. Their insertion can cause varying degrees of discomfort and pain, raising concerns about potential skin irritation, infection, or allergic reactions [62]. Furthermore, the fabrication of microneedle electrodes often requires intricate micromachining or microfabrication processes, which can be costly and complex [63]. One notable challenge is the lack of standardized evaluation criteria for assessing microneedle performance. Most studies compare microneedle electrodes with Ag/AgCl wet electrodes, but variations in the specific Ag/AgCl electrodes used across studies lead to inconsistent and non-comparable results. Additionally, there is room for improvement in the materials and processing techniques used to fabricate microneedle electrodes. The current approach, which typically involves coating flexible polymer substrates, is not well-suited for mass production.

Before exploring bioelectrical signal measurement electrodes in detail, it is essential to first understand the measurement principles behind various electrode types. This foundational knowledge provides context for the subsequent classification of electrodes. Below is a brief explanation of the measurement principles for four commonly used electrode types. The sensing mechanism of wet electrodes can be elucidated through the utilization of a simplified electrical equivalent circuit model, as shown in Fig. 2(a). Bioelectrical signals are transferred from the biological system to the electrode, resulting in a transition from ion conduction to electronic conduction. When wet electrodes make contact with the skin, the gel acts as an electrolyte, forming a half-cell at the interface between the skin and the electrode. E_{hc} represents the half-cell potential caused by polarization at this interface. The interface between the gel and the electrode is modeled as a parallel capacitor C_{eg} and a resistor R_{eg}. The series resistance R_g represents the resistance of the electrolyte. Since the stratum corneum is a semipermeable layer that contains ionic species, the gel is partially absorbed, leading to a difference in ion concentration along the epidermis. This concentration gradient creates a potential difference E_{gs}. The stratum corneum's impedance is modeled as a parallel resistor capacitance circuit, consisting of a resistor R_{sc} and capacitor C_{sc}. Finally, the epidermal layer and the underlying tissues are represented by a pure resistance, denoted as R.

Unlike wet electrodes, surface electrodes do not use conductive gel, as shown in Fig. 2(b). In this case, the R_s and E_{gs} present in the wet electrode model are replaced by a resistor R_{air} and a capacitor C_{air}, representing the air gap and the dry skin interface. This

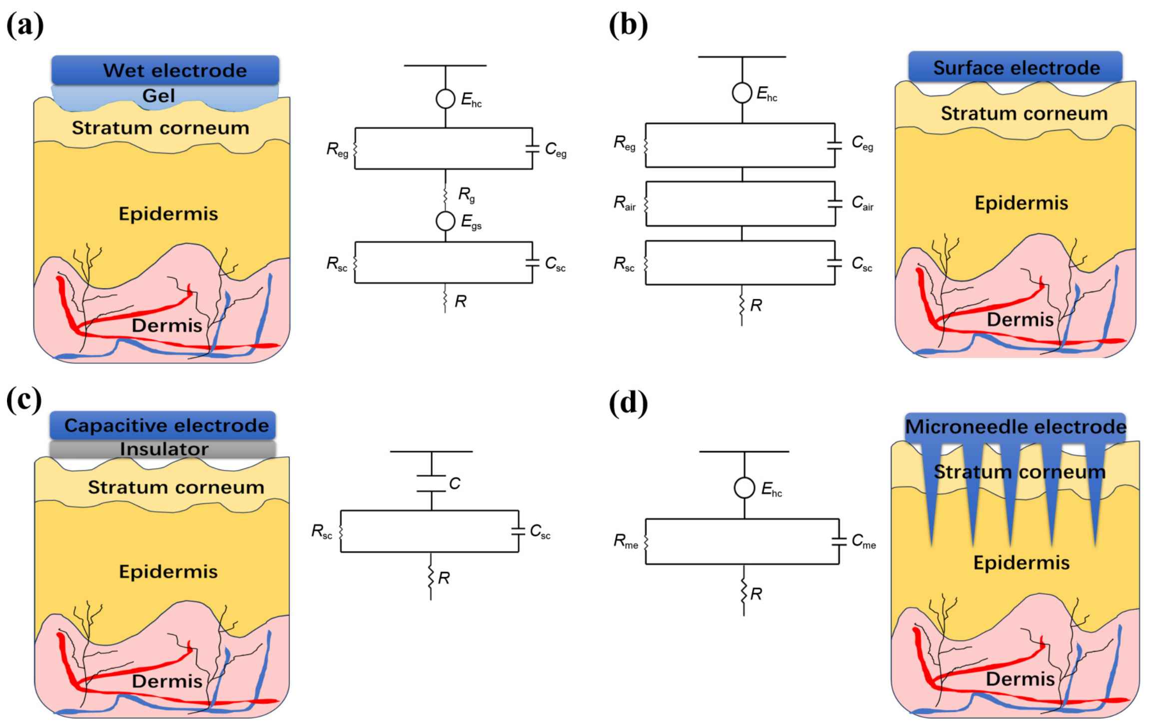

Figure 2 Equivalent circuit diagrams of four typical bioelectrical signal acquisition electrodes. (a) Ag/AgCl wet electrode; (b) surface electrode; (c) capacitive electrode; (d) microneedle electrode. Reproduced with permission from Ref. [1], © Fu, Y. L. et al. Licensee MDPI, Basel, Switzerland 2020.

additional interface significantly increases the overall skin-electrode impedance, which can lead to reduced signal quality and sensitivity compared to wet electrodes.

Compared to other electrodes that directly collect bioelectrical signals, capacitive electrodes are based on changes in capacitance caused by variations in the dielectric properties between the electrode and the skin [64], as shown in Fig. 2(c). The dielectric layer (e.g., air, clothing, or sweat) between the skin and the electrode is represented by the capacitance C in the equivalent circuit. Microneedle electrodes are minimally invasive compared to the other three electrode types. The interface is distinctly established between the microneedle and the epidermal layer, as shown in Fig. 2(d). This design reduces the distance over which ion charges are transmitted and minimizes the number of interfaces that could impede electrical signal transmission. In the equivalent circuit, the interface between the electrode and the epidermal layer is represented by parallel-connected components R_{me} and C_{me}. Due to their unique structural characteristics, microneedle electrodes provide enhanced signal quality, minimally invasive and patient-friendly measurements, targeted sensing capabilities, and the potential for long-term monitoring.

Microneedle structures have demonstrated significant advancements in biosensors [65], vaccination techniques [66], molecular detection [67], and transdermal drug delivery [68–71]. However, their potential for measuring bioelectrical signals has not received sufficient attention. Microneedle electrodes do not require additional skin preparation, as the microneedles penetrate the stratum corneum and extend to the boundary between the epidermis and dermis. This reduces the electrode-signal interface and enhances signal quality. Additionally, the microneedles avoid contact with blood vessels and nerves, improving user comfort. Consequently, microneedle electrodes combine high measurement accuracy with ease of use. Despite their broad applications and strong performance, microneedles have yet to achieve large-scale implementation, indicating unresolved challenges that warrant further research. The remainder of this article will explore the structure, preparation methods, performance, and applications of microneedle electrodes for bioelectrical signal measurement.

2 Microneedle electrodes for measuring bioelectrical signals

2.1 Overview of the development and history of microneedle electrodes

Figure 3 illustrates key milestones in the development of microneedle electrodes for bioelectrical signal acquisition. In 1928, Hans Berger, a German psychiatrist, achieved a groundbreaking feat by recording human electrical activity for the first time using electrodes attached to the scalp and an ammeter. Five years later, in 1933, he successfully documented low-frequency oscillations, which he termed Alpha waves [72]. Around the late 1920s, the concept of "Nadelelektroden" (needle electrodes) for recording bioelectrical signals from the brain began to take shape. In 1976, Martin. S and colleagues introduced the idea of microneedle structures capable of painlessly penetrating the stratum corneum, laying the foundation for their application in bioelectrical signal measurement [73].

Around 2000, Griss and colleagues made a seminal contribution by introducing the concept of using spiked biopotential electrodes for recording electroence-phalographic signals [74, 78]. These spiked electrodes consist of arrays of microneedles that penetrate the outer skin layers. Since then, microneedle electrodes have garnered significant attention for their potential in minimally invasive bioelectrical signal measurement. Research efforts have focused on developing microneedles with dimensions that allow skin penetration without causing significant pain or damage. Simultaneously, microneedles with integrated sensors and

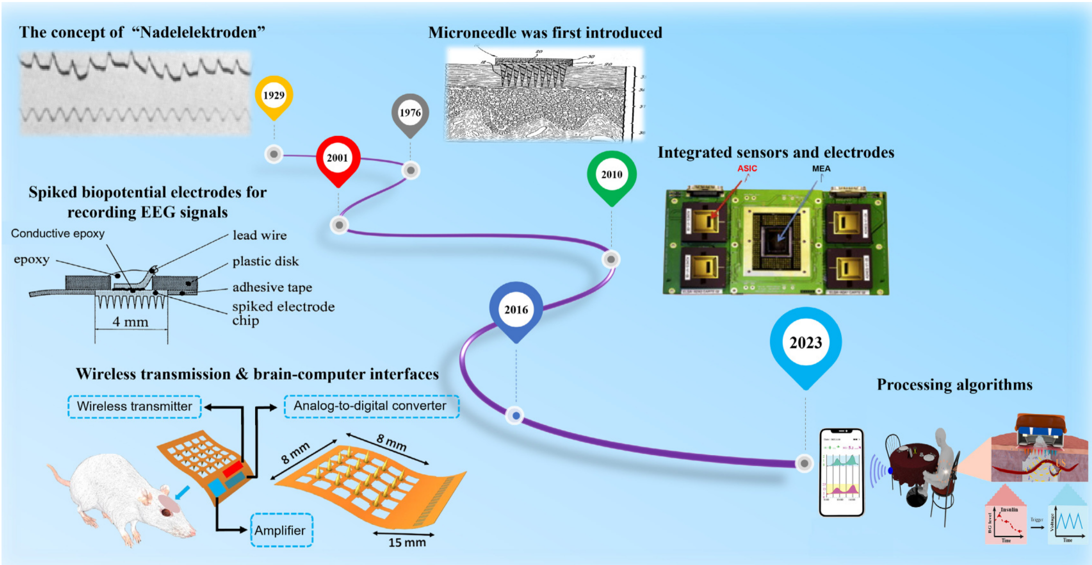

Figure 3 Overview of the development and history of microneedle electrodes. Reproduced with permission from Ref. [72], © Georg Thieme Verlag, Stuttgart 1934; Ref. [73], © Alza Corporation 1976; Ref. [74], © IEEE 2001; Ref. [75], © Elsevier B.V. All rights reserved 2010; Ref. [76], © Xiang, Z. et al. 2016; Ref. [77], © American Chemical Society 2023.

electrodes for bioelectrical signal measurement began to emerge. With their high degree of integration, the application domains for microneedle electrodes expanded rapidly to include wound management [79–83], healthcare monitoring [84–87], therapy [88–92], and brain-computer interfaces [93–95]. As the applications for microneedle electrodes continue to evolve, there has been a corresponding increase in performance requirements, such as enhanced biocompatibility, reliability, and long-term monitoring capabilities . To meet the growing demands of wearable applications [96], microneedle electrodes have gradually been integrated with power sources [97, 98], wireless transmission [99–101], and signal processing algorithms [77, 102]. Advancements in materials and manufacturing, coupled with integration into wearable and smart devices, are driving further progress in the field.

Initially, microneedles were constructed using silicon [103], However, silicon's inherent brittleness limits its ability to adapt to the dynamic movements of human skin, leading to noticeable motion artifacts and an increased risk of breakage within the skin. This can cause significant discomfort and raise the potential for infection. Additionally, silicon has limited electrical conductivity, which may hinder the transmission of subtle bioelectrical signals. Subsequent advancements led to the development of metal microneedles, which improved conductivity and provided greater toughness. However, similar to their silicon counterparts, they struggled to adapt to skin movement. To address these limitations, researchers began coating metal microneedles and transitioning to flexible polymer substrates [104]. While polymers provide the flexibility needed to accommodate skin movement, their inadequate rigidity can hinder penetration of the stratum corneum, leading to higher skin-electrode impedance and reduced signal quality. Moreover, most polymers lack inherent electrical conductivity, necessitating additional conductive coatings to collect bioelectrical signals effectively. This adds complexity to the electrode fabrication process [105]. In recent years, the advent of conductive polymer materials has offered a promising solution by combining both flexibility and conductivity. These materials are also easy to mold, making them suitable for mass production. Consequently, they are emerging as viable alternatives to conventional Ag/AgCl wet electrodes.

2.2 Structural design of microneedle electrodes for bioelectrical signals collection

With advancements in fabrication techniques and materials, researchers have been refining microneedle electrode designs to create diverse structures [106–111]. These structures include candle-like [112], conical [113], barb-like [114], and pyramidal structures [115, 116], as illustrated in Fig. 4. Candle-like microneedle electrodes are commonly used for EEG signal acquisition due to their suitability for regions with hair, such as the scalp [117]. However, their composite structure—featuring flexible pillars and rigid tips—can complicate the fabrication process and result in unstable electrode-skin interfaces. Conical and pyramidal microneedle shapes are widely adopted because they can be fabricated using simple methods such as silicon etching or polymer casting on templates [104]. These shapes offer a straightforward manufacturing process with well-established protocols, making them popular in many applications. Barb-like microneedles are inspired by natural structures, such as those found in bees and barbed plants. This design enables a secure fit within the skin after insertion, reducing the likelihood of dislodgment [118]. Despite this advantage, barb-like microneedles have notable limitations. Their fabrication process is more complex and requires meticulous attention to detail. Additionally, the materials used must be strong enough to maintain the structural integrity of the barbs while embedded in the skin.

Amid the diverse range of microneedle geometries, candle-like electrodes have drawn significant interest for their compatibility with hair-bearing regions, such as the scalp. Pyramidal and conical configurations offer robust mechanical properties, allowing them to penetrate the stratum corneum without deformation or breakage. Barbed microneedles are designed for secure skin integration, minimizing the risk of dislodgment after insertion. Each morphology presents unique advantages; however, conical and

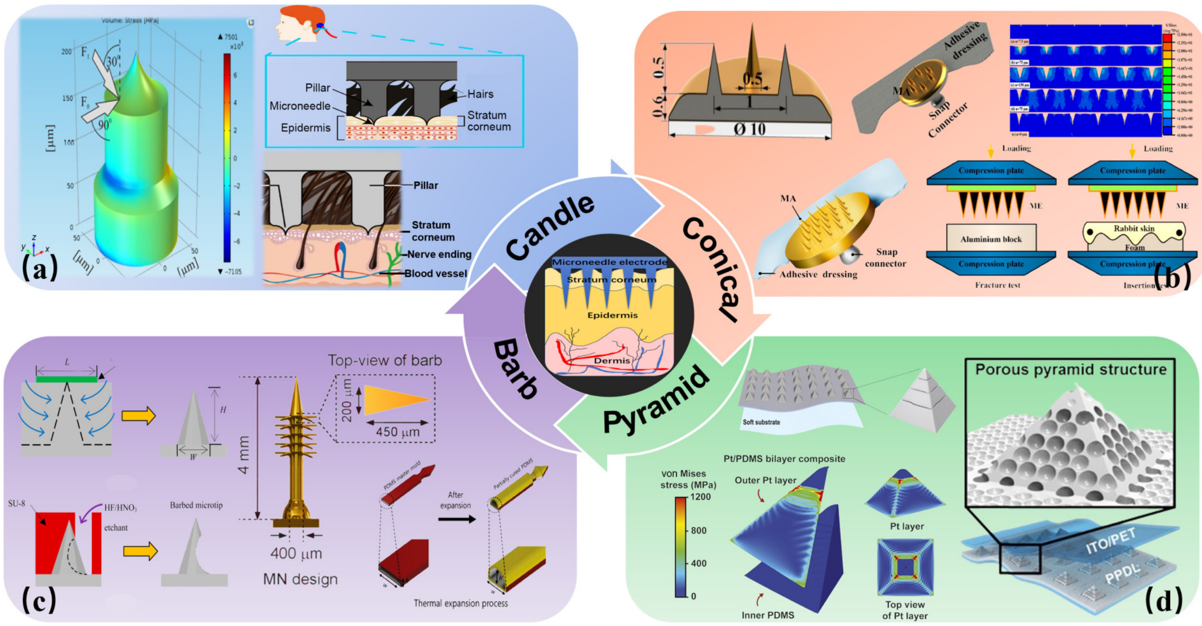

Figure 4 Schematic illustrations of microneedle electrodes with different shape. (a) Candle-like microneedle electrodes. Reproduced with permission from Ref. [112], © The Institution of Engineering and Technology 2017; Ref. [119], © Elsevier B.V. All rights reserved 2015; Ref. [120], © The Japan Society of Applied Physics 2016. (b) Conical microneedle electrodes. Reproduced with permission from Ref. [113], © Ren, L. et al. Licensee MDPI, Basel, Switzerland 2016; Ref. [121], © Chen, K. et al. Licensee MDPI, Basel, Switzerland 2016. (c) Barb-like microneedle electrodes. Reproduced with permission from Ref. [114], © WILEY-VCH Verlag GmbH & Co. KGaA, Weinheim 2020; Ref. [122], © Hsu, L.-S. et al. Licensee MDPI, Basel, Switzerland 2014; Ref. [123], © Elsevier B.V. All rights reserved 2024. (d) Pyramidal microneedle electrodes. Reproduced with permission from Ref. [124], © Published under the PNAS license 2020; Ref. [125], © American Chemical Society 2019.

pyramidal microneedles have emerged as the predominant choices in mainstream applications due to their balance of durability and ease of fabrication.

3 Microneedle electrodes classified by material for bioelectrical signal measurement

The performance of an electrode plays a pivotal role in ensuring the fidelity of collected bioelectrical signals, with electrode materials being a key determinant of this performance. Selecting appropriate materials is crucial for acquiring high-quality bioelectrical signals. In general, materials used in microneedle electrodes for bioelectrical signal acquisition must balance adequate rigidity, flexibility, electrical conductivity, and biocompatibility [126]. Rigidity is essential for penetrating the stratum corneum, thereby reducing electrode-skin impedance. Flexibility allows the electrode to accommodate skin deformation and minimizes motion artifacts. High electrical conductivity ensures the efficient conversion of ionic currents into electronic signals, while biocompatibility reduces the risk of discomfort and infection. Microneedle electrodes must address the competing demands of sufficient penetration and skin adaptability—a critical challenge in electrode design. To date, silicon, metals, polymers, carbon materials, and their composites have been employed in fabricating microneedle electrodes with diverse structural configurations.

3.1 Silicon-based microneedle electrodes

Silicon was one of the earliest materials chosen for microneedles used in recording bioelectrical signals, primarily due to its ease of fabrication into the desired microneedle dimensions. As early as 1985, Najafi et al. reported the development of multi-electrode arrays for studying central nervous system information processing and closed-loop control of neural prostheses [127]. The spikes were manufactured using deep boron diffusion and anisotropic etching with dimensions of 3 mm in length. Although silicon microneedles offer advantages such as mature fabrication methods and ease of skin penetration, they suffer from inherent drawbacks. For example, silicon material is brittle and poor conductivity, especially after fracturing, the remaining silicon can cause infections when left in the skin [62]. Particularly in the context of wearable devices, electrode adhesion to the human skin necessitates accommodating the skin's stretching to maintain close contact [128]. The rigid nature of silicon material clearly fails to meet our requirements. Furthermore, its conductivity increasingly fails to meet the precision requirements for acquiring bioelectrical signals. To enhance the electrical conductivity of silicon-based microneedles, investigators have employed surface coatings comprising highly conductive metals such as gold, titanium, and silver [119, 129–132]. Li et al. [133] developed a novel silicon microneedle electrode array (MEA) composed of 124 µm long microneedles on n-type (100) single-crystal silicon wafers using wet etching and photolithography techniques, followed by the deposition of a Ti/Au coating on the electrode surface, as shown in Fig. 5(a). The MEA has excellent test–retest reproducibility, with intraclass correlation coefficients exceeding 0.920. The introduction of this innovative MEA provides a practical and reusable solution for EMG assessment in neurogenic myopathy cases. Although metal coating solves the problem of poor conductivity to a certain extent, rigid silicon microneedle electrodes don't adapt to the stretching of the skin. The advancement of elastic materials has positioned the integration of silicon microneedles with flexible polymer substrates as a pivotal solution to address the challenge of inadequate contact between electrodes and the skin. Wang et al. [134] developed a flexible parylene-based microneedle electrode arrays (P-MNEA) with silicon microneedles, as shown in Fig. 5(b), which could provide not only conformal but also robust contact. P-MNEA exhibited low impedance density compared with

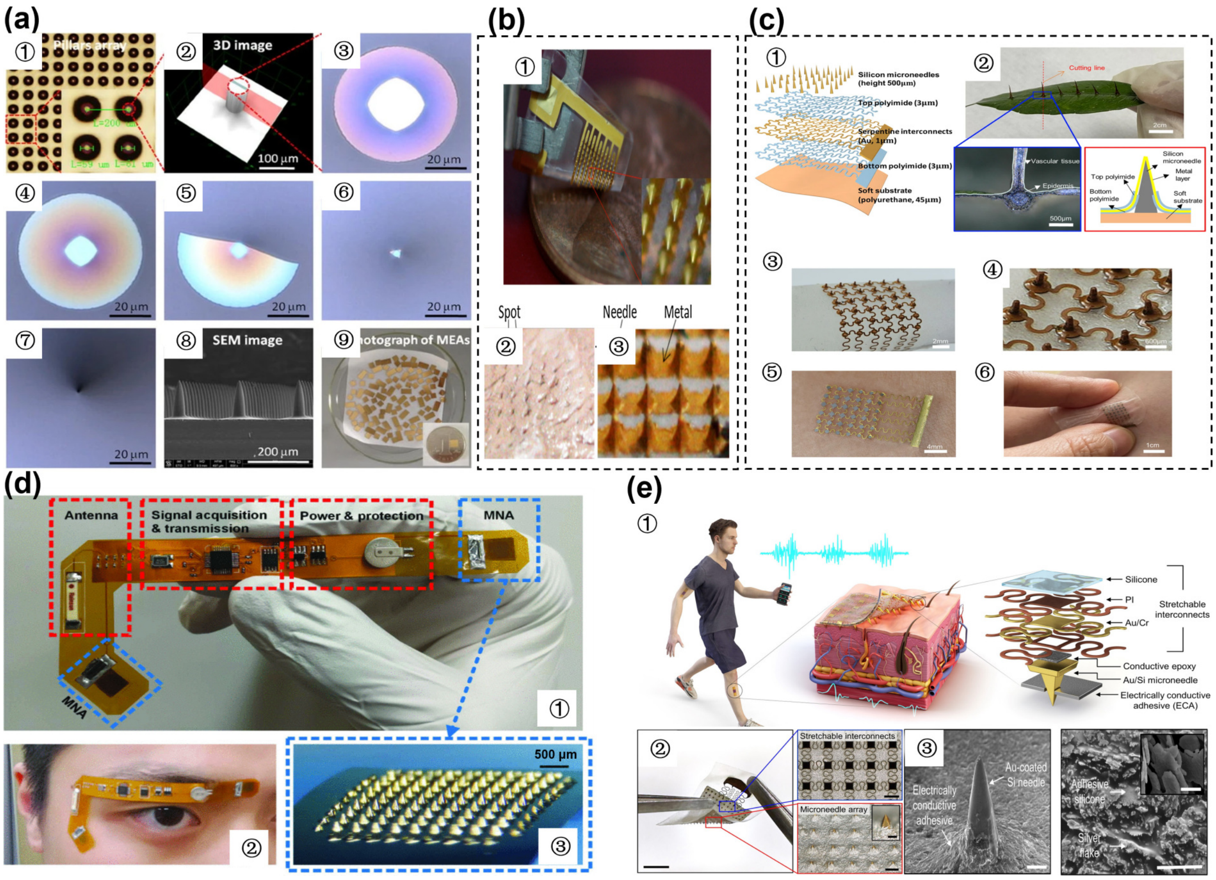

Figure 5 Image of silicon-based microneedle electrodes used for bioelectrical signal acquisition. (a) A novel microneedle electrode array was developed with a surface-deposited Ti/Au coating. Reproduced with permission from Ref. [133], © Biomedical Engineering Society 2015. (b) Flexible parylene-based microneedle electrode arrays with silicon microneedles. Reproduced with permission from Ref. [134], © Elsevier B.V. All rights reserved 2017. (c) A skin-integrated, biocompatible, and stretchable microneedle electrode. Reproduced with permission from Ref. [135], © Ji, H. et al. 2023. (d) A flexible wearable patch integrating a parylene-based microneedle array and a signal acquisition flexible PCB circuit. Reproduced with permission from Ref. [136], © IEEE 2019. (e) Silicon microneedle electrodes coated with Ti and Au layers were integrated with a flexible silicone substrate. Reproduced with permission from Ref. [137], © Kim, H. et al. some rights reserved; exclusive licensee American Association for the Advancement of Science 2024.

Ag/AgCl wet electrodes, allowing for excellent adhesion to curved and moving skin. The impedance density was measured at 7.5 kΩ·cm^2 at 10 Hz.

Ji et al. [135] developed a skin-integrated, biocompatible, and stretchable silicon microneedle electrode (SSME) inspired by radix zanthoxyli thorns. The 500 μm silicon microneedle arrays were fabricated via isotropic and anisotropic etching, as shown in Fig. 5(c). Using a semi-additive process, SSME, semi-encapsulated with polyimide (PI), achieved a stretch rate over 45%. SSME reduced interference from skin deformation during daily activities and demonstrated better long-term impedance stability compared to commercial wet electrodes. Huang et al. [136] developed a flexible wearable patch combining a parylene-based microneedle array (MNA) and a signal acquisition flexible PCB for long-term biopotential monitoring, as shown in Fig. 5(d). The MNA, featuring a PI substrate and a gold-parylene surface coating, effectively penetrates the stratum corneum, ensuring low-impedance skin contact. The flexible PI substrate conforms to curved body surfaces, while the integrated button battery, signal chip, and bluetooth transceiver enhance its wearability. This compact system enables multichannel biopotential monitoring across the body. Kim et al. [137] developed rigid silicon microneedle electrodes coated with Ti and Au layers, integrated into a flexible silicone substrate to create a stretchable microneedle adhesive patch (SNAP). Silver flakes and high-tack silicone were used as a conductive adhesive, as shown in Fig. 5(e), enhancing the electrode-skin interface and ensuring secure adhesion during prolonged use. Serpentine interconnects in the SNAP platform improved adaptability to skin dynamics, reducing impedance under contamination and increasing comfort during motion. The SNAP outperformed gel and flexible microneedle electrodes and demonstrated reliable wireless control of exoskeleton robots, showcasing its potential for human-machine interfaces under dynamic conditions.

The ease of fabrication and relatively low cost are key advantages of silicon-based microneedle electrodes. However, their development faces significant challenges due to silicon's inherent low electrical conductivity and high rigidity. Researchers have attempted to address these limitations by applying metal coatings to the microneedle surfaces or integrating silicon microneedles with polymers to enhance conductivity and flexibility. Despite these efforts, new issues have emerged, such as coating instability and weak adhesion to the polymer matrix. This raises the question: Can silicon, as a "legacy material", still offer innovative solutions? To address these challenges, future fabrication strategies should move beyond conventional forms and processing methods. One promising direction may involve synthesizing nanostructured silicon materials or doping silicon with other elements to enhance its electrical and mechanical properties.

3.2 Metal-based microneedle electrodes

Metal materials possess both rigidity and toughness, and their superior conductivity has drawn the attention of researchers [138]. In comparison to silicon, the reports on metal materials being fabricated into microneedles were considerably delayed due to processing limitations. Metals that possess both conductivity and biocompatibility, such as gold, titanium or silver, are expensive and have high melting points, while materials like iron or nickel lack sufficient biocompatibility [139].

Stainless steel has garnered significant attention among researchers due to its favorable biocompatibility and ease of transformation into microneedle morphology. Krieger et al. [140] used the direct-metal-laser-sintering 3D printing process to fabricate medical-grade stainless steel microneedle electrodes (MNEs) via a two-step method. Functional tests on healthy volunteers showed an approximation 63% reduction in electrode-skin impedance compared to needle-free electrodes. The MNEs also recorded surface electromyography signals from the biceps brachii with a signal-noise ratio (SNR) comparable to clinical-grade wet Ag/AgCl electrodes, maintaining performance for up to 6 h. Currently, the most widely used electrodes in clinical settings for measuring bioelectrical signals are Ag/AgCl wet electrode or disc metal electrode [141]. However, such electrodes often necessitate the use of conductive gels, which can compromise the quality of bioelectrical signals and are unsuitable for prolonged measurements. To harness the outstanding conductivity and biocompatibility of high-melting-point metals such as gold and titanium, they are commonly utilized as coatings on microneedle surfaces [121]. Wang et al. [142] utilized magnetically induced self-assembly to create ferromagnetic microneedles with a height of 550 μm. A conductive composite film, consisting of a 5 nm titanium layer and a 100 nm gold layer, was deposited via magnetron sputtering, as shown in Fig. 6(a). Compared to conventional dry electrode arrays, this microneedle electrode showed lower, more stable interfacial impedance and enabled high-quality signal recordings, even during body movements. Li et al. [143] developed a 10 × 10 steel-based micro-needle electrode array (M-MNEA) with a 500 μm pitch, 200 μm height, and 10 μm tip, as shown in Fig. 6(b). The system has the potential for circuit integration via flexible printed cables (FPC) or by directly flip-chip bonding an application-specific integrated circuit (ASIC) to a PCB/FPC substrate, enabling active signal processing with the M-MNEA. Researchers have also used a simple template method to fabricate microneedle electrodes from low-melting-point alloys. Dong et al.

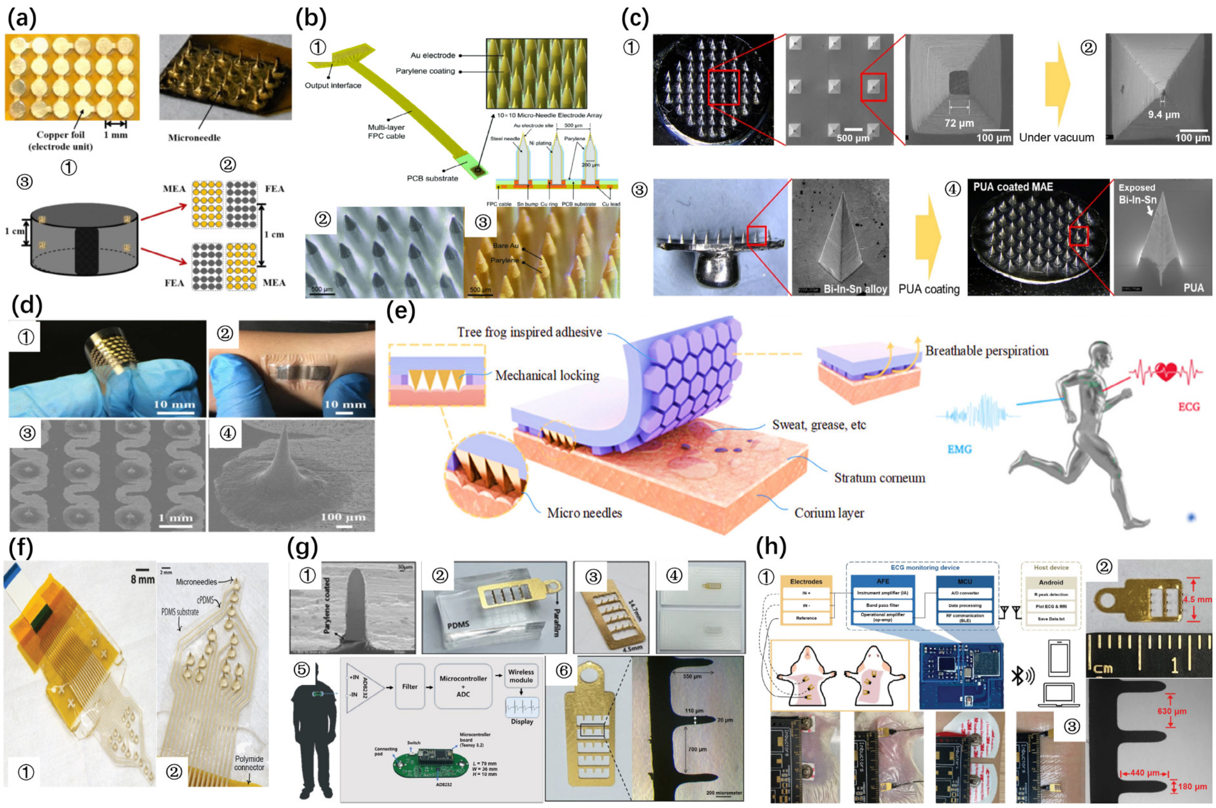

Figure 6 Image of metal-based microneedle electrodes used for bioelectrical signal acquisition. (a) Ferromagnetic microneedles constructed by magnetic induction self-assembly. Reproduced with permission from Ref. [142], © IEEE 2021. (b) Stainless steel microneedle electrodes coated with Au and parylene. Reproduced with permission from Ref. [143], © IEEE 2019. (c) Microneedle electrodes fabricated using Bismuth-Indium-Tin low-melting-point alloy. Reproduced with permission from Ref. [144], © Gwak, H. et al. 2023. (d) A micro-needle array was prepared on a polyethylene terephthalate substrate using curable magnetorheological fluid, with Ti and Au thin films deposited on its surface. Reproduced with permission from Ref. [145], © Ren, L. et al. Licensee MDPI, Basel, Switzerland 2018. (e) A bio-inspired adhesive microneedle electrode by mimicking the combined structure of gecko toe adhesion hooks and tree frog's polygonal adhesive pads. Reproduced with permission from Ref. [146], © Wiley-VCH GmbH 2022. (f) The stretchable microneedle electrode array comprises a PDMS substrate, conductive PDMS traces, and stainless steel microneedles. Reproduced with permission from Ref. [147], © IEEE 2017. (g) A microneedle array electrode is manufactured on a stainless steel substrate, coated with a thin gold film and a layer of poly(p-xylylene), and a two-lead wireless ECG measurement system was developed. Reproduced with permission from Ref. [148], © Satti, A. T. et al. Licensee MDPI, Basel, Switzerland 2020. (h) A stainless steel microneedle electrode coated with layers of gold and poly(p-xylylene) was developed, along with a miniature wearable electrocardiogram monitoring device. Reproduced with permission from Ref. [149], © IEEE 2023.

清华大学出版社 Tsinghua University Press | SciOpen

[144] utilized a polydimethylsiloxane (PDMS) template to prepare microneedle array electrodes (MAEs) employing Bismuth–Indium–Tin (Bi–In–Sn) alloys. The MAEs consist of 57 pyramid-shaped needles measuring 340 μm wide and 800 μm high, as shown in Fig. 6(c). Electrocardiogram measurements using the Bi–In–Sn MAEs demonstrated performance comparable to that of traditional Ag/AgCl electrodes, which shows promise for accurate data collection.

Although high-rigidity metal materials effectively facilitate stratum corneum penetration, their excessive stiffness hinders close conformity to the skin and limits their ability to accommodate skin stretching and movement. To address this issue, researchers have integrated a flexible substrate with rigid microneedles, forming a composite structure known as flexible microneedle electrodes [150]. Ren et al. [145] developed polyethylene terephthalate (PET) film as a flexible substrate, silver ink for conductive patterns, and curable magnetorheological fluid (CMRF) for microneedle array fabrication. Ti and Au films were then deposited through magnetron sputtering, as shown in Fig. 6(d). This electrode adapts well to skin deformation and maintains a lower electrode-skin interface impedance (EII) than Ag/AgCl wet electrodes after multiple uses. Yuan et al. [146] developed a bio-inspired adhesive microneedle electrode by mimicking the structures of gecko toe hooks and tree frog adhesive pads, as shown in Fig. 6(e). The microneedles were fabricated by laser direct writing on a 500 μm thick silver sheet, cut into 10 mm discs, with each microneedle being a 50 μm tall pyramid with a 50 μm base. The microneedles were then combined with a PDMS flexible substrate to create the biomimetic microneedle-based adhesive electrode (BMAE). The BMAE demonstrated excellent adhesion to both dry and wet skin, and the ECG signals collected were comparable to those from commercial wet electrodes. Guvanasen et al. [147] created a stretchable microneedle electrode array (SMEA) with a PDMS substrate, conductive PDMS traces, and stainless-steel microneedles made from 100-μm thick biocompatible steel sheets, as shown in Fig. 6(f). The SMEA showed an impedance of ~ 7.6 kΩ at 1 kHz in saline and maintained resistance below 10 kΩ under 63% strain. It demonstrated cytocompatibility for at least 28 days *in vivo*. This design shows promise for integrating microneedle electrodes with power and signal systems in wearable devices. Satti et al. [148] developed a microneedle array electrode (MNE) fabricated on a stainless steel substrate, with a thin Au film electroplated and a parylene coating applied to the surface, as shown in Fig. 6(g). Additionally, two-lead wireless ECG measurement systems were developed to investigate the performance of the MNE. The results indicate that compared to Ag/AgCl wet electrodes, MNE possess the capability to penetrate the skin and capture biological signals with lower contact impedance. Kim et al. [149] employed a stainless-steel substrate with gold and parylene coatings to create microneedle electrodes with a contact resistivity of 20 kΩ at 10 Hz, as shown in Fig. 6(h), lower than commercial Ag/AgCl electrodes. They also developed a compact wearable ECG device (< 50 mm^3, excluding the battery) that amplifies and transmits waveforms to a phone or laptop. The device enables real-time monitoring during surgery and stores data for later analysis.

Microneedle electrodes made from metals naturally provide excellent biocompatibility and high electrical conductivity. However, their inherent rigidity hinders close conformity to the skin, leading to motion artifacts during use. Consequently, metals are often employed as coatings rather than standalone electrode materials, which limits their wider application in microneedle electrodes. Looking ahead, integrating ultrathin, flexible metal layers with polymer substrates to create flexible electronic devices offer a promising direction for advancing metal-based microneedle electrodes. This approach could help overcome the challenges of rigidity, enabling better skin conformity and improved bioelectrical signal acquisition.

3.3 Polymer-based microneedle electrodes

The development of polymers used as electrodes for measuring bioelectrical signals has been an important area of research and innovation in the field of biomedical engineering and medical devices [151]. Microneedle electrodes made from polymers for measuring bioelectrical signals hold great promise in the field of bioelectrical signals measuring due to their ease of processing, biocompatibility and flexibility [51]. These advantages enable them to accommodate skin stretching, minimizing motion artifacts, facilitating prolonged measurements, and mitigating the risk of skin infections. However, two primary factors impact the performance of polymer microneedle electrodes in bioelectrical signals measurement. Firstly, the conductivity of polymer microneedle electrodes is not sufficient, which directly affects the quality of signal acquisition. Secondly, although polymers generally exhibit good flexibility, this characteristic also hinders their ability to easily penetrate the stratum corneum [152]. Frequently employed polymers (specifically refers to non-conductive polymers) in the formulation of microneedle electrodes encompass SU-8 [153], PDMS [154], poly(lactic-co-glycolic acid) (PLGA) [155], polylactic acid (PLA) [156], poly(vinyl alcohol) (PVA) [157], polyurethane (PU) [158], PI [159] among others. These polymer-based microneedle electrodes offer several advantages over traditional metal or silicon-based electrodes, including improved biocompatibility, flexibility, and ease of fabrication. Nevertheless, the polymers exhibit non-conductive attributes, prompting their amalgamation with metal like gold, silver, titanium, as well as carbon materials including conductive carbon black and carbon nanotubes [160–162]. These metals are often used as surface coatings on microneedles, while carbon materials are often used as fillers in polymers to improve their conductivity and mechanical properties. Lozano et al. [163] employed a templating method to fabricate microneedle structures using carbon black and epoxy resin, followed by a silver coating on the microneedle surface, as shown in Fig. 7(a). The resulting electrodes were suitable for recording EEG signals in the scalp's hairy region without the need for skin preparation, exhibiting an SNR comparable to Ag/AgCl wet electrodes. Hou et al. [164] employed a two-step process to fabricate microneedle electrodes by filling a mold with two epoxy resins: rigid resin for the tips and soft resin for the base, as shown in Fig. 7(b). A 50 nm titanium layer and 200 nm gold layer were added for conductivity. The electrode showed lower skin impedance (~ 220 kΩ at 10 Hz) than wet electrodes. Breathable channels improved ventilation, enabling perspiration and stable signal output. To reduce costs and simplify production, researchers suggested using a template method for microneedle array fabrication [61, 165–167]. Kim et al. [168] utilized PDMS molds and micro-molding techniques to fabricate a PLA microneedle array. To prevent degradation of PLA on the skin and enhance conductivity, silver and titanium coatings were sequentially deposited on the PLA microneedle arrays, as shown in Fig. 7(c). The microneedles exhibited minimal pain during the measurement

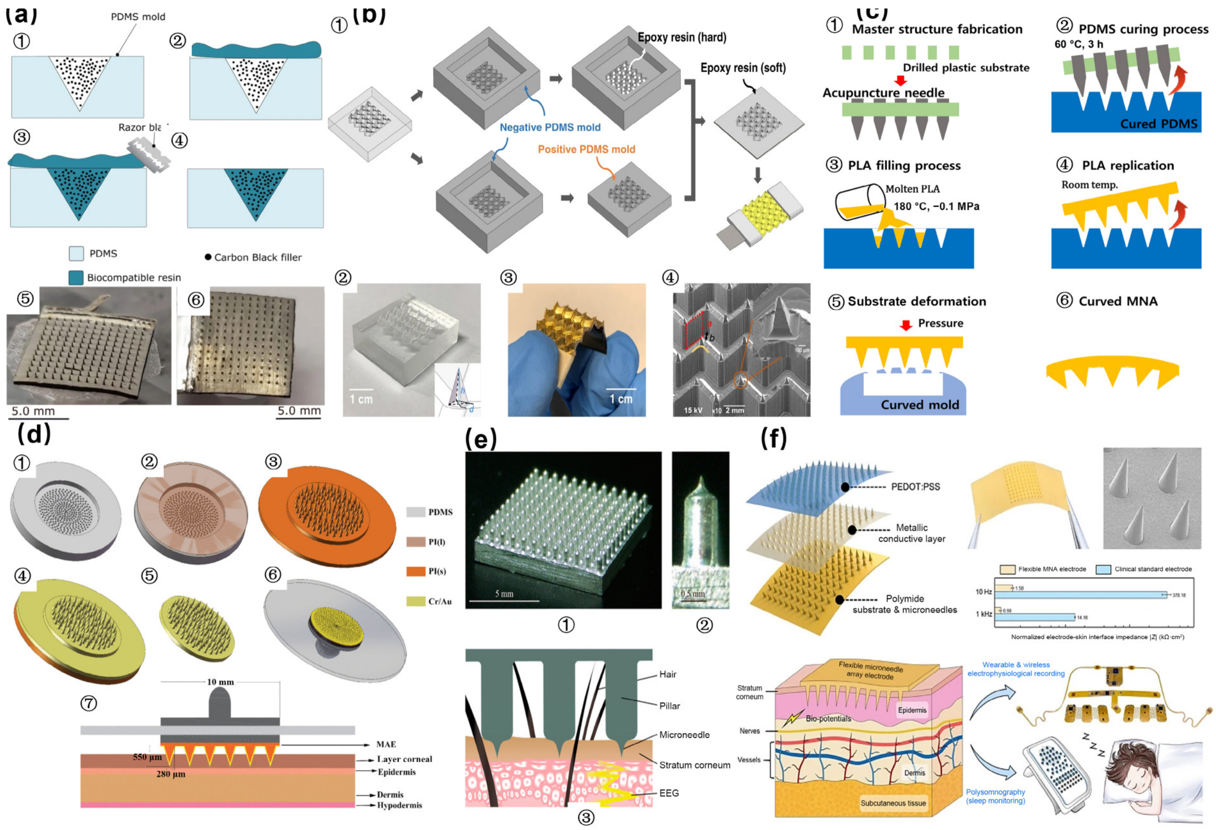

Figure 7 Image of polymer and conductive polymer-based microneedle electrodes used for bioelectrical signal acquisition. (a) The microneedle electrode is composed of conductive carbon black filler and epoxy resin, with a silver coating applied to its surface. Reproduced with permission from Ref. [163], © Lozano, J. et al. under exclusive licence to Springer Science Business Media, LLC, part of Springer Nature 2021. (b) The microneedle tips are formed using rigid epoxy resin, while the base utilizes a flexible resin for the microneedle electrode fabrication, followed by the application of titanium and gold layers. Reproduced with permission from Ref. [164], © Hou, Y. et al. 2021. (c) A polylactic acid microneedle array manufactured using PDMS molds and micro-molding techniques. Reproduced with permission from Ref. [168], © Kim, M. et al. Licensee MDPI, Basel, Switzerland 2015. (d) The utilization of PDMS templates facilitated the fabrication of PI into microneedle structures, subsequently coated with chromium and gold on their surfaces. Reproduced with permission from Ref. [169], © IEEE 2023. (e) A candle-shaped microneedle electrode capable of measuring bioelectrical signals in hairy areas. Reproduced with permission from Ref. [170], © Yoshida, Y. et al. Licensee MDPI, Basel, Switzerland 2020. (f) A PI microneedle array electrode compatible with wearable wireless systems. Reproduced with permission from Ref. [171], © Li, J. et al. 2022.

process, and no itching or inflammation was observed during or after the tests, demonstrating excellent biocompatibility.

Xu et al. [169] used PDMS templates to form PI microneedle structures, coating them with chromium and gold, as shown in Fig. 7(d). The microneedle array electrodes (MAEs) showed a significant impedance drop (251.95 to 7.81 kΩ at 10 Hz) and SNR increase (4.10 to 10.71). ECG recordings revealed the highest standard deviation of signal amplitude (830.40 μV) and SNR (10.71), aligning with impedance results. Mechanical tests confirmed that the MAEs could penetrate skin under 4 N force without damage, causing no significant irritation or allergic reactions after 6 h of use. While template methods significantly simplify the manufacturing process of microneedle arrays, they are prone to causing damage to the needles during demolding. Consequently, researchers have developed various methods for preparing microneedle arrays [104]. Ren et al. [113] prepared a thermal drawing method to prepare glassy-state PLGA microneedles coated with Ti/Au film. The brain electrical signals recorded were comparable in waveform and amplitude to those from commercial Ag/AgCl wet electrodes. At a pressing force above 1 N, the EII was about 85 kΩ, lower than the 120 kΩ measured for Ag/AgCl wet electrodes. Furthermore, bioelectrical signal measurements sometimes necessitate placement in areas with hair. For instance, electrodes for measuring EEG signals are commonly placed on the scalp. Traditional measurement techniques require shaving the hair to position the electrodes, causing inconvenience to both operators and subjects. Therefore, researchers are focusing on developing convenient methods for measuring bioelectrical signals in areas with hair [172, 173]. Yoshida et al. [170] employed candle-like microneedle electrodes to capture event-related potentials, as shown in Fig. 7(e). These electrodes allowed EEG recordings from hairy areas without skin preparation, producing SNR comparable to Ag/AgCl wet electrodes that require preparation, and were more robust. To improve the practicality and portability of microneedle electrodes, researchers are focusing on highly integrated wearable devices [174]. Li et al. [171] utilized microfabrication techniques to create an MNA electrode with a PI substrate. The microneedles were coated with a 10 nm thick titanium layer and a 200 nm thick gold layer using magnetron sputtering, as shown in Fig. 7(f). The electrode-skin contact impedance was exceptionally low, with values of 0.98 kΩ·cm² at 1 kHz and 1.50 kΩ·cm² at 10 Hz, which is about 1/250 of the impedance of standard electrodes. The MNA electrodes also demonstrated good compatibility with wearable wireless systems and reduced preparation time, enhancing comfort and convenience for electrophysiological recording. Although polymer microneedle electrodes provide excellent flexibility and ease of fabrication, their inherent lack of electrical conductivity poses a significant limitation to their broader application.

Fortunately, with the development and introduction of conductive polymer materials, it is expected to solve the problems of insufficient conductivity of non-conductive polymers, easy damage to the interface of polymer composite materials, and signal weakening or distortion due to electronic transmission between interfaces. Examples of conductive polymers include polyaniline (PANI) [175], polypyrrole (PPy) [176], polythiophene (PT) [177], and poly(3,4-ethylenedioxythiophene) (PEDOT) [178]. Conductive polymers offer convenient processing and easy scalability in production. Moreover, they exhibit both electrical conductivity and flexibility [179], making them a prominent research focus for the fabrication of microneedle electrodes. Currently, the utilization of conductive polymers for microneedle electrodes is constrained by their mechanical properties and conductivity. Consequently, they are often utilized as coatings in combination with polymers or filled with conductive metal particles and carbon materials to enhance their conductivity and mechanical properties [180, 181]. Zhou et al. [182] fabricated a flexible microneedle electrode array (P-FMNEA) by employing a template method on PI, followed by surface coating with a layer of Au and subsequent modification with poly(3,4-ethylenedioxythiophene) polystyrene sulfonate (PEDOT:PSS). The P-FMNEA can capture each electrical impulse in response to real-time direct nerve stimulation during neurosurgical procedures. The wireless conveyance of EMG signals to medical facilities via a server augments access to patient follow-up evaluation data. Furthermore, the device's soft mechanics minimize soft tissue hematomas associated with traditional needle electrode positioning.

The development of conductive polymers has effectively addressed the inherent conductivity limitations of traditional polymers. With their intrinsic flexibility and ease of processing, conductive polymers have become prominent electrode materials for biopotential signal measurement and are anticipated to find even broader applications in the future.

3.4 Carbon-based microneedles electrodes

Carbon-based materials have attracted great attention in biomedical and biological fields owing to their stability, chemical inertness, mechanical strength and rapid electron transfer kinetics [183–188]. These attributes contribute to the extended longevity of carbon-based electrodes while facilitating high-precision bioelectrical signals acquisition [189]. carbon nanotubes (CNTs) based biosensors have been shown to provide reliable interface to neuronal signals [190]. CNTs based biosensors are shown to be biosafe at low concentration external to the body [191]. In 1976, Mitskene V et al. [192] proposed the use of carbon electrodes for long-term recording of human brain signals. Opdam et al. [193] employed carbon fiber electrodes to acquire bilateral intracranial EEG signals. Ruffini et al. [194] designed dry electrode sensors for bioelectrical potential measurements with the aim of eliminating gel-related noise and inconvenience while maintaining good contact impedance to minimize interference noise. The electrode is made by coating the surface of the carbon nanotube array with Ag/AgCl, as shown in Fig. 8(a).

Nevertheless, achieving stratum corneum penetration proves challenging due to insufficient hardness of carbon nanotubes and carbon fibers. However, carbon materials as filler components or employing them as surface coatings presents a viable strategy to notably enhance the electrical characteristics of microneedle

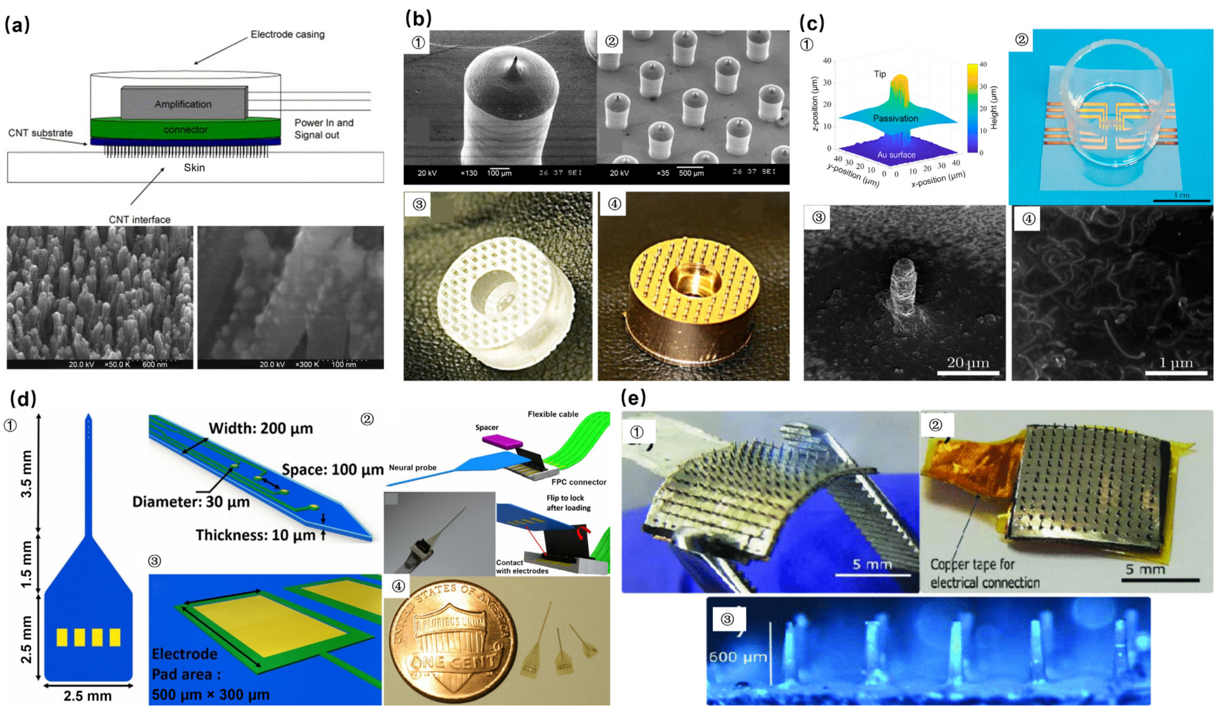

Figure 8 Image of bioelectrical signal acquisition using carbon-based microneedle electrodes. (a) The surface-coated carbon nanotube array electrode with Ag/AgCl. Reproduced with permission from Ref. [194], © Elsevier B.V. All rights reserved 2006. (b) Epoxy resin-carbon microneedle electrodes. Reproduced with permission from Ref. [195], © Elsevier B.V. All rights reserved 2009. (c) A three-dimensional microelectrode array with microneedle tips was fabricated using a composite ink of PEDOT:PSS and Multi-walled carbon nanotubes (MWCNTs). Reproduced with permission from Ref. [196], © American Chemical Society 2019. (d) The microneedle electrode with carbon nanotubes deposited on a PI substrate. Reproduced with permission from Ref. [197], © IOP Publishing Ltd 2014. (e) Conductive polymer microneedle electrodes composed of biocompatible epoxy resin and carbon black. Reproduced with permission from Ref. [198], © IEEE 2019.

electrodes. Ng et al. [195] employed a vacuum casting method to create epoxy resin-carbon microneedle electrodes. Each electrode featured a micro-column with a pointed tip, designed to penetrate through hair and establish electrical conduction by passing through the stratum corneum, as shown in Fig. 8(b). To enhance electrical conductivity, Ag/AgCl was deposited on the tip of the microneedle. The electrodes exhibited improved performance in terms of impedance levels and stability, demonstrating higher efficiency in EEG measurements. Xiang et al. [197] fabricated a microneedle electrode on a PI substrate with a 20 nm titanium layer, 200 nm gold layer, as shown in Fig. 8(c), and a carbon nanotube film. A maltose coating enhanced rigidity and dissolved in the body, exposing the CNTs-coated probes, which successfully captured neural signals from brain tissue. Zips et al. [196] developed a 3D MEA with microneedle tips using a composite ink of PEDOT:PSS and MWCNTs, as shown in Fig. 8(d), which exhibited 323 $S \cdot m^{-1}$ conductivity. The MEAs, with 128 kΩ impedance at 1 kHz, successfully recorded cell signals and showed long-term stability under cell culture conditions. Lozano et al. [198] utilized polymer casting techniques and metal deposition to fabricate conductive polymer microneedle electrodes composed of biocompatible epoxy resin and carbon black, with a sputtered silver coating of 100 nm thickness, as shown in Fig. 8(e). The device exhibits impedance comparable to that of a wet electrode, obviating the need for skin preparation.

In summary, carbon materials demonstrate exceptional electrical conductivity and mechanical strength when employed as base materials for microneedle electrodes. At present, carbon fibers and carbon nanotubes are leading research efforts in this field. Instead of directly fabricating microneedles from carbon materials, alternatives such as carbon fiber fabrics or carbon nanotube films may provide more promising solutions.

3.5 Others

2D transition metal carbides and/or nitrides (MXene) is a class of two-dimensional inorganic compounds discovered in 2011, consisting of atomically thin layers of transition metal carbides, nitrides or carbonitrides [199]. Hydrogel-based sensors with MXene functional fillers were developed to detect both strain and temperature stimulations [200]. Moreover, thin film and electronic skin sensors for collecting bioelectrical signals have also emerged [201, 202]. However, there is still inadequate research using Mxene to prepare microneedle electrodes.

Yang et al. [203] fabricated microneedle electrodes by PLA casting into the PDMS mold as a substrate and coating MXene as a conductive layer. The MXene nanosheet-based microneedles are highly conductive, stable, and biocompatible. The wearable MXene nanosheet-based microneedles can sense the tiny electric potential difference generated from the human eye movements or muscle contraction from the human arm. In addition, the transcutaneous electrical nerve stimulation treatment can be applied according to the feedback of the micro-biosensors. Finally, they demonstrated a “hospital-on-a-chip” system comprising integrated microchip biosensors for an efficient diagnosis and medical treatment elements for therapies, enabling both biosensing and electrical stimulation capabilities.

4 Preparation methods of microneedle electrodes

4.1 Etching

Etching methods, such as wet etching and dry etching [204], are fundamental to fabricating microneedle electrodes, particularly those based on silicon. These techniques offer straightforward operation and have been instrumental in advancing microneedle electrode technology.

Wet etching involves immersing the substrate in a liquid chemical solution, where material removal occurs through chemical reactions [205], as shown in Fig. 9(a). This method is especially suited for isotropic etching, where material is uniformly removed in all directions. Its simplicity, cost-effectiveness, and ability to achieve high selectivity and precision make wet etching a well-established fabrication technique. In contrast, dry etching, widely used in microdevice fabrication [206], removes material using plasma or reactive gases. Dry etching offers several advantages over wet etching, such as faster etching rates, anisotropic profiles, and the ability to process various materials [207]. Reactive ion etching (RIE) and deep reactive ion etching (DRIE) are the primary dry etching techniques used for microneedle electrode fabrication [208]. RIE employs low-pressure plasma for selective etching, while DRIE enables the formation of deep, high-aspect-ratio features. Ji et al. [209] employed RIE technology utilizing an inductively coupled plasma etch tool, using SF_6/O_2 gas, to successfully fabricate the pyramidal needle structure, as shown in Fig. 9(b). Li et al. [210] employed a modified (DRIE) process to achieve anisotropic etching of circular holes with diameters as small as 30 μm, reaching depths exceeding 300 μm through enhanced ion bombardment, as shown in Fig. 9(c). Subsequently, isotropic wet and/or dry etching techniques were employed to refine the needle structure by accelerating etching at the apex of the pillar. This resulted in the attainment of tip radii as small as 5 μm, ensuring sharp and precise needle tips. Additionally, the compatibility of dry etching with various materials, such as silicon, polymers, and metals, makes it a versatile and widely adopted method in microfabrication [211]. Both wet etching and dry etching have been extensively utilized in the preparation of microneedle electrodes, enabling the easy and controlled fabrication of microneedle structures. Furthermore, these techniques have greatly contributed to advancements in various fields, including biomedical sensing, drug delivery, and microfluidics [212].

4.2 Lithography

Lithography technology is a rising star in the preparation of microneedle structures. Although lithography technology developed late in the preparation of microneedle structures, it has already shined in other fields. Lithography uses a master template, which may be called a mask, to create a pattern or image on a substrate, encompassing X-ray lithography [213], magnetorheological drawing lithography (MRDL) [214] as well as drawing lithography [215]. Chen et al. [216] successfully fabricated the various specifications by employing distinct mask patterns and employing X-ray lithography to achieve precise hollow positions, as shown in Fig. 10(a). Drawing lithography is characterized by an elastic deformation of polymer materials in the glassy transition, and the 3D microneedle structures were fabricated from viscous polymers by extensional deformation. Lee et al. [217] discussed an integrated lithography model based on the fundamental principles of additive manufacturing, as shown in Fig. 10(b). The properties in glass transition of a polymer, the phenomena and theories of extensional deformation and capillary self-thinning caused by drawing. The continuous drawing technique, stepwise controlled drawing technique and drawing technique with antidromic

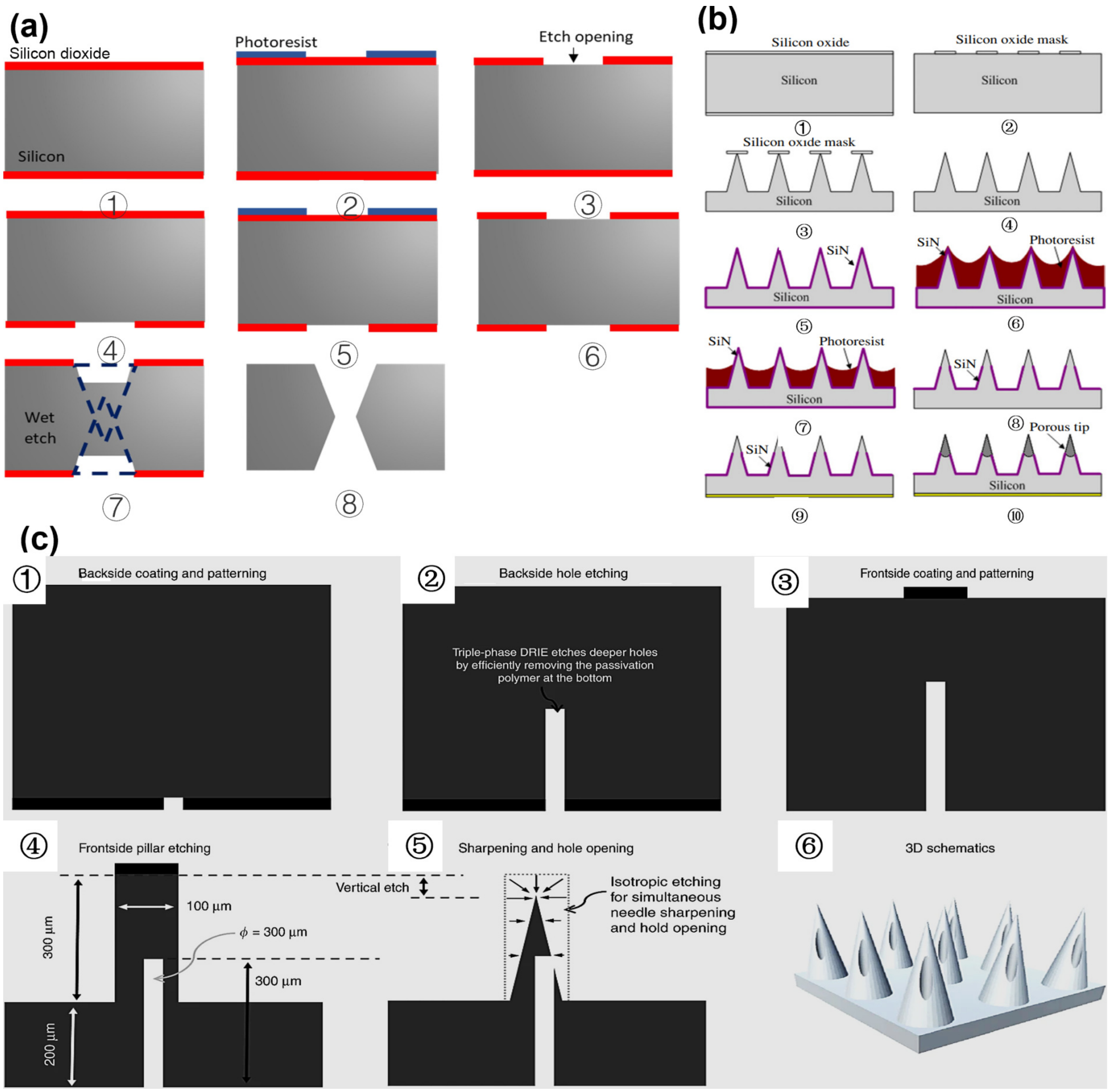

Figure 9 Schematic illustrations of the preparation of microneedle electrodes by etching. (a) A simple single wet etch step. Reproduced with permission from Ref. [205], © Published by Elsevier B.V. 2021. (b) RIE for microneedle electrode fabrication. Reproduced with permission from Ref. [209], © IOP Publishing Ltd 2006. (c) DRIE for microneedle electrode fabrication. Reproduced with permission from Ref. [210], © Li, Y. et al. 2019.

isolation that can be flexibly applied to the variable polymers to design an ultrahigh-aspect ratio hollow microneedle, dissolving microneedle and the hybrid electro-microneedle. Chen et al. [214] proposed a novel MRDL method to fabricate microneedle arrays, as shown in Fig. 10(c). In this technology, droplets of CMRF are drawn directly from virtually any substrate to create 3D microneedles under an external magnetic field. This method not only inherits the advantages of the thermal drawing method, eliminating the need for masks and light irradiation, but also does not require adjustment of the drawing temperature. The MRDL method is extremely simple and can even produce bionic microneedles with complex, multi-scale structures.

4.3 Micro-molding

The utilization of molds for microneedle fabrication offers several significant advantages, including ease of operation, low cost, and the ability to achieve mass production. Baek et al. [218] employed a fabrication method wherein PLA was poured into laser-machined polytetrafluoroethylene molds to create microneedles, as shown in Fig. 11(a). This approach is suitable for mass production and enables the simultaneous production of multiple microneedle sensors. Anbazhagan et al. [219] utilized a CO_2 laser and polymer molding technique to fabricate a 10 × 10 microneedle array structure with a specific design. The developed master mold is efficient to replicate several PDMS microneedle patches, as shown in Fig. 11(b). The proposed combined method of laser processing and molding mechanism is simple and low-cost for rapid prototyping of microneedle array.

4.4 Hot embossing and injection molding

Hot embossing and injection molding are common methods for creating microstructures using molds. These techniques are ideal

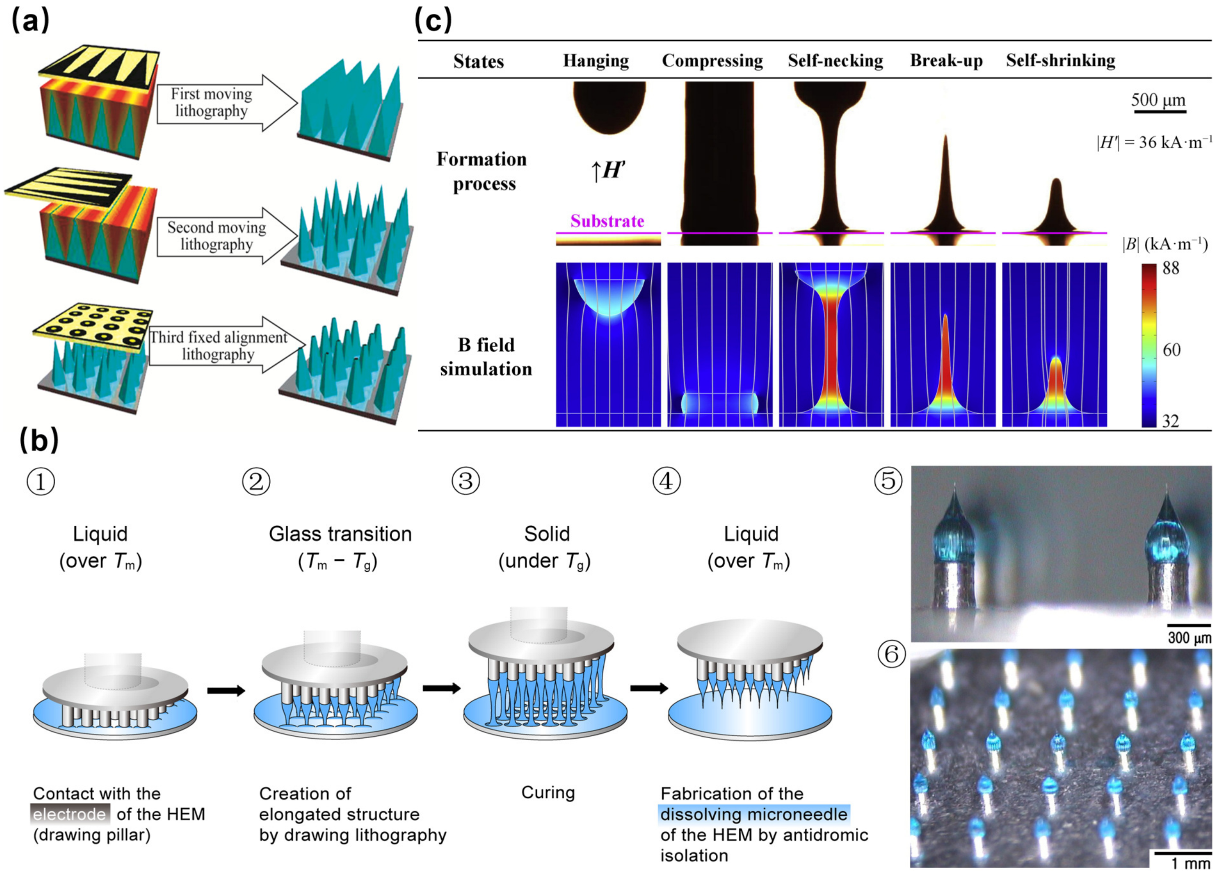

Figure 10 Schematic illustrations of the preparation of microneedle electrodes by lithography. (a) X-ray lithography. Reproduced with permission from Ref. [216], © *Optics and Precision Engineering* Editorial Office 2018. (b) Drawing lithography. Reproduced with permission from Ref. [217], © Elsevier Ltd. All rights reserved 2012. (c) Magnetorheological drawing lithography. Reproduced with permission from Ref. [214], ©Acta Materialia Inc. Published by Elsevier Ltd. All rights reserved 2017.

for mass production due to their controllable cost and simplicity. A typical process of injection molding technique and the hot embossing technique was presented [220], as shown in Fig. 12(a). Abubaker et al. [221] used a series of experiments to investigate the effects of embossing temperature, pressure, and time on microneedles. Li et al. [222] proposed a modified hot embossing approach to fabricate the gradient porous microneedle array from poly(lactic-co-glycolic acid) powders within a cavity array mold under the coupling combination of gradient thermal and pressure multi-fields, as shown in Fig. 12(b). Kang et al. [223] used mold-flow simulation software to analyze the filling process of PLA eye-sticking microneedles during microinjection molding. This study explored the effects of different injection speeds on filling time, shear rate, shrinkage, and warpage of the microneedle patch. Furthermore, the filling process, temperature field, and velocity field changes of a single microneedle were also examined. Gulcur et al. [224] proposed laser machining as a cost-effective method for making microneedle molds and micro-injection molding of thermoplastic microneedle arrays as a highly-suitable manufacturing technique for large-scale production with low marginal cost, as shown in Fig. 12(c). Evens et al. [225] present a novel method to produce polymer microneedles using laser ablated molds in an injection molding process, and successfully created cone-shaped micro holes with low tip radii in a tool steel mold, using a femtosecond laser with a cross-hatching strategy, as shown in Fig. 12(d). Finally, the attained mold was used in an injection molding process to replicate polypropylene microneedles.

4.5 3D printing

Three-dimensional (3D) printing is a versatile manufacturing technique ideal for creating personalized and intricate structures [226]. It is increasingly used to fabricate microneedle arrays [227]. Common 3D printing methods for microneedle fabrication include stereolithography (SLA), two-photon polymerization (TPP), digital light processing (DLP), continuous liquid interface production (CLIP), and fused deposition modeling (FDM) [228]. SLA, the oldest still-in-use 3D printing technology, differs from DLP by using a laser beam to cure the polymer. In SLA, an ultraviolet (UV) laser is directed through two galvanometers to the correct X and Y coordinates, tracing out the model's cross-section [229]. As the laser moves across the print area, it continuously hardens the photopolymer. The resolution of SLA depends on the laser beam diameter. With a resolution of several tens of micrometers, it is suitable for microneedle fabrication. Jeong et al. [229] developed a novel method using 3D printing to control needle bevel angles. By adjusting the printing direction, the needle bevel angles were modified, as shown in Fig. 13(a). TPP is a method within the SLA-based laser technology family. Since it induces polymer polymerization through two-photon absorption, it offers greater precision than conventional SLA technology, which relies on a single focal point. This enables the production of microneedles with nanometer-level accuracy. McKee et al. [230] successfully fabricated pentaerythritol triacrylate microneedle arrays using TPP 3D printing technology, as shown in Fig. 13(b). Finite element simulations were then performed to investigate the interaction

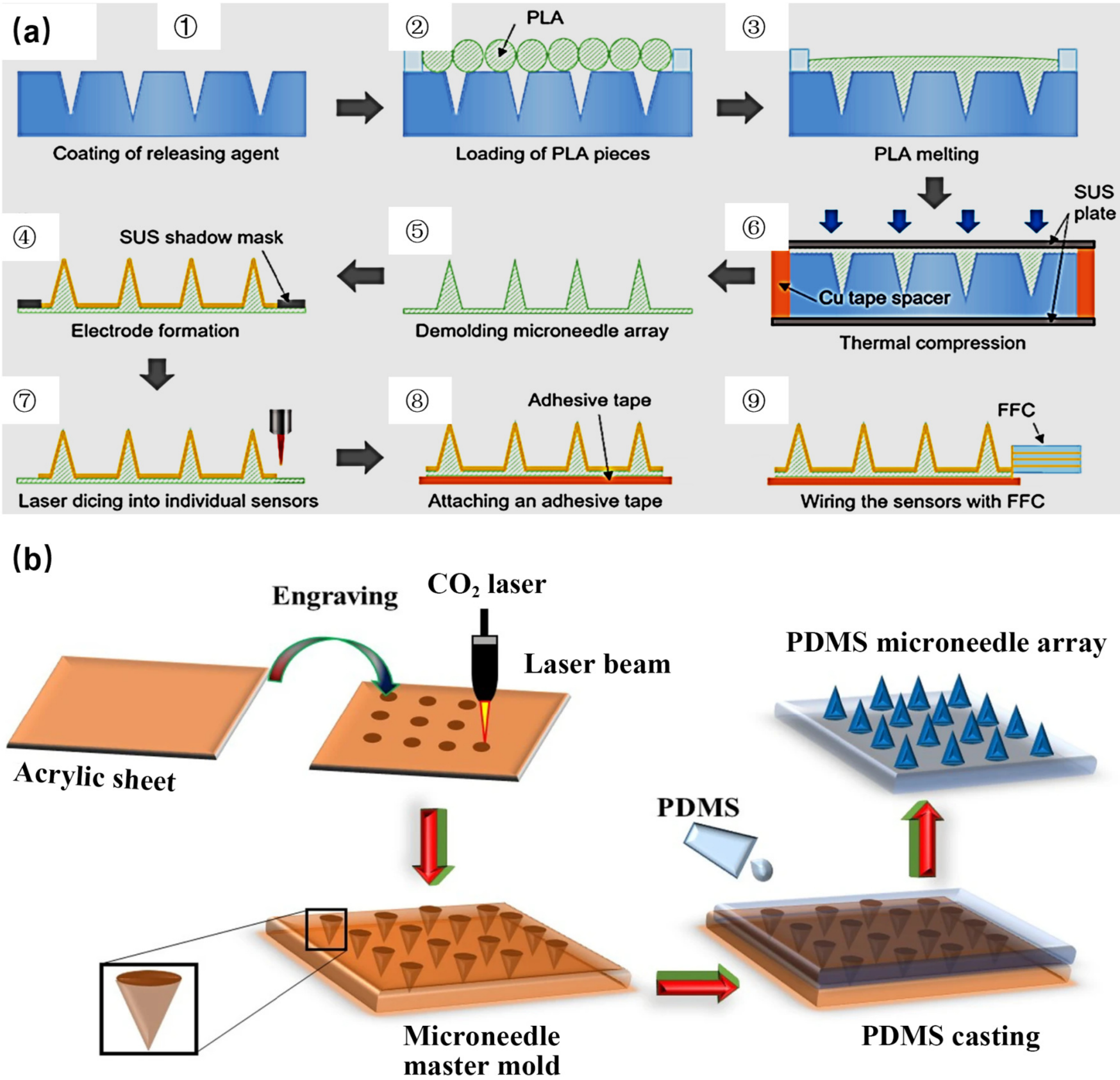

Figure 11 Schematic illustrations of the preparation of microneedle electrodes by micro-mold. (a) Laser processed mold. Reproduced with permission from Ref. [218], © Baek, J. Y. et al. Licensee MDPI, Basel, Switzerland 2023. (b) 3D printed mold, CO_2 laser processed mold. Reproduced with permission from Ref. [219], © Controlled Release Society 2023.

between a single microneedle and human skin. Rad et al. [231] reported the fabrication of highly detailed microneedles using the two-photon direct laser writing process. They also discussed optimization strategies and parameter selection for microprinting tall microneedles with side channels and other complex designs. Furthermore, this manufacturing process is currently best suited for printing master microneedles. DLP 3D printing is similar to SLA in that both use light to manufacture objects, but the irradiation method differs [232], as shown in Fig. 13(c). Unlike SLA, which induces localized photopolymerization by focusing a laser beam on specific areas, DLP technology projects an entire image of the layer onto the resin at once using a high-definition projector. Compared to SLA, the DLP method significantly shortens printing time. CLIP printing is an advanced technique derived from the DLP method. The CLIP 3D printing process further enhances output speed while continuously creating smooth surfaces [233]. Lipkowitz et al. [234] introduced a previously unexplored ultraviolet-based photopolymerization three-dimensional printing process, as shown in Fig. 13(d). This method can accelerate printing speeds by 5 to 10 times compared to current approaches such as CLIP. The FDM printing method, which creates 3D objects through extrusion, has a disadvantage in that its resolution is significantly lower than that of photopolymerization-based printing methods. Due to the current limitations of FDM printer resolution, conventional micron-scale microneedle structures cannot be fabricated without a post-processing step. Wu et al. [235] employed additive manufacturing to produce microneedles with preprogrammed structures, as shown in Fig. 13(e). Inclined microneedles were successfully fabricated using FDM 3D printing followed by chemical etching. Khosraviboroujeni et al. [236] reported the preparation of a reservoir-based biodegradable polymeric microneedle array containing estradiol valerate. These microneedles were fabricated using PLA through a combination of FDM 3D printing and injection volume filling techniques.

4.6 Thermal drawing

Thermal drawing is a versatile and rapid prototyping method capable of forming microneedle structures with ultra-high aspect ratios without requiring complex or expensive processes. However, factors such as temperature, viscosity, and drawing speed affect the

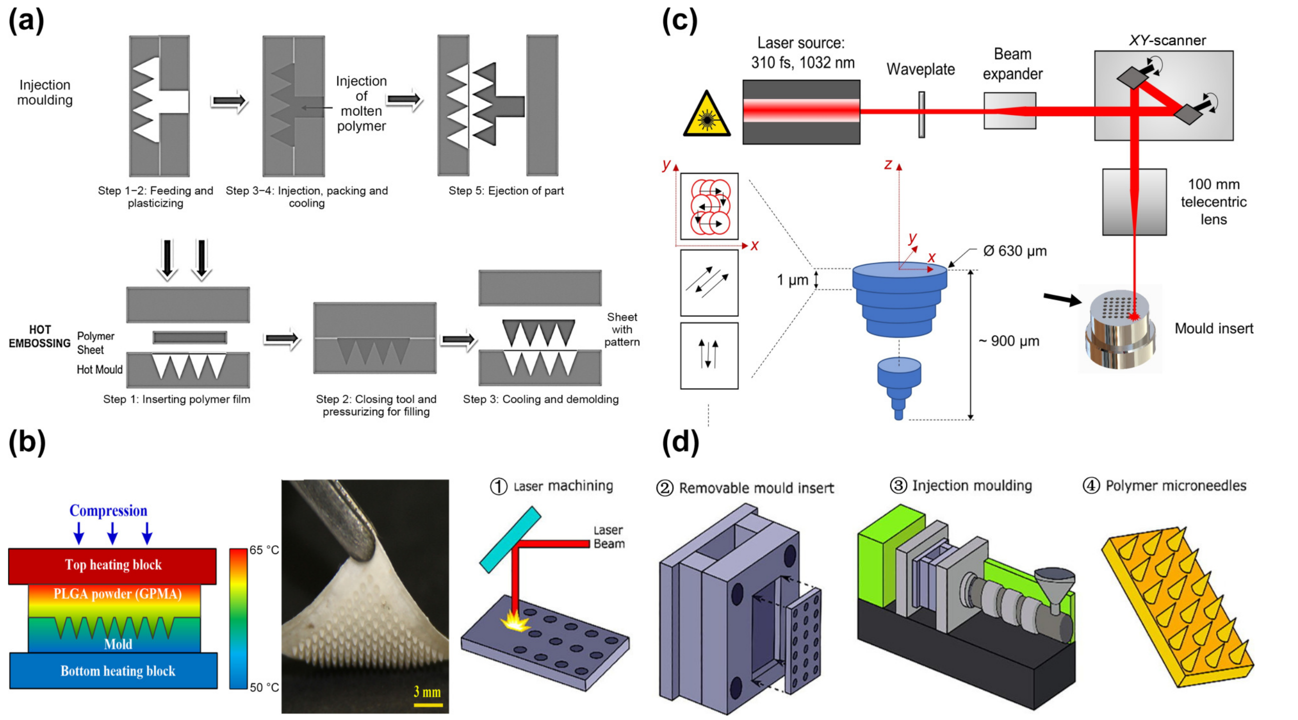

Figure 12 Schematic illustrations of the preparation of microneedle electrodes by hot embossing and injection molding. (a) Hot embossing and injection molding. Reproduced with permission from Ref. [220], © Society of Plastics Engineers 2019. (b)Hot embossing. Reproduced with permission from Ref. [222], © Elsevier B.V. All rights reserved 2019. (c) Micro-injection moulding. Reproduced with permission from Ref. [224], © CIRP 2021. (d) Injection molding. Reproduced with permission from Ref. [225], © Society of Manufacturing Engineers (SME). Published by Elsevier Ltd. All rights reserved 2020.

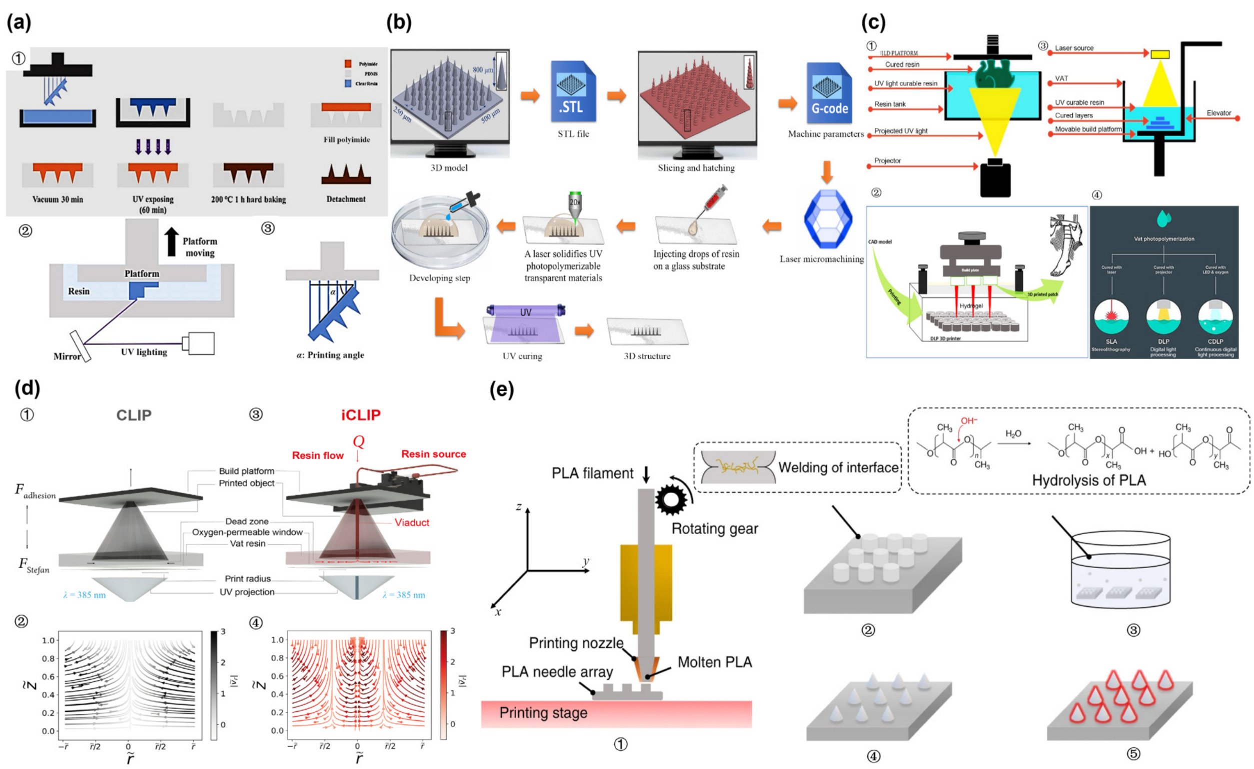

Figure 13 Schematic illustrations of the preparation of microneedle electrodes by 3D printing. (a) The schematic diagram of SLA 3D printed microneedle. Reproduced with permission from Ref. [229], © Jeong, J. et al. 2023. (b) Fabrication steps performed to produce microneedle arrays using the TPP method. Reproduced with permission from Ref. [230], © Elsevier B.V. All rights reserved 2022. (c) Photopolymerization technology comparison of DLP and SLA technology. Reproduced with permission from Ref. [232], © Tsegay, F. et al. Licensee MDPI, Basel, Switzerland 2022. (d) Traditional CLIP process vs. ultraviolet-based photopolymerization three-dimensional printing process. Reproduced with permission from Ref. [234], © Lipkowitz, G. et al. some rights reserved; exclusive licensee American Association for the Advancement of Science 2022. (e) A PLA needle arrays with predesigned structures printed by FDM. Reproduced with permission from Ref. [235], © Wu, L. et al. 2021.

controllability and repeatability of the fabricated microneedles, leading to inconsistencies. Choi et al. [237] introduced spatially discrete thermal drawing as a novel method for the fabrication of biodegradable microneedles with ultra-sharp tip ends, as shown in Fig. 14(a). Lee et al. [238] utilized thermal drawing to fabricate master molds with high aspect ratios and replicate the shape by micro-molding, as shown in Fig. 14(b). Lee et al. [239] proposed a three-step thermal drawing for rapid, prototyping microneedles that can have a variety of shapes and can be fabricated on curved surfaces, as shown in Fig. 14(c).

Selecting different fabrication techniques based on the material type is the most effective approach for successfully preparing microneedle electrodes. For example, the etching method is suitable for silicon-based materials. While this technique is simple and fast, it poses challenges such as environmental contamination and relatively low precision. The lithography method is ideal for materials with photoresist properties, offering high speed and precision; however, its applicability is limited. The micro-molding technique, which requires a mold, is well-suited for raw materials that can form pastes, such as metal and carbon-based particles, soluble polymers, and their composites. Hot embossing and injection molding are commonly used for materials that undergo phase transitions upon heating or cooling. 3D printing requires raw materials to be processed into specialized pastes, which are then shaped and solidified through printing. Due to the strict requirements for paste formulation, only a limited number of materials currently meet the criteria for microneedle fabrication. The thermal drawing technique demands materials with suitable flow properties when heated and rapid solidification upon cooling. Among these mainstream fabrication methods, polymers have emerged as the dominant materials for microneedle electrode preparation. Their ease of shaping, tunable conductivity, and flexibility make them a research hotspot in the field.

5 Methods for benchmarking and evaluating bioelectrical signal measurements with microneedle electrodes

This review mainly evaluates the ability of microneedle electrodes to measure bioelectrical signals from three aspects, including electrochemical properties, mechanical properties and biocompatibility. Among them, the electrochemical properties mainly include electrode-skin impedance and SNR; the mechanical properties include flexibility, rigidity and stability; and good biocompatibility properties ensure the effectiveness of bioelectrical signals and avoid immune reactions.

5.1 Electrode-skin interface impedance

Biopotential electrodes are transducers that convert ionic currents within the human body into electronic currents in the electrode. EII is utilized as a metric or indicator to assess the effectiveness of charge transfer. The EII is a crucial parameter in the assessment of electrodes utilized for the measurement of bioelectrical signals. A reduced EII is beneficial in facilitating the acquisition of bioelectrical signals with superior quality and intensity [240]. Compared with other electrodes for measuring bioelectrical signals, microneedle electrodes can penetrate the stratum corneum, thereby reducing EII and further improving signal quality and intensity. Currently, there are two primary techniques utilized in the measurement of EII. The first is the two-electrode system, whereby the inductance-capacitance-resistance meter (LCR) is commonly employed as the measuring tool [93, 241]. The second method is the three-electrode system, which typically utilizes the electrochemical workstation [242, 243] or potentiostat [244–246] to determine EII.

The commonly used method for measuring EII in current literature is by employing a two-electrode system with an LCR meter. The LCR meter is designed specifically for high-precision measurements of inductance, capacitance, and impedance [247]. In accordance with the equivalent circuit diagram of the electrode-skin interface, there exist resistance and capacitance effects between the skin and the electrode. Impedance testing generally involves applying a sinusoidal alternating current (AC) wave, so there may be inductive effects during the testing process. In conclusion, measuring EII using an LCR meter is a reliable method. Nevertheless, LCR meters are designed to operate within a certain frequency range, which may not cover the full range of frequencies relevant to EII measurements. This can lead to inaccurate measurements or inconsistencies in the data obtained. Ren et al.

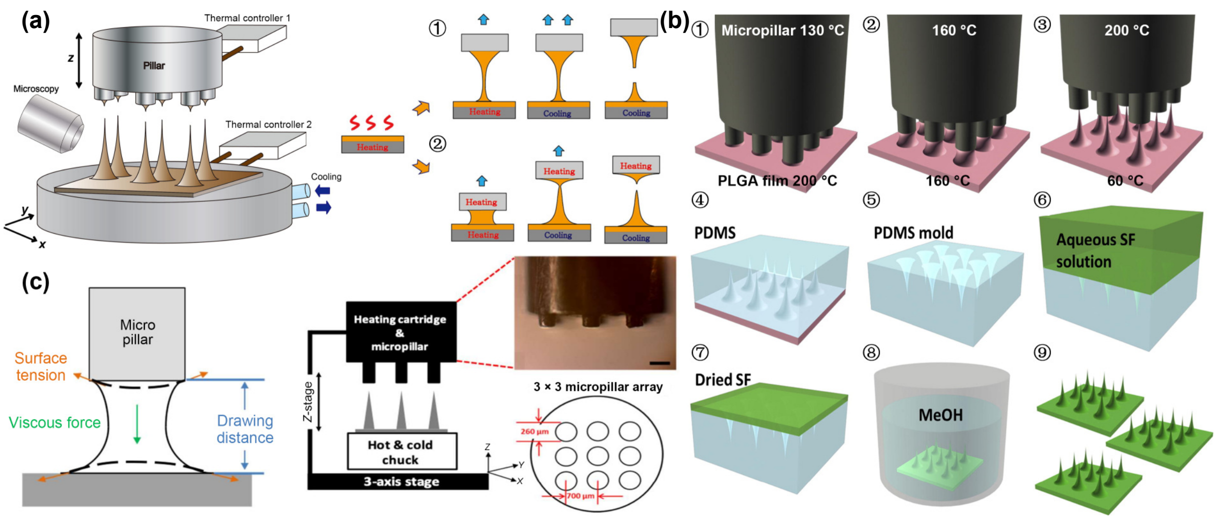

Figure 14 Schematic illustrations of the preparation of microneedle electrodes by thermal drawing. (a) Spatially discrete thermal drawing system. Reproduced with permission from Ref. [237], © Elsevier B.V. All rights reserved 2012. (b) Thermally-drawn micromolds. Reproduced with permission from Ref. [238], © Elsevier B.V. All rights reserved 2015. (c) Three-step thermal drawing. Reproduced with permission from Ref. [239], © Lee, K. et al. Licensee MDPI, Basel, Switzerland 2019.

[113] successfully demonstrated that EII changes with applied pressure using a two-electrode system, as shown in Fig. 15(a). When the compression force on the MAE is larger than 1 N, EII of the MAE reaches a steady state, and its value is about 85 kΩ. Hou et al. [164] measured EII using a two-electrode technique, whereby an Ag/AgCl wet electrode served as the reference electrode, as shown in Fig. 15(b). Two electrodes were placed on the forearm and connected to an LCR meter. At a frequency of 10 Hz, the EII of the Ag/AgCl wet electrode was measured to be approximately 650 KΩ, while the self-made microelectrode had an EII of approximately 240 kΩ.

In a three-electrode system, electrochemical workstations and potentiostats are commonly used to measure EII. While these two devices share many similarities in measuring EII, the electrochemical workstation offers more comprehensive functionalities. Furthermore, the electrochemical workstation provides high-level precision and accuracy required for EII measurement. Moreover, it can measure skin electrode interface impedance in real-time. However, the electrochemical workstation's impedance data stability is poorer in the low-frequency region, and environmental influences are more apparent during testing. In comparison to the two-electrode system, the three-electrode system can accurately control the potential difference applied to the sample. The reference electrode is used to establish a reference potential, which can measure the potential difference between the working and counter electrodes, thereby ensuring measurement accuracy and reproducibility. Zhang et al. [248] measured skin-contact impedance with an electrochemical workstation, the self-made electrodes was placed on the skin of the back of the hand, and the Ag/AgCl wet electrodes were fixed on the skin of both sides of the hand, as shown in Fig. 15(c). The average EII values for the self-made electrode and Ag/AgCl wet electrode were measured to be 5 kΩ, respectively. Yang et al. [242] used a three-electrode system with a CHI760E electrochemical workstation to measure EII, as shown in Fig. 15(d). During the measurement, three electrodes were placed on the forearm. At a frequency of 10 Hz, the EII of the Ag/AgCl wet electrode was recorded at approximately 35 kΩ, while that of the semi-dry electrode and dry electrode were recorded at approximately 15 and 65 kΩ, respectively. Roberts et al. [249] utilized a potentiostat with a three-electrode configuration to measure EII on the forearm, as shown in Fig. 15(e). At a frequency of 10 Hz, the surface-normalized impedance of the Ag/AgCl wet electrode was approximately 15 kΩ, whereas the self-made electrode was approximately 12 kΩ.

5.2 Signal quality

The SNR is defined as the ratio of signal power to noise power, often expressed in decibels, and can be calculated using the following equation to assess the quality of the signal obtained from both electrodes [250] (Eqs. (1) and (2)):

$$\mathrm{SNR_{dB}} = 20 \times \log \frac{Y(\mathrm{f1})}{Y(\mathrm{f2})} \tag{1}$$

$$Y(\mathrm{f1}) = \frac{\mathrm{Amplitude}\,(\mu\mathrm{V})}{\sqrt{f}(\mathrm{Hz})} \tag{2}$$

where SNR is in decibels; $Y(\mathrm{f}_1)$ is the amplitude spectrum calculated using the fast Fourier transform, and Y(f1) and $Y(\mathrm{f}_2)$ represent the signal and noise correlation functions, respectively [248]. SNR is critical because signals are small and measurements are susceptible

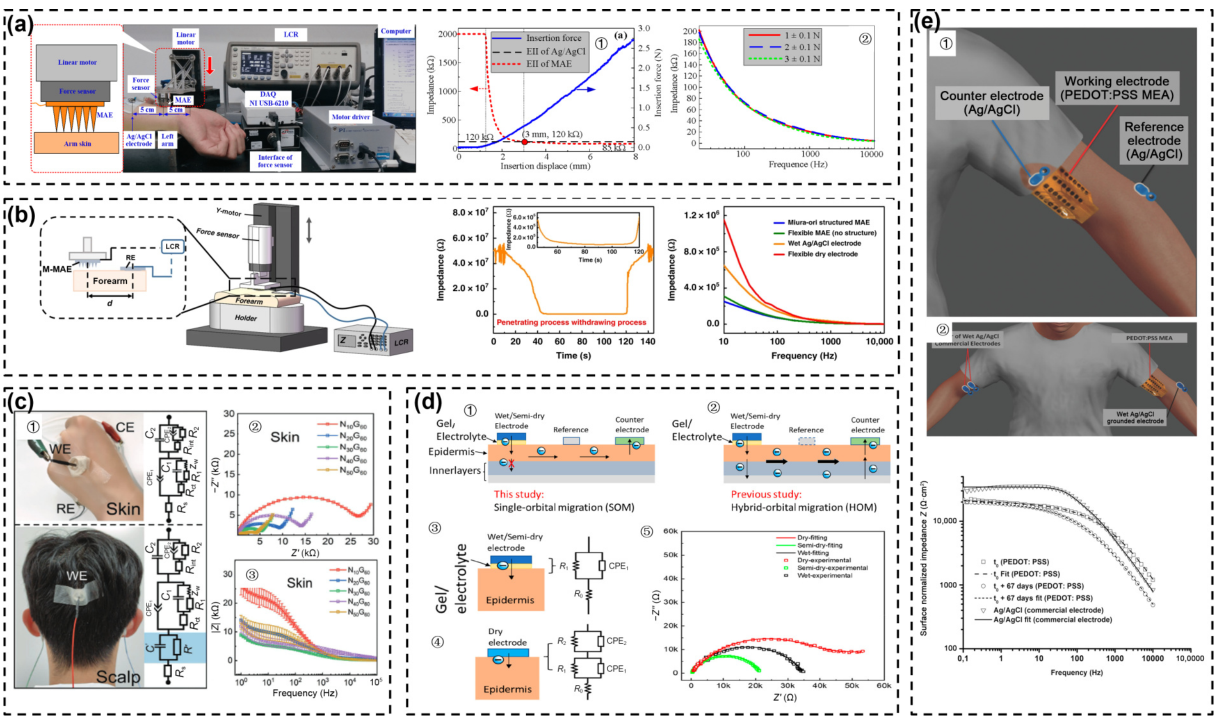

Figure 15 Two-electrode system test EII: (a) setup for EII recording during the insertion process. Reproduced with permission from Ref. [113], © Ren, L. et al. Licensee MDPI, Basel, Switzerland 2016. (b) Schematic drawing of the EII test setup. Reproduced with permission from Ref. [164], © Hou, Y. et al. 2021. Three-electrode system test EII: (c) photograph of electrode positions for measuring skin-contact resistance on hand. Reproduced with permission from Ref. [248], © Wiley-VCH GmbH 2023. (d) The position of the electrodes during the test. Reproduced with permission from Ref. [242], © Yang, L. et al. Published by American Chemical Society 2022. (e) Electrochemical impedance spectroscopy: setup and comparison study. Reproduced with permission from Ref. [249], © WILEY-VCH Verlag GmbH & Co. KGaA, Weinheim 2016.

Tsinghua University Press | SciOpen

to environmental noise, baseline drift, and contamination from other electrophysiological signals [251]. SNR also determines the maximum amount of data that can be transmitted reliably over a given channel, which depends on its bandwidth and SNR. This relationship is described by the Shannon–Hartley theorem, a fundamental law of information theory [252].

Due to its ability to penetrate the stratum corneum during measurements, the microneedle electrode eliminates EII and reduces noise levels caused by environmental factors and dead cells (in the stratum corneum), effectively filtering unwanted noise. As a result, the strength of bioelectrical signals is enhanced, leading to an improvement in the SNR. Singh et al. [253] fabricated flexible microneedle electrodes by employing epoxy resin and thermoplastic PU as the base materials, complemented by a surface coating of titanium and platinum. The SNR values were then quantified for both the microneedle electrode and the wet electrode, yielding respective values of 23.1 and 24.0 dB. These results contribute to the comprehensive characterization of the microneedle electrode and enable a comparative assessment with the Ag/AgCl wet electrode.

5.3 Mechanical properties

The paramount advantage of microneedle electrodes lies in their capability to penetrate the stratum corneum, whereby the mechanical strength assumes a pivotal role. Microneedles are characterized by their diminutive size, typically ranging from tens to hundreds of microns in length. To facilitate smooth stratum corneum penetration, it is imperative to achieve an optimal balance between rigidity and flexibility. Sufficient rigidity ensures effective penetration of the skin, while a certain level of flexibility accommodates the skin's expansion and contraction. Inadequate rigidity would cause premature bending of the microneedles before penetrating the skin, while insufficient flexibility could lead to motion artifacts, signal instability.

Typically, silicon-based microneedles exhibit sufficient rigidity to penetrate the skin; however, their brittleness renders them prone to fracture when subjected to skin stretching. Conversely, polymer-based microneedle electrodes generally lack the necessary rigidity, causing them to bend before piercing the stratum corneum. To address the issue of inadequate rigidity, researchers have proposed various solutions. A common approach involves the deposition of a film, such as gold [254, 255], silver [256], titanium [113], platinum [257], MXene [203], onto the microneedle surface. Alternatively, polymer-based microneedles can be fabricated using composite materials, wherein the incorporation of particles with rigidity-enhancing properties, such as graphene [258], carbon nanotubes [259], metal particles, can effectively mitigate the flexibility-related challenges. Biocompatible metals like gold, silver, and titanium exhibit desirable properties for microneedle applications, including adequate rigidity for skin penetration and enhanced durability within the skin compared to silicon. Their inherent strength ensures prolonged retention without the risk of fracture commonly observed with silicon microneedles. However, the fabrication of microneedles from these metals presents challenges due to their high cost and difficulties in shaping. Furthermore, their limited ability to conform to skin contractions impairs SNR and may result in motion artifacts during use. These considerations highlight the need for alternative approaches that strike a balance between biocompatibility, mechanical properties, and cost-effectiveness to optimize the performance of microneedle electrodes. The advent of conductive polymers signifies a promising advancement in the realm of microneedle electrodes. Polymers with inherent conductivity, including PANI, PPy, PT, among others, offer a solution to the limitations associated with mechanical properties. By incorporating additional materials, the mechanical deficiencies of these polymers can be easily addressed. The versatile nature of these polymers allows for their formulation as solutions or slurries, facilitating their utilization as templates for microneedle fabrication. Moreover, the exceptional flexibility of these conductive polymers enables the development of flexible microneedle patches, effectively circumventing the inherent rigidity and brittleness of metal and silicon microneedles. Consequently, conductive polymers present a viable and promising avenue to surmount the challenges associated with hard, brittle structures and insufficient stretchability in the field of microneedle technology. However, long-term stability within physiological environments remains a key challenge for conductive polymers. Degradation or structural changes over time can impact its electrical conductivity and mechanical properties, prompting the need for further investigation to enhance its durability and long-term performance.

5.4 Biocompatibility

Given the direct contact of the microneedle component with living cells, it is imperative that the matrix material employed in microneedle electrode fabrication exhibits excellent biocompatibility. The intimate interface between the microneedle and the skin necessitates meticulous consideration. Optimal selection of biocompatible materials plays a vital role in ensuring consistent signal acquisition and accommodating long-term measurements. The utilization of biocompatible materials is therefore crucial for maintaining stable signals and facilitating close contact of microneedle electrodes with the skin. Silicon is generally considered to be biocompatible, meaning it is well-tolerated by biological systems and does not cause significant adverse reactions or toxicity [260, 261]. Nevertheless, the inherent brittleness of silicon necessitates careful consideration, as it introduces the possibility of debris migrating to neighboring tissues or organs in specific scenarios. This migration carries the potential to elicit inflammatory responses and induce localized tissue damage [62]. Therefore, understanding and mitigating the challenges associated with silicon's brittleness are vital for enhancing the biocompatibility and long-term performance of silicon-based microneedles. Certain metals, including titanium, stainless steel, gold, platinum, and others, exhibit enhanced biocompatibility characteristics [262]. However, when these metals come into contact with human body fluids, varying degrees of corrosion can transpire, particularly during long-term exposure. This corrosion can result in the release and accumulation of metal ions. Additionally, the presence of an implant can serve as a potential substrate for bacterial colonization and biofilm formation [263]. These factors must be carefully considered to ensure the long-term stability and biocompatibility of metal electrodes within the biological environment. In comparison to metal and silicon-based materials, polymer materials offer a wider range of biocompatible options. Notable examples include polyethylene glycol [264], PLGA [265], PU [266], PVA [267], polyethylene oxide [268], PDMS [269], and PEDOT:PSS [270]. PVA is widely used in the production of contact lenses [271], while PLGA is commonly employed in drug delivery systems and tissue engineering [272]. PDMS, on the other hand, is extensively utilized in implants, prosthetics, and medical tubing [273]. Although

PEDOT:PSS is still under active research, promising findings suggest its general biocompatibility with various cell types, including neuronal cells, muscle cells, and stem cells [274]. PEDOT:PSS exhibits excellent compatibility with biological tissues, conforming seamlessly to tissue surfaces and minimizing the risk of tissue damage or irritation [275]. This characteristic is particularly advantageous in applications such as neural interfaces and bioelectronic devices [276]. Furthermore, PEDOT:PSS demonstrates compatibility with biological fluids and shows resistance to protein adsorption.

6 Advantages and challenges

6.1 Advantages of microneedle electrodes

In contrast to conventional Ag/AgCl wet electrodes, microneedle electrodes offer distinct advantages by eliminating the need for prior skin preparation and conductive gel application. This feature facilitates convenient, rapid, and long-lasting biological signal detection, substantially enhancing the practicality of microneedle electrodes. Although surface electrodes and capacitive electrodes—both classified as dry electrodes—can also sustain long-term measurements without conductive gel, they only collect bioelectrical signals from the body's surface. This leads to the susceptibility of weak bioelectrical signals to environmental interference, resulting in significant signal attenuation and reduced accuracy. In stark contrast, implanted electrodes make direct contact with living cells, rendering them the most precise instruments for bioelectrical signal measurement, even capable of capturing single-neuron discharge signals. Nonetheless, the implantation procedure demands meticulous surgery, is constrained by using time and cost considerations, and presents substantial portability challenges. In summary, microneedle electrodes occupy an intermediate position between dry electrodes and implanted electrodes, offering an array of unique advantages. They have more measurement precision than other dry electrode, enabling the utilization of bioelectrical signals in diverse scenarios, including medical applications, entertainment, and military contexts. Furthermore, microneedle electrodes eliminate the need for intricate surgical implantation, rendering them more user-friendly and practical.

6.2 Challenges of microneedle electrodes

Currently, the development of microneedle electrodes faces two major challenges: First, the absence of an ideal material or structure for microneedle electrode fabrication, and second, the lack of established standards for assessing the performance of microneedle electrodes. The mainstream materials used to fabricate microneedle electrodes include silicon, metals, carbon, and polymers. However, these materials cannot simultaneously meet the conductivity, biocompatibility, and mechanical properties required by microneedle electrodes. For instance, silicon-based materials lack sufficient conductivity and flexibility. Researchers have resorted to coating the surface of silicon microneedles with gold, silver, or titanium layers to enhance their conductivity. To improve the flexibility of silicon-based microneedle electrodes, researchers have integrated silicon microneedles with flexible polymer substrates. While these methods address the issues of poor conductivity and flexibility in silicon-based microneedle electrodes, they also introduce new challenges. Given the substantial disparities between the materials used in the substrate or coating and microneedle, which increases the number of interfaces for charge transport and leads to structural instability. For example, the combination of a flexible substrate and silicon or metal microneedles will cause the interface increased during the bioelectrical signal transmission, thus weakening the signals. The interface between the surface coating and the microneedles is also unstable and easy to fall off. For polymers, insufficient conductivity and rigidity represent their foremost challenges. Although the use of metal coatings and conductive fillers can effectively improve the problems of poor conductivity and insufficient rigidity of polymers, at the same time, when polymer microneedle electrodes transmit bioelectrical signals, their complex interfaces often weaken or distort the signals. Fortunately, conductive polymer coatings have been shown to enhance the electrochemical performance of microneedle electrodes. Compared with other electrode materials, conductive polymers have an integrated structure and are sufficiently flexible. However, conductive polymers are not rigid enough when penetrating the skin and become soft when exposed to sweat [203]. In the future, developing conductive polymers that are both flexible and appropriately rigid will be the key to their application in microneedle electrodes. Judging from current research progress, carbon materials (such as carbon nanotubes, carbon fibers and graphene, etc.) are not effective in preparing microneedle electrodes alone. However, carbon materials have high electrical conductivity, high mechanical strength and good biocompatibility, making them more suitable as fillers or coatings for composite materials. And existing research has proven that carbon materials can be well combined with polymers and improve their mechanical and electrochemical properties. In the future, carbon materials should have greater room for development in the field of microneedle electrodes.

To assess the performance of microneedle electrodes, commonly employed tests encompass conductivity, electrode-skin impedance, rigidity, flexibility, and biocompatibility. Among these, electrode-skin impedance stands out as one of the most critical parameters for microneedle electrodes. Although, the measured data were compared with Ag/AgCl wet electrodes in a previously published paper, there is no standardized method for measuring the impedance of electrode-skin interface. There is neither a universal measuring instrument nor a gold standard for measuring position. The sensitivity of skin to factors such as temperature, humidity, pressure, and different skin pretreatment methods may vary across different measurement locations, which can affect the results of impedance test [277]. Therefore, even when comparing the data with that measured with an Ag/AgCl wet electrode, the data varies greatly between different papers, and there is no comparability, which is extremely detrimental to further research on microneedle electrodes. Finally, we overview the developments of silicon (Table 1), metal (Table 2), polymer (Table 3) and carbon (Table 4)-based microneedle electrodes in bioelectrical signal measuring by listing representative works in recent years.

7 Outlook

Based on prolonged measurements and precision requirements, wet electrodes no longer suffice for current demands. Non-invasive electrodes lack adequate precision, while the implantation process of invasive electrodes is complex, leading to heightened risks of infection post-implantation, necessitating further research.

Table 1 Summary of silicon-based microneedle electrodes for measuring bioelectrical signals

Materials/coating	Preparation	Advantages	Disadvantages	Instrument	Impedance	Ref.
Si/Au	Etching	Biocompatibility, low impedance	Fragile, limited lifespan	CHI660C, 0.9% NaCl	100 Hz, ~ 5.2×10^{-2} kΩ	[278]
Si/Ag/AgCl	Etching	Easily penetrates the skin	Short lifespan	—	—	[131]
Si/Ti&Ag	Wet etching	Improved signal quality	Complex fabrication process	—	—	[129]
Si/Au	MEMS[a]	High signal quality	Complex fabrication process	LCR meter	10 Hz, 7 kΩ	[115]
p-Si/Ti&Ag	Etching	Enhanced adhesion, low impedance	Fabrication, complexity	—	—	[122]
Si/Cr&Au	DRIE	Enhanced conductivity, improved skin penetration	Fragile	LCR meter	10 Hz, 500 kΩ	[119]
n-Si/Ti&Au	DRIE	High signal quality	Fabrication complexity	—	20 Hz, ~ 150 kΩ	[133]
Si&parylene/Au	Wet etching	Flexible, long-lasting	Complex fabrication, high cost	HP4192A	10 Hz, 7.5 kΩ·cm^2	[134]
Si&PU/Ti&Au	DRIE	Biocompatible, stretchable	Fabrication complexity	Impedance; analyzer	10 Hz, ~ 750 kΩ	[135]
Si&PI/Au&Parylene	Etching	Wireless, flexible, biocompatible	High power consumption	—	10 Hz, ~ 30 kΩ	[136]
Si&silicone/Ti&Au	Wet etching	Skin-friendly, stretchable	Adhesion challenges, limited durability	LCR meter	100 Hz, 21 kΩ·cm^2	[137]
Si/Ti&Au	Etching	No skin preparation, durable	Low signal quality	LCR meter	100 Hz, ~ 20 kΩ	[130]
Si/Ti&Au&parylene	Wet etching	Long-term stability, biocompatibility	Higher skin–electrode impedance	CHI660D	10 Hz, 120 kΩ·cm^2	[132]

[a]MEMS: microelectromechanical systems.

Table 2 Summary of metal-based microneedle electrodes for measuring bioelectrical signals

Materials/Coating	Preparation	Advantages	Disadvantages	Instrument	Impedance	Ref.
Magnetic fluid/Ti&Au	Magnetization-induced self-assembly	Low-cost, scalable	Magnetization challenges	LCR meter	100 Hz, ~ 70 kΩ	[121]
Magnetorheological fluid&PI/Ti&Au	MRDL	Flexibility	Fabrication complexity	—	50 Hz, 104 kΩ	[150]
Magnetorheological fluid & PET/Ti&Au	Laser direct writing/magneto-rheological drawing lithography	High fidelity, low impedance	High cost	—	70 kΩ, 10 Hz	[145]
Stainless steel/Au&parylene	Etching	Biocompatible, durable	Fabrication complexity	EVAL-AD5940BIOZ	100 Hz,100 kΩ	[148]
Ferromagnetic fluid/Ti&Au	Magnetically induced self-assembly	High-quality signals	Poor skin penetration	—	20 Hz, 200 kΩ	[142]
Stainless steel/Au&parylene	Mechanical grinding	Low-cost, durable	Rigidity	CHI660E; 0.01M, PBS	100 Hz, ~ 70 kΩ	[143]
Bismuth–indium–tin; Alloys/Polyurethane acrylate	Micro-molding	Easy to form	Low strength	Palmsens4 impedance measurement systems, 0.9% NaCl	10 Hz, ~ 0.5 kΩ	[144]
Ag sheet	Direct writing with laser	Highly sensitive	Poor durability	CHI660E	10 Hz, ~ 500 kΩ	[146]
Stainless steel&PDMS	Photochemically milled	Excellent stretchability	Signal noise	Stanford Research SR785, conducting media bath	1 kHz, 7.6 kΩ	[147]
Stainless steel/Au&parylene	Etching	Suitable for small animals	High fragility	Impedance analyzer	10 Hz, 20 kΩ	[149]

Microneedle electrodes, with their minimally invasive nature, amalgamate the advantages of prolonged usage and precision. Furthermore, microneedle structures have been extensively researched in fields such as transdermal drug delivery, biosensors, vaccination techniques, and intrabody molecular detection. Existing studies indicate that microneedle electrodes perform comparably to, if not better than, traditional wet electrodes in measuring biological electrical signals such as ECG, EMG, and EEG. However, materials used for microneedle electrode fabrication still require further breakthroughs. Irrespective of the chosen material for fabrication microneedle electrodes, it must ultimately meet the following basic requirements: (1) satisfactory electrical conductivity. Good electrical conductivity is the basis for successfully measuring bioelectrical signals. Thus, materials with inherent poor conductivity, such as silicon or non-conductive polymers, necessitate admixing with conductive fillers like carbon black or surface coating with highly conductive materials such as metals (e.g., titanium, gold, silver) or carbon materials (e.g., CNTs, carbon black) to enhance their conductivity so that microneedle electrodes can measure and transmit bioelectrical signals. Although the introduction of fillers

Table 3 Summary of polymer-based microneedle electrodes for measuring bioelectrical signals

Materials/Coating	Preparation	Advantages	Disadvantages	Instrument	Impedance	Ref.
SU-8/Sliver&parylene	Micro-molding	Biocompatible	Fabrication complexity	Impedance meter	15 Hz,10 kΩ	[105]
PLA/Silver&Ti	Micro-molding	High selectivity	High fitting requirement	—	—	[168]
SU-8/Sliver&parylene	Micro-molding	Long-term stability	High initial impedance	—	6 kΩ	[61]
SU-8/Au	Photolithography	Low cost	Signal attenuation	—	50 kΩ	[174]
PLGA/Ti&Au	Thermal drawing	Simple process	Low mechanical strength	LCR meter	100 Hz, 70 kΩ	[113]
SU-8/Sliver&parylene	Micro-molding	Hair penetration	Signal noise	LCR meter	10 Hz, 100 kΩ	[120]
SU-8/Ag	Photolithography	No skin preparation	Mechanical brittleness	—	2.7 kΩ	[104]
Epoxy resin/Ti&Au	Micro-molding	Excellent skin contact	Fabrication complexity	Potentiostat	10 Hz, 200 kΩ	[165]
SU-8/Sliver&parylene	Micro-molding	Preparation-free	Signal noise	—	—	[172]
SU-8/Sliver&parylene	Micro-molding	Comfortable wear	Signal interference	—	10 Hz, ~ 20 kΩ	[173]
SU-8/Sliver&parylene	Micro-molding	High sensitivity, flexibility	Signal noise	—	—	[170]
PDMS/Ti&Au	MRDL	Bendability	Complex fabrication	LCR meter	50 Hz, 15 kΩ	[166]
Epoxy resin/Ti&Au	Micro-molding	Structural flexibility	Complex fabrication	LCR meter	10 Hz, 220 kΩ	[164]
PU/Ag	—	Flexible, biocompatible	Low mechanical strength	Impedance analyzer	10 Hz, 20 kΩ	[163]
PDMS/Ti&Au&parylene	MEMS	Long-term stability	Signal noise	E4990A	10 Hz, 92 kΩ	[167]
PI/Ti&Au	Micro-molding	Low impedance	High cost	CHI 660E	10 Hz, 1.5 kΩ·cm^2	[171]
Silicon/Ti&Au&PEDOT	Etching	Enhanced performance	Poor flexibility	CHI 660D	100 Hz, 2.7 kΩ	[180]
Epoxy/PEDOT:PSS	3D printing	Biocompatible	Low mechanical strength	Four point probe	4 kΩ/sq	[181]
PI/Cr&Au&Ag&PEDOT:PSS	Micro-molding	Superior signal quality	Complex fabrication	CHI660E	10 Hz, 7.81 kΩ	[169]

Table 4 Summary of carbon-based microneedle electrodes for measuring bioelectrical signals

Materials/Coating	Preparation	Advantages	Disadvantages	Instrument	Impedance	Ref.
Carbon/Au&Agepoxy resin	Vacuum casting	Mass-producible	High initial cost	—	~ 7 kΩ	[195]
PI/Maltose& NTs	—	Flexible, biocompatible, low-impedance	Complex fabrication process	Metrohm Autolab; PG Stat; 0.9%NaCl	1 kHz, 59 kΩ	[197]
GO nano fiber/Parylene	Wet-spun	Flexible, conductive, biocompatible	Fabrication complexity	Impedance analyzer; PBS	10 Hz, 2 kΩ	[188]
MWCNTs/Al_2O_3&iron	CVD[a]	Low impedance, stable over time	Fabrication complexity	Agilent 4294A; Agar gel	40 Hz, 8.15 × 10^{-3} kΩ	[279]
CNTs/PDMS	Micro-molding	Flexible, stable	High impedance	CHI660C	30 Hz, 348 kΩ	[280]
CNTs/PPy	—	Good conductivity	High cost	Agilent 4294A	40 Hz, 18.76 × 10^{-3} kΩ	[281]
PEDOT:PSS&MWCNTs	Inkjet	Fully printed, cell-compatible	Moderate conductivity	Potentiostat	1 kHz, 128 kΩ	[196]
Epoxy resin&Carbon black/Silver	Casting	Low cost, simple process	Not durable	—	10 kHz, 130 kΩ	[198]

[a]CVD: chemical vapor deposition.

and surface coatings solves the problem of poor conductivity, it will also increase the interface during the transmission of bioelectrical signals, and the increased interface may result in structural instability and signal attenuation or distortion. Regrettably, comprehensive analyses of the impacts induced by interfaces have yet to be conducted in the existing body of research. (2) Sufficient mechanical properties. Unlike conventional surface or implanted electrodes, microneedle electrodes rely on their structural design to penetrate the stratum corneum, reducing EII. Moreover, microneedle electrodes must be adaptable to skin movement. Balancing the required rigidity for stratum corneum penetration with the flexibility necessary to accommodate skin stretching poses a substantial challenge. (3) Excellent biocompatibility. Good biocompatibility is the basis for long-term monitoring of bioelectrical signals by microneedle electrodes, and is an important indicator of whether microneedle electrodes can be used in practical applications in life. As bioelectrical signals emanate from living cells, the material's biocompatibility plays a crucial role. Subpar biocompatibility may adversely affect cell activity, resulting in erroneous signal acquisition.

In summary, it is challenging for a single material to simultaneously meet the aforementioned requirements. Therefore, composite materials or composite structures are pivotal for the future development of microneedle electrodes. Material advancements not only enhance the performance of microneedle electrodes but also revolutionize their fabrication methods, facilitating large-scale production and practical application. For instance, earlier silicon and metal microneedles were primarily fabricated through etching and cutting processes, which lacked precision control and hindered mass production. Subsequently, polymer microneedle electrodes emerged, utilizing 3D printing and simpler templating methods, thus reducing costs and expediting practical implementation. Additionally, the development of flexible, wearable biosignals acquisition systems is critical for advancing microneedle electrodes. For example, studies have proposed integrating microneedle electrodes, power sources, and wireless transmission systems, enabling intuitive measurement results on smartphones or computers. In the future, combining microneedle electrodes with brain-machine interfaces, portable medical devices, and wearable technology holds vast potential for bioelectrical signals measurement systems.

Data availability

All data needed to support the conclusions in the paper are presented in the manuscript. Additional data related to this paper may be requested from the corresponding author upon request.

Acknowledgements

All the authors thank the National Natural Science Foundation of China (Nos. 51672221, and 51872231) and the Key Industrial Chain Project of Shaanxi Province (No. 2018ZDCXL-GY-08-07).

Declaration of competing interest

All contributing authors report no conflicts of interest in this work.

Author contribution statement

X. H. L.: Data curation, project administration, validation, writing manuscript, experimental design. T. K. Z.: Project administration, funding acquisition.

Informed consent

Not applicable.

Ethics statement

Not applicable.

Use of AI statement

None.

References

[1] Fu, Y. L.; Zhao, J. J.; Dong, Y.; Wang, X. H. Dry electrodes for human bioelectrical signal monitoring. *Sensors* **2020**, *20*, 3651.

[2] Hardenacke, K.; Shubina, E.; Bührle, C. P.; Zapf, A.; Lenartz, D.; Klosterkötter, J.; Visser-Vandewalle, V.; Kuhn, J. Deep brain stimulation as a tool for improving cognitive functioning in Alzheimer’s dementia: A systematic review. *Front. Psychiatry* **2013**, *4*, 159.

[3] Vance, C. G. T.; Dailey, D. L.; Rakel, B. A.; Sluka, K. A. Using TENS for pain control: The state of the evidence. *Pain Manag.* **2014**, *4*, 197–209.

[4] Wang, J. J.; Wang, T. J.; Liu, H. Y.; Wang, K.; Moses, K.; Feng, Z. Y.; Li, P.; Huang, W. Flexible electrodes for brain-computer interface system. *Adv. Mater.* **2023**, *35*, 2211012.

[5] Nunez, P. L.; Srinivasan, R. *Electric Fields of the Brain: The Neurophysics of EEG*, 2nd ed.; Oxford University Press: Oxford, 2006.

[6] Ma, Y. X.; Gong, A. M.; Nan, W. Y.; Ding, P.; Wang, F.; Fu, Y. F. Personalized brain-computer interface and its applications. *J. Pers. Med.* **2023**, *13*, 46.

[7] Hong, Y. J.; Jeong, H.; Cho, K. W.; Lu, N. S.; Kim, D. H. Wearable and implantable devices for cardiovascular healthcare: From monitoring to therapy based on flexible and stretchable electronics. *Adv. Funct. Mater.* **2019**, *29*, 1808247.

[8] Mirvis, D. M.; Goldberger, A. L. Electrocardiography. *Heart Dis.* **2001**, *1*, 82–128.

[9] De Luca, C. J. *Electromyography Encyclopedia of Medical Devices and Instrumentation*; Wiley-Interscience: Hoboken, 2006; pp 98–109.

[10] Song, M. Y.; Kim, U. S. Current usage of electrophysiological tests in a secondary referral hospital in Korea. *Doc. Ophthalmol.* **2022**, *145*, 127–131.

[11] Zhang, B. L.; Xie, R. J.; Jiang, J. M.; Hao, S. P.; Fang, B.; Zhang, J. X.; Bai, H.; Peng, B.; Li, L.; Liu, Z. Y. et al. Implantable neural electrodes: From preparation optimization to application. *J. Mater. Chem. C* **2023**, *11*, 6550–6572.

[12] Huang, Z. B.; Zhou, Z. N.; Zeng, J. S.; Lin, S.; Wu, H. Flexible electrodes for non-invasive brain-computer interfaces: A perspective. *APL Mater.* **2022**, *10*, 090901.

[13] Parvizi, J.; Kastner, S. Promises and limitations of human intracranial electroencephalography. *Nat. Neurosci.* **2018**, *21*, 474–483.

[14] Wang, S.; Zhao, M. M.; Yan, Y. B.; Li, P.; Huang, W. Flexible monitoring, diagnosis, and therapy by microneedles with versatile materials and devices toward multifunction scope. *Research* **2023**, *6*, 0128.

[15] Kim, T.; Park, J.; Sohn, J.; Cho, D.; Jeon, S. Bioinspired, highly stretchable, and conductive dry adhesives based on 1D-2D hybrid carbon nanocomposites for all-in-one ECG Electrodes. *ACS Nano* **2016**, *10*, 4770–4778.

[16] Pan, K. G.; Hagiwara, T.; Tso, K. C.; Siwadamrongpong, R.; Akbar, L.; Nakano, Y.; Kono, T.; Terasawa, Y.; Haruta, M.; Takehara, H. A flexible retinal device with CMOS smart electrodes fabricated on parylene C thin-film and bioceramic substrate. *Jpn. J. Appl. Phys.* **2023**, *62*, SC1022.

[17] Nigusse, A. B.; Malengier, B.; Mengistie, D. A.; Tseghai, G. B.; Van Langenhove, L. Development of washable silver printed textile electrodes for long-term ECG monitoring. *Sensors* **2020**, *20*, 6233.

[18] Ferrari, L. M.; Ismailov, U.; Badier, J. M.; Greco, F.; Ismailova, E. Conducting polymer tattoo electrodes in clinical electro- and magneto-encephalography. *NPJ Flex. Electron.* **2020**, *4*, 4.

[19] Baek, H. J.; Lee, H. J.; Lim, Y. G.; Park, K. S. Conductive polymer foam surface improves the performance of a capacitive EEG electrode. *IEEE Trans. Biomed. Eng.* **2012**, *59*, 3422–3431.

[20] Li, L. J.; Li, G. L.; Cao, Y. L.; Duan, Y. Y. A novel highly durable carbon/silver/silver chloride composite electrode for high-definition transcranial direct current stimulation. *Nanomaterials* **2021**, *11*, 1962.

[21] Rossetti, N.; Hagler, J.; Kateb, P.; Cicoira, F. Neural and electromyography PEDOT electrodes for invasive stimulation and recording. *J. Mater. Chem. C* **2021**, *9*, 7243–7263.

[22] Chatterjee, S.; Sakorikar, T.; Bs, A.; Joshi, R. K.; Sikaria, A.; Jayachandra, M.; V, V.; Pandya, H. J. A flexible implantable microelectrode array for recording electrocorticography signals from rodents. *Biomed. Microdevices* **2022**, *24*, 31.

[23] Chen, S. T.; Chu, C. Y. Fabrication and testing of a novel biopotential electrode array. *J. Mater. Process. Technol.* **2017**, *250*, 345–356.

[24] Ruffini, G.; Dunne, S.; Fuentemilla, L.; Grau, C.; Farrés, E.; Marco-Pallarés, J.; Watts, P. C. P.; Silva, S. R. P. First human trials of a dry electrophysiology sensor using a carbon nanotube array interface.

Sens. Actuators A: Phys. **2008**, *144*, 275–279.
[25] Niu, X.; Gao, X. H.; Liu, Y. F.; Liu, H. Surface bioelectric dry Electrodes: A review. *Measurement* **2021**, *183*, 109774.
[26] Luo, Y. F.; Li, W. L.; Lin, Q. Y.; Zhang, F. L.; He, K.; Yang, D. P.; Loh, X. J.; Chen, X. D. A morphable ionic electrode based on thermogel for non-invasive hairy plant electrophysiology. *Adv. Mater.* **2021**, *33*, 2007848.
[27] Won, S. M.; Song, E. M.; Zhao, J. N.; Li, J. H.; Rivnay, J.; Rogers, J. A. Recent advances in materials, devices, and systems for neural interfaces. *Adv. Mater.* **2018**, *30*, 1800534.
[28] Niu, X.; Gao, X. H.; Wang, T. Y.; Wang, W.; Liu, H. Ordered nanopillar arrays of low dynamic noise dry bioelectrodes for electrocardiogram surface monitoring. *ACS Appl. Mater. Interfaces* **2022**, *14*, 33861–33870.
[29] Fang, Y.; Prominski, A.; Rotenberg, M. Y.; Meng, L. Y.; Acarón Ledesma, H.; Lv, Y. Y.; Yue, J. P.; Schaumann, E.; Jeong, J.; Yamamoto, N. et al. Micelle-enabled self-assembly of porous and monolithic carbon membranes for bioelectronic interfaces. *Nat. Nanotechnol.* **2021**, *16*, 206–213.
[30] Park, T.; Jeong, J.; Kim, Y. J.; Yoo, H. Weak molecular interactions in organic composite dry film lead to degradable, robust wireless electrophysiological signal sensing. *Adv. Mater. Interfaces* **2022**, *9*, 2200594.
[31] Spanu, A.; Taki, M.; Baldazzi, G.; Mascia, A.; Cosseddu, P.; Pani, D.; Bonfiglio, A. Epidermal electrodes with ferrimagnetic/ conductive properties for biopotential recordings. *Bioengineering* **2022**, *9*, 205.
[32] Acar, G.; Ozturk, O.; Golparvar, A. J.; Elboshra, T. A.; Böhringer, K.; Yapici, M. K. Wearable and flexible textile electrodes for biopotential signal monitoring: A review. *Electronics* **2019**, *8*, 479.
[33] Nigusse, A. B.; Mengistie, D. A.; Malengier, B.; Tseghai, G. B.; van Langenhove, L. Wearable smart textiles for long-term electrocardiography monitoring-A review. *Sensors* **2021**, *21*, 4174.
[34] Barrera, C. S.; Pina-Martinez, E.; Roberts, R.; Rodriguez-Leal, E. Impact of size and shape for textile surface electromyography electrodes: A study of the biceps brachii muscle. *Text. Res. J.* **2022**, *92*, 3097–3110.
[35] Xu, X. W.; Luo, M.; He, P.; Yang, J. L. Washable and flexible screen printed graphene electrode on textiles for wearable healthcare monitoring. *J. Phys. D: Appl. Phys.* **2020**, *53*, 125402.
[36] Kubicek, J.; Fiedorova, K.; Vilimek, D.; Cerny, M.; Penhaker, M.; Janura, M.; Rosicky, J. Recent trends, construction, and applications of smart textiles and clothing for monitoring of health activity: A comprehensive multidisciplinary review. *IEEE Rev. Biomed. Eng.* **2022**, *15*, 36–60.
[37] Xu, X. W.; Luo, M.; He, P.; Guo, X. J.; Yang, J. L. Screen printed graphene electrodes on textile for wearable electrocardiogram monitoring. *Appl. Phys. A* **2019**, *125*, 714.
[38] Bihar, E.; Roberts, T.; Ismailova, E.; Saadaoui, M.; Isik, M.; Sanchez-Sanchez, A.; Mecerreyes, D.; Hervé, T.; De Graaf, J. B.; Malliaras, G. G. Fully printed electrodes on stretchable textiles for long-term electrophysiology. *Adv. Mater. Technol.* **2017**, *2*, 1600251.
[39] Baldazzi, G.; Spanu, A.; Mascia, A.; Viola, G.; Bonfiglio, A.; Cosseddu, P.; Pani, D. Validation of a novel tattoo electrode for ECG monitoring. In *Proceedings of 2021 Computing in Cardiology*, Brno, Czech Republic, 2021, pp 1–4.
[40] Su, P. C.; Hsueh, Y. H.; Ke, M. T.; Chen, J. J.; Lai, P. C. Noncontact ECG monitoring by capacitive coupling of textiles in a chair. *J. Healthc. Eng.* **2021**, *2021*, 6698567.
[41] Sun, Y.; Yu, X. B. Capacitive biopotential measurement for electrophysiological signal acquisition: A review. *IEEE Sens. J.* **2016**, *16*, 2832–2853.
[42] Umar, A. H.; Othman, M. A.; Harun, F. K. C.; Yusof, Y. Dielectrics for non-contact ECG bioelectrodes: A review. *IEEE Sens. J.* **2021**, *21*, 18353–18367.
[43] Shay, T.; Velev, O. D.; Dickey, M. D. Soft electrodes combining hydrogel and liquid metal. *Soft Matter.* **2018**, *14*, 3296–3303.
[44] Wang, L. F.; Liu, J. Q.; Peng, H. L.; Yang, B.; Zhu, H. Y.; Yang, C. S. MEMS-based flexible capacitive electrode for ECG measurement. *Electron. Lett.* **2013**, *49*, 739–740.
[45] Inácio, P. M. C.; Mestre, A. L. G.; De Medeiros, M. D. C. R.; Asgarifar, S.; Elamine, Y.; Canudo, J.; Santos, J. M. A.; Bragança, J.; Morgado, J.; Biscarini, F. et al. Bioelectrical signal detection using conducting polymer electrodes and the displacement current method. *IEEE Sens. J.* **2017**, *17*, 3961–3966.
[46] Ueno, A.; Yamaguchi, T.; Iida, T.; Fukuoka, Y.; Uchikawa, Y.; Noshiro, M. Feasibility of capacitive sensing of surface electromyographic potential through cloth. *Sens. Mater.* **2012**, *24*, 335–346.
[47] Wang, T. W.; Zhang, H.; Lin, S. F. Influence of capacitive coupling on high-fidelity non-contact ecg measurement. *IEEE Sens. J.* **2020**, *20*, 9265–9273.
[48] Chen, C. C.; Chen, C. W.; Hsieh, C. W. Noise-resistant CECG using novel capacitive electrodes. *Sensors* **2020**, *20*, 2577.
[49] Ullah, H.; Wahab, A.; Will, G.; Karim, M. R.; Pan, T. S.; Gao, M.; Lai, D. K.; Lin, Y.; Miraz, M. H. Recent advances in stretchable and wearable capacitive electrophysiological sensors for long-term health monitoring. *Biosensors* **2022**, *12*, 630.
[50] Liu, H.; Chen, X. D.; Wang, Z. H.; Liu, Y.; Liang, C. Y.; Zhu, M.; Qi, D. P. Development of soft dry electrodes: From materials to structure design. *Soft Sci.* **2023**, *3*, 27.
[51] Yang, L. T.; Liu, Q.; Zhang, Z. L.; Gan, L.; Zhang, Y.; Wu, J. L. Materials for dry electrodes for the electroencephalography: Advances, challenges, perspectives. *Adv. Mater. Technol.* **2022**, *7*, 2100612.
[52] Lopez-Gordo, M. A.; Sanchez-Morillo, D.; Valle, F. P. Dry EEG electrodes. *Sensors* **2014**, *14*, 12847–12870.
[53] Teplan, M. Fundamentals of EEG measurement. *Meas. Sci. Rev.* **2002**, *2*, 1–11.
[54] Gargiulo, G.; Calvo, R. A.; Bifulco, P.; Cesarelli, M.; Jin, C.; Mohamed, A.; Van Schaik, A. A new EEG recording system for passive dry electrodes. *Clin. Neurophysiol.* **2010**, *121*, 686–693.
[55] Yan, D. X.; Jiman, A. A.; Bottorff, E. C.; Patel, P. R.; Meli, D.; Welle, E. J.; Ratze, D. C.; Havton, L. A.; Chestek, C. A.; Kemp, S. W. P. et al. Ultraflexible and stretchable intrafascicular peripheral nerve recording device with axon-dimension, cuff-less microneedle electrode array. *Small* **2022**, *18*, 2200311.
[56] Yu, K. J.; Kuzum, D.; Hwang, S. W.; Kim, B. H.; Juul, H.; Kim, N. H.; Won, S. M.; Chiang, K.; Trumpis, M.; Richardson, A. G. et al. Bioresorbable silicon electronics for transient spatiotemporal mapping of electrical activity from the cerebral cortex. *Nat. Mater.* **2016**, *15*, 782–791.
[57] Xi, Y.; Ji, B. W.; Guo, Z. J.; Li, W.; Liu, J. Q. Fabrication and characterization of micro-nano electrodes for implantable BCI. *Micromachines* **2019**, *10*, 242.
[58] Nam, D.; Cha, J. M.; Park, K. Next-generation wearable biosensors developed with flexible bio-chips. *Micromachines* **2021**, *12*, 64.
[59] Liu, Q.; Yang, L. T.; Zhang, Z. L.; Yang, H.; Zhang, Y.; Wu, J. L. The feature, performance, and prospect of advanced electrodes for electroencephalogram. *Biosensors* **2023**, *13*, 101.
[60] Ren, L.; Liu, B.; Zhou, W.; Jiang, L. L. A mini review of microneedle array electrode for bio-signal recording: A review. *IEEE Sens. J.* **2020**, *20*, 577–590.
[61] Arai, M.; Nishinaka, Y.; Miki, N. Long-term electroencephalogram measurement using polymer-based dry microneedle electrode. In *Proceedings of the 2015 18th International Conference on Solid-State Sensors, Actuators and Microsystems*, Anchorage, 2015, pp 81–84.
[62] Rad, Z. F.; Prewett, P. D.; Davies, G. J. An overview of microneedle applications, materials, and fabrication methods. *Beilstein J. Nanotechnol.* **2021**, *12*, 1034–1046.
[63] Yang, J. B.; Zhang, H. X.; Hu, T. L.; Xu, C. J.; Jiang, L. L.; Shrike

Zhang, Y.; Xie, M. B. Recent advances of microneedles used towards stimuli-responsive drug delivery, disease theranostics, and bioinspired applications. *Chem. Eng. J.* **2021**, *426*, 130561.
[64] Qin, J.; Yin, L. J.; Hao, Y. N.; Zhong, S. L.; Zhang, D. L.; Bi, K.; Zhang, Y. X.; Zhao, Y.; Dang, Z. M. Flexible and stretchable capacitive sensors with different microstructures. *Adv. Mater.* **2021**, *33*, 2008267.
[65] Vora, L. K.; Sabri, A. H.; McKenna, P. E.; Himawan, A.; Hutton, A. R. J.; Detamornrat, U.; Paredes, A. J.; Larrañeta, E.; Donnelly, R. F. Microneedle-based biosensing. *Nat. Rev. Bioeng.* **2024**, *2*, 64–81.
[66] Miller, P. R.; Skoog, S. A.; Edwards, T. L.; Wheeler, D. R.; Xiao, X. Y.; Brozik, S. M.; Polsky, R.; Narayan, R. J. Hollow microneedle-based sensor for multiplexed transdermal electrochemical sensing. *J. Vis. Exp.* **2012**, *64*, e4067.
[67] Miller, P. R.; Xiao, X. Y.; Brener, I.; Burckel, D. B.; Narayan, R.; Polsky, R. Microneedle-based transdermal sensor for on-chip potentiometric determination of K^+. *Adv. Healthc. Mater.* **2014**, *3*, 876–881.
[68] Goud, K. Y.; Moonla, C.; Mishra, R. K.; Yu, C. M.; Narayan, R.; Litvan, I.; Wang, J. Wearable electrochemical microneedle sensor for continuous monitoring of levodopa: Toward parkinson management. *ACS Sens.* **2019**, *4*, 2196–2204.
[69] Chu, H. Q.; Zhang, Y. Y.; Yang, Y.; Xue, J. T.; Li, C.; Zhang, W.; Li, Z.; Zheng, H. Flurbiprofen microneedle patches for the management of acute postoperative pain. *Nano Res.* **2024**, *17*, 7493–7503.
[70] Yang, Y.; Chu, H. Q.; Zhang, Y.; Xu, L. L.; Luo, R. Z.; Zheng, H.; Yin, T. L.; Li, Z. Rapidly separable bubble microneedle patch for effective local anesthesia. *Nano Res.* **2022**, *15*, 8336–8344.
[71] Chu, H. Q.; Xue, J. T.; Yang, Y.; Zheng, H.; Luo, D.; Li, Z. Advances of smart stimulus-responsive microneedles in cancer treatment. *Small Methods* **2024**, *8*, 2301455.
[72] Berger, H. Über das elektrenkephalogramm des menschen. *Dtsch. Med. Wochenschr.* **1934**, *60*, 1947–1949.
[73] Gerstel, M. S.; Place, V. A. Drug delivery device. U.S. Patent 3964482A, June 22, 1976.
[74] Griss, P.; Enoksson, P.; Tolvanen-Laakso, H. K.; Merilainen, P.; Ollmar, S.; Stemme, G. Micromachined electrodes for biopotential measurements. *J. Microelectromech. Syst.* **2001**, *10*, 10–16.
[75] Charvet, G.; Rousseau, L.; Billoint, O.; Gharbi, S.; Rostaing, J. P.; Joucla, S.; Trevisiol, M.; Bourgerette, A.; Chauvet, P.; Moulin, C. et al. BioMEA™: A versatile high-density 3D microelectrode array system using integrated electronics. *Biosens. Bioelectron.* **2010**, *25*, 1889–1896.
[76] Xiang, Z. L.; Liu, J. Q.; Lee, C. A flexible three-dimensional electrode mesh: An enabling technology for wireless brain-computer interface prostheses. *Microsyst. Nanoeng.* **2016**, *2*, 16012.
[77] Luo, X. J.; Yu, Q.; Yang, L.; Cui, Y. Wearable, sensing-controlled, ultrasound-based microneedle smart system for diabetes management. *ACS Sens.* **2023**, *8*, 1710–1722.
[78] Griss, P.; Tolvanen-Laakso, H. K.; Merilainen, P.; Stemme, G. Characterization of micromachined spiked biopotential electrodes. *IEEE Trans. Biomed. Eng.* **2002**, *49*, 597–604.
[79] Lu, H. H.; Shao, W. Y.; Gao, B. B.; Zheng, S. Y.; He, B. F. Intestine-inspired wrinkled MXene microneedle dressings for smart wound management. *Acta Biomater.* **2023**, *159*, 201–210.
[80] Sun, L. Y.; Fan, L.; Bian, F. K.; Chen, G. P.; Wang, Y. T.; Zhao, Y. J. MXene-integrated microneedle patches with innate molecule encapsulation for wound healing. *Research* **2021**, *2021*, 9838490.
[81] Shao, Y.; Dong, K. Y.; Lu, X. Y.; Gao, B. B.; He, B. F. Bioinspired 3D-printed mxene and spidroin-based near-infrared light-responsive microneedle scaffolds for efficient wound management. *ACS Appl. Mater. Interfaces* **2022**, *14*, 56525–56534.
[82] Guo, M. Z.; Wang, Y. Q.; Gao, B. B.; He, B. F. Shark tooth-inspired microneedle dressing for intelligent wound management. *ACS Nano* **2021**, *15*, 15316–15327.
[83] Wang, Y. Q.; Gao, B. B.; He, B. F. Toward efficient wound management: Bioinspired microfluidic and microneedle patch. *Small* **2023**, *19*, 2206270.
[84] Miller, P.; Moorman, M.; Manginell, R.; Ashlee, C.; Brener, I.; Wheeler, D.; Narayan, R.; Polsky, R. Towards an integrated microneedle total analysis chip for protein detection. *Electroanalysis* **2016**, *28*, 1305–1310.
[85] Gao, J.; Huang, W. Z.; Chen, Z. P.; Yi, C. Q.; Jiang, L. L. Simultaneous detection of glucose, uric acid and cholesterol using flexible microneedle electrode array-based biosensor and multi-channel portable electrochemical analyzer. *Sens. Actuators B Chem.* **2019**, *287*, 102–110.
[86] Rezali, F. A. M.; Soin, N.; Hatta, S. F. W. M.; Daut, M. H. M.; Nouxman, M. H. A. H.; Hussin, H. Design strategies and prospects in developing wearable glucose monitoring system using printable organic transistor and microneedle: A review. *IEEE Sens. J.* **2022**, *22*, 13785–13799.
[87] Dervisevic, M.; Alba, M.; Yan, L.; Senel, M.; Gengenbach, T. R.; Prieto-Simon, B.; Voelcker, N. H. Transdermal electrochemical monitoring of glucose via high-density silicon microneedle array patch. *Adv. Funct. Mater.* **2022**, *32*, 2009850 .
[88] Lijnse, T. M.; Haider, K.; Dalton, C. High throughput fabrication of robust solid microneedles. In *Proceedings of SPIE 11955, Microfluidics, BioMEMS, and Medical Microsystems XX*, San Francisco, 2022, pp 80–88.
[89] Wu, D.; Shou, X.; Yu, Y. R.; Wang, X. C.; Chen, G. P.; Zhao, Y. J.; Sun, L. Y. Biologics-loaded photothermally dissolvable hyaluronic acid microneedle patch for psoriasis treatment. *Adv. Funct. Mater.* **2022**, *32*, 2205847.
[90] Feng, X. Q.; Xian, D. Y.; Fu, J. T.; Luo, R.; Wang, W. H.; Zheng, Y. W.; He, Q.; Ouyang, Z.; Fang, S. B.; Zhang, W. C. et al. Four-armed host-defense peptidomimetics-augmented vanadium carbide MXene-based microneedle array for efficient photo-excited bacteria-killing. *Chem. Eng. J.* **2023**, *456*, 141121.
[91] Lin, S. Y.; Lin, H.; Yang, M.; Ge, M.; Chen, Y.; Zhu, Y. F. A two-dimensional MXene potentiates a therapeutic microneedle patch for photonic implantable medicine in the second NIR biowindow. *Nanoscale* **2020**, *12*, 10265–10276.
[92] Huang, S.; He, M. Y.; Yao, C. J.; Huang, X. S.; Ma, D. Y.; Huang, Q. Q.; Yang, J. B.; Liu, F. M.; Wen, X. Q.; Wang, J. et al. Petromyzontidae-biomimetic multimodal microneedles-integrated bioelectronic catheters for theranostic endoscopic surgery. *Adv. Funct. Mater.* **2023**, *33*, 2214485.
[93] Shi, Z. Y.; Jiang, B.; Liang, S. C.; Zhang, J. T.; Suo, D. J.; Wu, J. L.; Chen, D. D.; Pei, G. Y.; Yan, T. Y. Claw-shaped flexible and low-impedance conductive polymer electrodes for EEG recordings: Anemone dry electrode. *Sci. China Technol. Sci.* **2023**, *66*, 255–266.
[94] Lee, S. H.; Thunemann, M.; Lee, K.; Cleary, D. R.; Tonsfeldt, K. J.; Oh, H.; Azzazy, F.; Tchoe, Y.; Bourhis, A. M.; Hossain, L. et al. Scalable thousand channel penetrating microneedle arrays on flex for multimodal and large area coverage brainmachine interfaces. *Adv. Funct. Mater.* **2022**, *32*, 2112045.
[95] Ibayashi, K.; Kunii, N.; Matsuo, T.; Ishishita, Y.; Shimada, S.; Kawai, K.; Saito, N. Decoding speech with integrated hybrid signals recorded from the human ventral motor cortex. *Front. Neurosci.* **2018**, *12*, 221.
[96] Zhang, X. X.; Lu, M. H.; Cao, X. Y.; Zhao, Y. J. Functional microneedles for wearable electronics. *Smart Med.* **2023**, *2*, e20220023.
[97] Kil, H. J.; Kim, S. R.; Park, J. W. A self-charging supercapacitor for a patch-type glucose sensor. *ACS Appl. Mater. Interfaces* **2022**, *14*, 3838–3848.
[98] Ke, K. H.; Chung, C. K. High-performance Al/PDMS TENG with novel complex morphology of two-height microneedles array for high-sensitivity force-sensor and self-powered application. *Small*

2020, *16*, 2001209.

[99] Mahmood, M.; Kwon, S.; Kim, H.; Kim, Y. S.; Siriaraya, P.; Choi, J.; Otkhmezuri, B.; Kang, K.; Yu, K. J.; Jang, Y. C. et al. Wireless soft scalp electronics and virtual reality system for motor imagery-based brain-machine interfaces. *Adv. Sci.* **2021**, *8*, 2101129.

[100] Kim, M.; Gu, G. Y.; Cha, K. J.; Kim, D. S.; Chung, W. K. Wireless sEMG system with a microneedle-based high-density electrode array on a flexible substrate. *Sensors* **2017**, *18*, 92.

[101] Kim, Y. J.; Chinnadayyala, S. R.; Le, H. T. N.; Cho, S. Sensitive electrochemical non-enzymatic detection of glucose based on wireless data transmission. *Sensors* **2022**, *22*, 2787.

[102] Liu, Y. Q.; Yu, Q.; Ye, L.; Yang, L.; Cui, Y. A wearable, minimally-invasive, fully electrochemically-controlled feedback minisystem for diabetes management. *Lab Chip* **2023**, *23*, 421–436.

[103] Wang, R. X.; Zhao, W.; Wang, W.; Li, Z. H. A flexible microneedle electrode array with solid silicon needles. *J. Microelectromech. Syst.* **2012**, *21*, 1084–1089.

[104] Stavrinidis, G.; Michelakis, K.; Kontomitrou, V.; Giannakakis, G.; Sevrisarianos, M.; Sevrisarianos, G.; Chaniotakis, N.; Alifragis, Y.; Konstantinidis, G. SU-8 microneedles based dry electrodes for electroencephalogram. *Microelectron. Eng.* **2016**, *159*, 114–120.

[105] Nishinaka, Y.; Jun, R.; Prihandana, G. S.; Miki, N. Fabrication of polymer microneedle electrodes coated with nanoporous parylene. *Jpn. J. Appl. Phys.* **2013**, *52*, 06GL10.

[106] Omatsu, T.; Chujo, K.; Miyamoto, K.; Okida, M.; Nakamura, K.; Aoki, N.; Morita, R. Metal microneedle fabrication using twisted light with spin. *Opt. Express* **2010**, *18*, 17967–17973.

[107] Yu, L. M.; Tay, F. E. H.; Guo, D. G.; Xu, L.; Yap, K. L. A microfabricated electrode with hollow microneedles for ECG measurement. *Sens. Actuators A phys.* **2009**, *151*, 17–22.

[108] Rodriguez, A.; Molinero, D.; Valera, E.; Trifonov, T.; Marsal, L. F.; Pallarès, J.; Alcubilla, R. Fabrication of silicon oxide microneedles from macroporous silicon. *Sens. Actuators B Chem.* **2005**, *109*, 135–140.

[109] Zhou, H. B.; Li, G.; Sun, X. N.; Zhu, Z. H.; Xu, B. J.; Jin, Q. H.; Zhao, J. L.; Ren, Q. S. A new process for fabricating tip-shaped polymer microstructure array with patterned metallic coatings. *Sens. Actuators A Phys.* **2009**, *150*, 296–301.

[110] Dabbagh, S. R.; Sarabi, M. R.; Rahbarghazi, R.; Sokullu, E.; Yetisen, A. K.; Tasoglu, S. 3D-printed microneedles in biomedical applications. *iScience* **2021**, *24*, 102012.

[111] Wang, R. X.; Wang, W.; Li, Z. H. An improved manufacturing approach for discrete silicon microneedle arrays with tunable height-pitch ratio. *Sensors* **2016**, *16*, 1628.

[112] Kudo, Y.; Arai, M.; Miki, N. Fatigue assessment by electroencephalogram measured with candle-like dry microneedle electrodes. *Micro Nano Lett.* **2017**, *12*, 545–549.

[113] Ren, L.; Jiang, Q.; Chen, K. Y.; Chen, Z. P.; Pan, C. F.; Jiang, L. L. Fabrication of a micro-needle array electrode by thermal drawing for bio-signals monitoring. *Sensors* **2016**, *16*, 908.

[114] Han, D.; Morde, R. S.; Mariani, S.; La Mattina, A. A.; Vignali, E.; Yang, C.; Barillaro, G.; Lee, H. 4D printing of a bioinspired microneedle array with backward-facing barbs for enhanced tissue adhesion. *Adv. Funct. Mater.* **2020**, *30*, 1909197.

[115] Wang, L. F.; Liu, J. Q.; Yan, X. X.; Yang, B.; Yang, C. S. A MEMS-based pyramid micro-needle electrode for long-term EEG measurement. *Microsyst. Technol.* **2013**, *19*, 269–276.

[116] Liu, B.; Yang, Z. L.; Zheng, Y.; Yin, Z.; Fu, T.; Ren, L.; Jiang, L. L. Fabrication of metal microneedle array electrode for bio-signals monitoring. *J. Mech. Eng.* **2021**, *57*, 61–68.

[117] Kawana, T.; Yoshida, Y.; Kudo, Y.; Iwatani, C.; Miki, N. Design and characterization of an EEG-hat for reliable EEG measurements. *Micromachines* **2020**, *11*, 635.

[118] Chen, Z. P.; Lin, Y. Y.; Lee, W.; Ren, L.; Liu, B.; Liang, L.; Wang, Z.; Jiang, L. L. Additive manufacturing of honeybee-inspired microneedle for easy skin insertion and difficult removal. *ACS Appl. Mater. Interfaces* **2018**, *10*, 29338–29346.

[119] Resnik, D.; Možek, M.; Pečar, B.; Dolžan, T.; Janež, A.; Urbančič, V.; Vrtačnik, D. Characterization of skin penetration efficacy by Au-coated Si microneedle array electrode. *Sens. Actuators A Phys.* **2015**, *232*, 299–309.

[120] Arai, M.; Kudo, Y.; Miki, N. Polymer-based candle-shaped microneedle electrodes for electroencephalography on hairy skin. *Jpn. J. Appl. Phys.* **2016**, *55*, 06GP16.

[121] Chen, K. Y.; Ren, L.; Chen, Z. P.; Pan, C. F.; Zhou, W.; Jiang, L. L. Fabrication of micro-needle electrodes for bio-signal recording by a magnetization-induced self-assembly method. *Sensors* **2016**, *16*, 1533.

[122] Hsu, L. S.; Tung, S. W.; Kuo, C. H.; Yang, Y. J. Developing barbed microtip-based electrode arrays for biopotential measurement. *Sensors* **2014**, *14*, 12370–12386.

[123] Dong, C. W.; Lee, C. J.; Lee, D. H.; Moon, S. H.; Park, W. T. Fabrication of barbed-microneedle array for bio-signal measurement. *Sens. Actuators A Phys.* **2024**, *367*, 115040.

[124] Yao, H. C.; Yang, W. D.; Cheng, W.; Tan, Y. J.; See, H. H.; Li, S.; Ali, H. P. A.; Lim, B. Z. H.; Liu, Z. J.; Tee, B. C. K. Near-hysteresis-free soft tactile electronic skins for wearables and reliable machine learning. *Proc. Natl. Acad. Sci. USA* **2020**, *117*, 25352–25359.

[125] Yang, J. C.; Kim, J. O.; Oh, J.; Kwon, S. Y.; Sim, J. Y.; Kim, D. W.; Choi, H. B.; Park, S. Microstructured porous pyramid-based ultrahigh sensitive pressure sensor insensitive to strain and temperature. *ACS Appl. Mater. Interfaces* **2019**, *11*, 19472–19480.

[126] Abdullah, H.; Phairatana, T.; Jeerapan, I. Tackling the challenges of developing microneedle-based electrochemical sensors. *Microchim. Acta.* **2022**, *189*, 440.

[127] Najafi, K.; Wise, K. D.; Mochizuki, T. A high-yield IC-compatible multichannel recording array. *IEEE Trans. Electron Devices* **1985**, *32*, 1206–1211.

[128] Sun, W. B.; Guo, Z. L.; Yang, Z. Q.; Wu, Y. Z.; Lan, W. X.; Liao, Y. J.; Wu, X.; Liu, Y. Y. A review of recent advances in vital signals monitoring of sports and health via flexible wearable sensors. *Sensors* **2022**, *22*, 7784.

[129] O'Mahony, C.; Pini, F.; Blake, A.; Webster, C.; O'Brien, J.; McCarthy, K. G. Microneedle-based electrodes with integrated through-silicon via for biopotential recording. *Sens. Actuators A Phys.* **2012**, *186*, 130–136.

[130] Wang, Y.; Pei, W. H.; Guo, K.; Gui, Q.; Li, X. Q.; Chen, H. D.; Yang, J. H. Dry electrode for the measurement of biopotential signals. *Sci. China Inf. Sci.* **2011**, *54*, 2435–2442.

[131] Wang, Y.; Guo, K.; Pei, W. H.; Gui, Q.; Li, X. Q.; Chen, H. D.; Yang, J. H. Fabrication of dry electrode for recording bio-potentials. *Chin. Phys. Lett.* **2011**, *28*, 010701.

[132] Pei, W. H.; Zhang, H.; Wang, Y. J.; Guo, X. H.; Xing, X.; Huang, Y.; Xie, Y. X.; Yang, X. W.; Chen, H. D. Skin-potential variation insensitive dry electrodes for ECG recording. *IEEE Trans. Biomed. Eng.* **2017**, *64*, 463–470.

[133] Li, Z.; Li, Y.; Liu, M. S.; Cui, L. Y.; Yu, Y. D. Microneedle electrode array for electrical impedance myography to characterize neurogenic myopathy. *Ann. Biomed. Eng.* **2016**, *44*, 1566–1575.

[134] Wang, R. X.; Jiang, X. M.; Wang, W.; Li, Z. H. A microneedle electrode array on flexible substrate for long-term EEG monitoring. *Sens. Actuators B Chem.* **2017**, *244*, 750–758.

[135] Ji, H. W.; Wang, M. Y.; Wang, Y. T.; Wang, Z. H.; Ma, Y. J.; Liu, L. L.; Zhou, H. L.; Xu, Z.; Wang, X.; Chen, Y. et al. Skin-integrated, biocompatible, and stretchable silicon microneedle electrode for long-term EMG monitoring in motion scenario. *npj Flex. Electron.* **2023**, *7*, 46.

[136] Huang, D.; Wang, H. C.; Li, J. S.; Chen, Y. F.; Li, Z. H. A wireless flexible wearable biopotential acquisition system utilizing parylene based microneedle array. In *Proceedings of the 2019 20th International Conference on Solid-State Sensors, Actuators and*

Microsystems & Eurosensors XXXIII, Berlin, Germany, 2019, pp 298–301.

[137] Kim, H.; Lee, J.; Heo, U.; Jayashankar, D. K.; Agno, K. C.; Kim, Y.; Kim, C. Y.; Oh, Y.; Byun, S. H.; Choi, B. et al. Skin preparation-free, stretchable microneedle adhesive patches for reliable electrophysiological sensing and exoskeleton robot control. *Sci. Adv.* **2024**, *10*, eadk5260.

[138] Hermawan, H.; Ramdan, D.; Djuansjah, J. R. P. Metals for biomedical applications. In *Biomedical Engineering-from Theory to Applications*. Fazel-Rezai, R., Ed.; InTech: Rijeka, 2011; pp 411–430.

[139] Ali, S.; Abdul Rani, A. M.; Baig, Z.; Ahmed, S. W.; Hussain, G.; Subramaniam, K.; Hastuty, S.; Rao, T. V. V. L. N. Biocompatibility and corrosion resistance of metallic biomaterials. *Corros. Rev.* **2020**, *38*, 381–402.

[140] Krieger, K. J.; Liegey, J.; Cahill, E. M.; Bertollo, N.; Lowery, M. M.; O'Cearbhaill, E. D. Development and evaluation of 3D-printed dry microneedle electrodes for surface electromyography. *Adv. Mater. Technol.* **2020**, *5*, 2000518.

[141] Lo, L. W.; Zhao, J. Y.; Aono, K.; Li, W. L.; Wen, Z. C.; Pizzella, S.; Wang, Y.; Chakrabartty, S.; Wang, C. Stretchable sponge electrodes for long-term and motion-artifact-tolerant recording of high-quality electrophysiologic signals. *ACS Nano* **2022**, *16*, 11792–11801.

[142] Wang, Y. Y.; Jiang, L. L.; Ren, L.; Huang, P. A.; Yu, M.; Tian, L.; Li, X. X.; Xie, J.; Fang, P.; Li, G. L. Towards improving the quality of electrophysiological signal recordings by using microneedle electrode arrays. *IEEE Trans. Biomed. Eng.* **2021**, *68*, 3327–3335.

[143] Li, J. S.; Huang, D.; Chen, Y. F.; Li, Z. H. Low-cost, metal-based micro-needle electrode array (M-MNEA): A three-dimensional intracortical neural interface. In *Proceedings of the 2019 20th International Conference on Solid-State Sensors, Actuators and Microsystems & Eurosensors XXXIII*, Berlin, Germany, 2019, pp 1635–1638.

[144] Gwak, H.; Cho, S.; Song, Y. J.; Park, J. H.; Seo, S. A study on the fabrication of metal microneedle array electrodes for ECG detection based on low melting point Bi–In–Sn alloys. *Sci. Rep.* **2023**, *13*, 22931.

[145] Ren, L.; Xu, S. J.; Gao, J.; Lin, Z.; Chen, Z. P.; Liu, B.; Liang, L.; Jiang, L. L. Fabrication of flexible microneedle array electrodes for wearable bio-signal recording. *Sensors* **2018**, *18*, 1191.

[146] Yuan, C.; Ji, K. J.; Zhang, Q.; Yuan, P.; Xu, Y. L.; Liu, J.; Huo, T. W.; Zhao, J. H.; Chen, J.; Song, Y. et al. Bionic design and performance of electrode for bioelectrical signal monitoring. *Adv. Mater. Interfaces* **2022**, *9*, 2200532.

[147] Guvanasen, G. S.; Guo, L.; Aguilar, R. J.; Cheek, A. L.; Shafor, C. S.; Rajaraman, S.; Nichols, T. R.; DeWeerth, S. P. A stretchable microneedle electrode array for stimulating and measuring intramuscular electromyographic activity. *IEEE Trans. Neural Syst. Rehabil. Eng.* **2017**, *25*, 1440–1452.

[148] Satti, A. T.; Park, J.; Park, J.; Kim, H.; Cho, S. Fabrication of parylene-coated microneedle array electrode for wearable ECG device. *Sensors* **2020**, *20*, 5183.

[149] Kim, C.; Jang, A.; Kim, S.; Cho, S.; Lee, D.; Kim, Y. J. A wearable ECG monitoring system using microneedle electrodes for small animals. *IEEE Sens. J.* **2023**, *23*, 21873–21881.

[150] Ren, L.; Jiang, Q.; Chen, Z. P.; Chen, K. Y.; Xu, S. J.; Gao, J.; Jiang, L. L. Flexible microneedle array electrode using magnetorheological drawing lithography for bio-signal monitoring. *Sens. Actuators A Phys.* **2017**, *268*, 38–45.

[151] Muskovich, M.; Bettinger, C. J. Biomaterials-based electronics: Polymers and interfaces for biology and medicine. *Adv. Healthc. Mater.* **2012**, *1*, 248–266.

[152] Chen, Z. W.; Li, H. J.; Bian, Y. J.; Wang, Z. J.; Chen, G. J.; Zhang, X. D.; Miao, Y. M.; Wen, D.; Wang, J. Q.; Wan, G. et al. Bioorthogonal catalytic patch. *Nat. Nanotechnol.* **2021**, *16*, 933–941.

[153] Nemani, K. V.; Moodie, K. L.; Brennick, J. B.; Su, A.; Gimi, B. *In vitro* and *in vivo* evaluation of SU-8 biocompatibility. *Mater. Sci. Eng. C* **2013**, *33*, 4453–4459.

[154] Wolf, M. P.; Salieb-Beugelaar, G. B.; Hunziker, P. PDMS with designer functionalities—Properties, modifications strategies, and applications. *Prog. Polym. Sci.* **2018**, *83*, 97–134.

[155] Makadia, H. K.; Siegel, S. J. Poly lactic-co-glycolic acid (PLGA) as biodegradable controlled drug delivery carrier. *Polymers* **2011**, *3*, 1377–1397.

[156] Elmowafy, E. M.; Tiboni, M.; Soliman, M. E. Biocompatibility, biodegradation and biomedical applications of poly(lactic acid)/poly(lactic-co-glycolic acid) micro and nanoparticles. *J. Pharm. Investig.* **2019**, *49*, 347–380.

[157] Teodorescu, M.; Bercea, M.; Morariu, S. Biomaterials of Poly(vinyl alcohol) and Natural Polymers. *Polym. Rev.* **2018**, *58*, 247–287.

[158] Atiqah, A.; Mastura, M. T.; Ali, B. A. A.; Jawaid, M.; Sapuan, S. M. A review on polyurethane and its polymer composites. *Curr. Org. Synth.* **2017**, *14*, 233–248.

[159] Liaw, D. J.; Wang, K. L.; Huang, Y. C.; Lee, K. R.; Lai, J. Y.; Ha, C. S. Advanced polyimide materials: Syntheses, physical properties and applications. *Prog. Polym. Sci.* **2012**, *37*, 907–974.

[160] Liu, Z. Y.; Wang, H.; Huang, P. A.; Huang, J. P.; Zhang, Y.; Wang, Y. Y.; Yu, M.; Chen, S. X.; Qi, D. P.; Wang, T. et al. Highly stable and stretchable conductive films through thermal-radiation-assisted metal encapsulation. *Adv. Mater.* **2019**, *31*, 1901360.

[161] Ohm, Y.; Pan, C. F.; Ford, M. J.; Huang, X. N.; Liao, J. H.; Majidi, C. An electrically conductive silver-polyacrylamide-alginate hydrogel composite for soft electronics. *Nat. Electron.* **2021**, *4*, 185–192.

[162] Cordill, M. J.; Kreiml, P.; Mitterer, C. Materials engineering for flexible metallic thin film applications. *Materials* **2022**, *15*, 926.

[163] Lozano, J.; Stoeber, B. Fabrication and characterization of a microneedle array electrode with flexible backing for biosignal monitoring. *Biomed. Microdevices* **2021**, *23*, 53.

[164] Hou, Y.; Li, Z. Y.; Wang, Z. Y.; Yu, H. Y. Miura-ori structured flexible microneedle array electrode for biosignal recording. *Microsyst. Nanoeng.* **2021**, *7*, 53.

[165] O'Mahony, C.; Grygoryev, K.; Ciarlone, A.; Giannoni, G.; Kenthao, A.; Galvin, P. Design, fabrication and skin-electrode contact analysis of polymer microneedle-based ECG electrodes. *J. Micromech. Microeng.* **2016**, *26*, 084005.

[166] Ren, L.; Chen, Z. P.; Wang, H. J.; Dou, Z. L.; Liu, B.; Jiang, L. L. Fabrication of bendable microneedle-array electrode by magnetorheological drawing lithography for electroencephalogram recording. *IEEE Trans. Instrum. Meas.* **2020**, *69*, 8328–8334.

[167] Wang, R. X.; Bai, J. X.; Zhu, X. H.; Li, Z. D.; Cheng, L. X.; Zhang, G. J.; Zhang, W. D. A PDMS-based microneedle array electrode for long-term ECG recording. *Biomed. Microdevices* **2022**, *24*, 27.

[168] Kim, M.; Kim, T.; Kim, D. S.; Chung, W. K. Curved microneedle array-based sEMG electrode for robust long-term measurements and high selectivity. *Sensors* **2015**, *15*, 16265–16280.

[169] Xu, J. H.; Fan, Y.; Wang, M. H.; Ji, B. W.; Li, L.; Jin, M. Y.; Shang, S. Y.; Ni, C. E.; Cheng, Y. H.; Dong, L. X. et al. Microneedle array electrode with Ag-PPS modification for superior bio-signal recording on skin. *IEEE Sens. J.* **2023**, *23*, 24196–24204.

[170] Yoshida, Y.; Kawana, T.; Hoshino, E.; Minagawa, Y.; Miki, N. Capturing human perceptual and cognitive activities via event-related potentials measured with candle-like dry microneedle electrodes. *Micromachines* **2020**, *11*, 556.

[171] Li, J. S.; Ma, Y. D.; Huang, D.; Wang, Z. Y.; Zhang, Z. T.; Ren, Y. J.; Hong, M. Y.; Chen, Y. F.; Li, T. Y.; Shi, X. Y. et al. High-performance flexible microneedle array as a low-impedance surface biopotential dry electrode for wearable electrophysiological recording and polysomnography. *Nano-Micro Lett.* **2022**, *14*, 132.

[172] Yoshida, Y.; Kudo, Y.; Hoshino, E.; Minagawa, Y.; Miki, N. Preparation-free measurement of event-related potential in oddball tasks from hairy parts using candle-like dry microneedle electrodes.

In *Proceedings of the 2018 40th Annual International Conference of the IEEE Engineering in Medicine and Biology Society*, Honolulu, USA, 2018, pp 4685–4688.
[173] Kawana, T.; Yoshida, Y.; Kudo, Y.; Miki, N. Eeg-hat with candle-like microneedle electrode. In *Proceedings of the 2019 41st Annual International Conference of the IEEE Engineering in Medicine and Biology Society*, Berlin, Germany, 2019, pp 1111–1114.
[174] Srivastava, A. K.; Bhartia, B.; Mukhopadhyay, K.; Sharma, A. Long term biopotential recording by body conformable photolithography fabricated low cost polymeric microneedle arrays. *Sens. Actuators A Phys.* **2015**, *236*, 164–172.
[175] Rasmussen, S. C. The early history of polyaniline: Discovery and origins. *Substantia* **2017**, *1*, 99–109.
[176] Rasmussen, S. C. Early history of polypyrrole: The first conducting organic polymer. *Bull. Hist. Chem. Div. Hist. Chem. Am. Chem. Soc.* **2015**, *40*, 45–55.
[177] Elsenbaumer, R. L.; Jen, K. Y.; Miller, G. G.; Shacklette, L. W. Processible, environmentally stable, highly conductive forms of polythiophene. *Synth. Met.* **1987**, *18*, 277–282.
[178] Nie, S. S.; Li, Z. F.; Yao, Y. Y.; Jin, Y. Z. Progress in synthesis of conductive polymer poly (3,4-ethylenedioxythiophene). *Front. Chem.* **2021**, *9*, 803509.
[179] Nezakati, T.; Seifalian, A.; Tan, A.; Seifalian, A. M. Conductive polymers: Opportunities and challenges in biomedical applications. *Chem. Rev.* **2018**, *118*, 6766–6843.
[180] Chen, Y. F.; Pei, W. H.; Chen, S. Y.; Wu, X.; Zhao, S. S.; Wang, H.; Chen, H. D. Poly(3,4-ethylenedioxythiophene) (PEDOT) as interface material for improving electrochemical performance of microneedles array-based dry electrode. *Sens. Actuators B Chem.* **2013**, *188*, 747–756.
[181] Keirouz, A.; Mustafa, Y. L.; Turner, J. G.; Lay, E.; Jungwirth, U.; Marken, F.; Leese, H. S. Conductive polymer-coated 3D printed microneedles: Biocompatible platforms for minimally invasive biosensing interfaces. *Small* **2023**, *19*, 2206301.
[182] Zhou, W. J. L.; Wang, Z. Y.; Xu, Q.; Liu, X. X.; Li, J. S.; Yu, H. Q.; Qiao, H.; Yang, L. R.; Chen, L. P.; Zhang, Y. et al. Wireless facial biosensing system for monitoring facial palsy with flexible microneedle electrode arrays. *npj Digital Med.* **2024**, *7*, 13.
[183] Gencoglu, M. F.; Spurri, A.; Franko, M.; Chen, J. H.; Hensley, D. K.; Heldt, C. L.; Saha, D. Biocompatibility of soft-templated mesoporous carbons. *ACS Appl. Mater. Interfaces* **2014**, *6*, 15068–15077.
[184] Zhu, Y. W.; Murali, S.; Stoller, M. D.; Ganesh, K. J.; Cai, W. W.; Ferreira, P. J.; Pirkle, A.; Wallace, R. M.; Cychosz, K. A.; Thommes, M. et al. Carbon-based supercapacitors produced by activation of graphene. *Science* **2011**, *332*, 1537–1541.
[185] De Volder, M. F. L.; Tawfick, S. H.; Baughman, R. H.; Hart, A. J. Carbon nanotubes: Present and future commercial applications. *Science* **2013**, *339*, 535–539.
[186] Vomero, M.; Castagnola, E.; Ciarpella, F.; Maggiolini, E.; Goshi, N.; Zucchini, E.; Carli, S.; Fadiga, L.; Kassegne, S.; Ricci, D. Highly stable glassy carbon interfaces for long-term neural stimulation and low-noise recording of brain activity. *Sci. Rep.* **2017**, *7*, 40332.
[187] Negishi, M.; Abildgaard, M.; Laufer, I.; Nixon, T.; Constable, R. T. An EEG (electroencephalogram) recording system with carbon wire electrodes for simultaneous EEG-fMRI (functional magnetic resonance imaging) recording. *J. Neurosci. Methods* **2008**, *173*, 99–107.
[188] Apollo, N. V.; Maturana, M. I.; Tong, W.; Nayagam, D. A. X.; Shivdasani, M. N.; Foroughi, J.; Wallace, G. G.; Prawer, S.; Ibbotson, M. R.; Garrett, D. J. Soft, flexible freestanding neural stimulation and recording electrodes fabricated from reduced graphene oxide. *Adv. Funct. Mater.* **2015**, *25*, 3551–3559.
[189] Garcia-Cortadella, R.; Masvidal-Codina, E.; De La Cruz, J. M.; Schäfer, N.; Schwesig, G.; Jeschke, C.; Martinez-Aguilar, J.; Sanchez-Vives, M. V.; Villa, R.; Illa, X. et al. Distortion-free sensing of neural activity using graphene transistors. *Small* **2020**, *16*, 1906640.
[190] Zhang, Y.; Bai, Y. H.; Yan, B. Functionalized carbon nanotubes for potential medicinal applications. *Drug Discov. Today* **2010**, *15*, 428–435.
[191] Smart, S. K.; Cassady, A. I.; Lu, G. Q.; Martin, D. J. The biocompatibility of carbon nanotubes. *Carbon* **2006**, *44*, 1034–1047.
[192] Mitskene, V.; Miliuskas, R. Carbon electrodes for prolonged human EEG recording. *Zh. Vyssh. Nervn. Deyat. Im. I. P. Pavlova* **1976**, *26*, 218–219.
[193] Opdam, H. I.; Federico, P.; Jackson, G. D.; Buchanan, J.; Abbott, D. F.; Fabinyi, G. C. A.; Syngeniotis, A.; Vosmansky, M.; Archer, J. S.; Wellard, R. M. et al. A sheep model for the study of focal epilepsy with concurrent intracranial EEG and functional MRI. *Epilepsia* **2002**, *43*, 779–787.
[194] Ruffini, G.; Dunne, S.; Farrés, E.; Marco-Pallarés, J.; Ray, C.; Mendoza, E.; Silva, R.; Grau, C. A dry electrophysiology electrode using CNT arrays. *Sens. Actuators A Phys.* **2006**, *132*, 34–41.
[195] Ng, W. C.; Seet, H. L.; Lee, K. S.; Ning, N.; Tai, W. X.; Sutedja, M.; Fuh, J. Y. H.; Li, X. P. Micro-spike EEG electrode and the vacuum-casting technology for mass production. *J. Mater. Process. Technol.* **2009**, *209*, 4434–4438.
[196] Zips, S.; Grob, L.; Rinklin, P.; Terkan, K.; Adly, N. Y.; Weiß, L. J. K.; Mayer, D.; Wolfrum, B. Fully printed µ-needle electrode array from conductive polymer ink for bioelectronic applications. *ACS Appl. Mater. Interfaces* **2019**, *11*, 32778–32786.
[197] Xiang, Z. L.; Yen, S. C.; Xue, N.; Sun, T.; Tsang, W. M.; Zhang, S. S.; Liao, L. D.; Thakor, N. V.; Lee, C. Ultra-thin flexible polyimide neural probe embedded in a dissolvable maltose-coated microneedle. *J. Micromech. Microeng.* **2014**, *24*, 065015.
[198] Lozano, J.; Stoeber, B. Microspike array electrode with flexible backing for biosignal monitoring. In *Proceedings of 2019 IEEE SENSORS*, Montreal, Canada, 2019, pp 1–4.
[199] Naguib, M.; Kurtoglu, M.; Presser, V.; Lu, J.; Niu, J. J.; Heon, M.; Hultman, L.; Gogotsi, Y.; Barsoum, M. W. Two-dimensional nanocrystals produced by exfoliation of Ti_3AlC_2. *Adv. Mater.* **2011**, *23*, 4248–4253.
[200] Liu, H. D.; Du, C. F.; Liao, L. L.; Zhang, H. J.; Zhou, H. Q.; Zhou, W. C.; Ren, T. N.; Sun, Z. C.; Lu, Y. F.; Nie, Z. T. et al. Approaching intrinsic dynamics of MXenes hybrid hydrogel for 3D printed multimodal intelligent devices with ultrahigh superelasticity and temperature sensitivity. *Nat. Commun.* **2022**, *13*, 3420.
[201] Song, Y. Y.; Ren, W. J.; Zhang, Y. Q.; Liu, Q.; Peng, Z.; Wu, X. D.; Wang, Z. Q. Synergetic monitoring of both physiological pressure and epidermal biopotential based on a simplified on-skin-printed sensor modality. *Small* **2023**, *19*, 2303301.
[202] Hao, Y. N.; Yan, Q. Y.; Liu, H. J.; He, X. Y.; Zhang, P. H.; Qin, X. H.; Wang, R. R.; Sun, J.; Wang, L. M.; Cheng, Y. A Stretchable, breathable, and self-adhesive electronic skin with multimodal sensing capabilities for human-centered healthcare. *Adv. Funct. Mater.* **2023**, *33*, 2303881.
[203] Yang, Y. C.; Lin, Y. T.; Yu, J. S.; Chang, H. T.; Lu, T. Y.; Huang, T. Y.; Preet, A.; Hsu, Y. J.; Wang, L. G.; Lin, T. E. MXene nanosheet-based microneedles for monitoring muscle contraction and electrostimulation treatment. *ACS Appl. Nano Mater.* **2021**, *4*, 7917–7924.
[204] Jung, J. H.; Jin, S. G. Microneedle for transdermal drug delivery: Current trends and fabrication. *J. Pharm. Investig.* **2021**, *51*, 503–517.
[205] Howells, O.; Blayney, G. J.; Gualeni, B.; Birchall, J. C.; Eng, P. F.; Ashraf, H.; Sharma, S.; Guy, O. J. Design, fabrication, and characterisation of a silicon microneedle array for transdermal therapeutic delivery using a single step wet etch process. *Eur. J. Pharm. Biopharm.* **2022**, *171*, 19–28.

[206] Eş, I.; Kafadenk, A.; Inci, F. A high-precision method for manufacturing tunable solid microneedles using dicing saw and xenon difluoride-induced dry etching. *J. Mater. Process. Technol.* **2024**, *325*, 118268.

[207] Donnelly, V. M.; Kornblit, A. Plasma etching: Yesterday, today, and tomorrow. *J. Vac. Sci. Technol. A* **2013**, *31*, 050825.

[208] Bodhale, D. W.; Nisar, A.; Afzulpurkar, N. Design, fabrication and analysis of silicon microneedles for transdermal drug delivery applications. In *Proceedings of the 3rd International Conference on the Development of Biomedical Engineering in Vietnam*, Ho Chi Minh City, Vietnam, 2010, pp 84–89.

[209] Ji, J.; Tay, F. E. H.; Miao, J. M.; Iliescu, C. Microfabricated microneedle with porous tip for drug delivery. *J. Micromech. Microeng.* **2006**, *16*, 958–964.

[210] Li, Y.; Zhang, H.; Yang, R. F.; Laffitte, Y.; Schmill, U.; Hu, W. H.; Kaddoura, M.; Blondeel, E. J. M.; Cui, B. Fabrication of sharp silicon hollow microneedles by deep-reactive ion etching towards minimally invasive diagnostics. *Microsyst. Nanoeng.* **2019**, *5*, 41.

[211] Laermer, F.; Franssila, S.; Sainiemi, L.; Kolari, K. Chapter 16—Deep reactive ion etching. In *Handbook of Silicon Based MEMS Materials and Technologies*; 3rd ed. Tilli, M.; Paulasto-Krockel, M.; Petzold, M.; Theuss, H.; Motooka, T.; Lindroos, V., Eds.; Elsevier: Amsterdam, 2020; pp 417–446.

[212] Zheng, M. J.; Sheng, T.; Yu, J. C.; Gu, Z.; Xu, C. J. Microneedle biomedical devices. *Nat. Rev. Bioeng.* **2024**, *2*, 324–342.

[213] Maldonado, J. R.; Peckerar, M. X-ray lithography: Some history, current status and future prospects. *Microelectron. Eng.* **2016**, *161*, 87–93.

[214] Chen, Z. P.; Ren, L.; Li, J. Y.; Yao, L. B.; Chen, Y.; Liu, B.; Jiang, L. L. Rapid fabrication of microneedles using magnetorheological drawing lithography. *Acta Biomater.* **2018**, *65*, 283–291.

[215] Lee, K.; Lee, H. C.; Lee, D. S.; Jung, H. Drawing lithography: Three-dimensional fabrication of an ultrahigh-aspect-ratio microneedle. *Adv. Mater.* **2010**, *22*, 483–486.

[216] Li, Y. G.; Wu, W. Y.; Wang, H.; Cai, J. D.; Lü, T. Fabrication, testing and simulation of microneedle array based on X-ray lithography. *Opt. Precis. Eng.* **2018**, *26*, 1156–1164.

[217] Lee, K.; Jung, H. Drawing lithography for microneedles: A review of fundamentals and biomedical applications. *Biomaterials* **2012**, *33*, 7309–7326.

[218] Baek, J. Y.; Kang, K. M.; Kim, H. J.; Kim, J. H.; Lee, J. H.; Shin, G.; Jeon, J. G.; Lee, J.; Han, Y. S.; So, B. J. et al. Manufacturing process of polymeric microneedle sensors for mass production. *Micromachines* **2021**, *12*, 1364.

[219] Anbazhagan, G.; Suseela, S. B.; Sankararajan, R. Design, analysis and fabrication of solid polymer microneedle patch using CO_2 laser and polymer molding. *Drug Deliv. Transl. Res.* **2023**, *13*, 1813–1827.

[220] Juster, H.; Van Der Aar, B.; de Brouwer, H. A review on microfabrication of thermoplastic polymer-based microneedle arrays. *Polym. Eng. Sci.* **2019**, *59*, 877–890.

[221] Abubaker, S. S.; Zhang, Y. J. Optimization design and fabrication of polymer micro needle by hot embossing method. *Int. J. Precis. Eng. Manuf.* **2019**, *20*, 631–640.

[222] Li, J. Y.; Zhou, Y. Y.; Yang, J. B.; Ye, R.; Gao, J.; Ren, L.; Liu, B.; Liang, L.; Jiang, L. L. Fabrication of gradient porous microneedle array by modified hot embossing for transdermal drug delivery. *Mater. Sci. Eng. C* **2019**, *96*, 576–582.

[223] Kang, T. T.; Zhuang, J.; Lin, L.; Zhao, Z. W.; Zhu, L.; Sun, J. Y.; Yang, Z. Z.; Wu, D. M. Simulation analysis of injection speed in micro injection molding of PLA cosmetic microneedle. *Plastics* **2022**, *51*, 23–28.

[224] Gülçür, M.; Romano, J. M.; Penchev, P.; Gough, T.; Brown, E.; Dimov, S.; Whiteside, B. A cost-effective process chain for thermoplastic microneedle manufacture combining laser micro-machining and micro-injection moulding. *CIRP J. Manuf. Sci. Technol.* **2021**, *32*, 311–321.

[225] Evens, T.; Malek, O.; Castagne, S.; Seveno, D.; van Bael, A. A novel method for producing solid polymer microneedles using laser ablated moulds in an injection moulding process. *Manuf. Lett.* **2020**, *24*, 29–32.

[226] Murphy, S. V.; Atala, A. 3D bioprinting of tissues and organs. *Nat. Biotechnol.* **2014**, *32*, 773–785.

[227] Cho, Y. H.; Park, Y. G.; Kim, S.; Park, J. U. 3D electrodes for bioelectronics. *Adv. Mater.* **2021**, *33*, 2005805.

[228] Choo, S.; Jin, S.; Jung, J. Fabricating high-resolution and high-dimensional microneedle mold through the resolution improvement of stereolithography 3D printing. *Pharmaceutics* **2022**, *14*, 766.

[229] Jeong, J.; Park, J.; Lee, S. 3D printing fabrication process for fine control of microneedle shape. *Micro Nano Syst. Lett.* **2023**, *11*, 1.

[230] Mckee, S.; Lutey, A.; Sciancalepore, C.; Poli, F.; Selleri, S.; Cucinotta, A. Microfabrication of polymer microneedle arrays using two-photon polymerization. *J. Photochem. Photobiol. B Biol.* **2022**, *229*, 112424.

[231] Rad, Z. F.; Prewett, P. D.; Davies, G. J. Parametric optimization of two-photon direct laser writing process for manufacturing polymeric microneedles. *Addit. Manuf.* **2022**, *56*, 102953.

[232] Tsegay, F.; Elsherif, M.; Butt, H. Smart 3D printed hydrogel skin wound bandages: A review. *Polymers* **2022**, *14*, 1012.

[233] Tumbleston, J. R.; Shirvanyants, D.; Ermoshkin, N.; Janusziewicz, R.; Johnson, A. R.; Kelly, D.; Chen, K.; Pinschmidt, R.; Rolland, J. P.; Ermoshkin, A. et al. Continuous liquid interface production of 3D objects. *Science* **2015**, *347*, 1349–1352.

[234] Lipkowitz, G.; Samuelsen, T.; Hsiao, K.; Lee, B.; Dulay, M. T.; Coates, I.; Lin, H.; Pan, W.; Toth, G.; Tate, L. et al. Injection continuous liquid interface production of 3D objects. *Sci. Adv.* **2022**, *8*, eabq3917.

[235] Wu, L. B.; Park, J.; Kamaki, Y.; Kim, B. Optimization of the fused deposition modeling-based fabrication process for polylactic acid microneedles. *Microsyst. Nanoeng.* **2021**, *7*, 58.

[236] Khosraviboroujeni, A.; Mirdamadian, S. Z.; Minaiyan, M.; Taheri, A. Preparation and characterization of 3D printed PLA microneedle arrays for prolonged transdermal drug delivery of estradiol valerate. *Drug Deliv. Transl. Res.* **2022**, *12*, 1195–1208.

[237] Choi, C. K.; Lee, K. J.; Youn, Y. N.; Jang, E. H.; Kim, W.; Min, B. K.; Ryu, W. Spatially discrete thermal drawing of biodegradable microneedles for vascular drug delivery. *Eur. J. Pharm. Biopharm.* **2013**, *83*, 224–233.

[238] Lee, J.; Park, S. H.; Seo, I. H.; Lee, K. J.; Ryu, W. Rapid and repeatable fabrication of high A/R silk fibroin microneedles using thermally-drawn micromolds. *Eur. J. Pharm. Biopharm.* **2015**, *94*, 11–19.

[239] Lee, K.; Park, S. H.; Lee, J.; Ryu, S.; Joo, C.; Ryu, W. Three-step thermal drawing for rapid prototyping of highly customizable microneedles for vascular tissue insertion. *Pharmaceutics* **2019**, *11*, 100.

[240] Goyal, K.; Borkholder, D. A.; Day, S. W. Dependence of skin-electrode contact impedance on material and skin hydration. *Sensors* **2022**, *22*, 8510.

[241] Zhou, W.; Song, R.; Pan, X. L.; Peng, Y. J.; Qi, X. Y.; Peng, J. H.; Hui, K. S.; Hui, K. N. Fabrication and impedance measurement of novel metal dry bioelectrode. *Sens. Actuators A Phys.* **2013**, *201*, 127–133.

[242] Yang, L. T.; Gan, L.; Zhang, Z. G.; Zhang, Z. L.; Yang, H.; Zhang, Y.; Wu, J. L. Insight into the contact impedance between the electrode and the skin surface for electrophysical recordings. *ACS Omega* **2022**, *7*, 13906–13912.

[243] Liu, J. T.; Liu, X. Y.; He, E. H.; Gao, F.; Li, Z. Y.; Xiao, G. H.; Xu, S. W.; Cai, X. X. A novel dry-contact electrode for measuring electroencephalography signals. *Sens. Actuators A Phys.* **2019**, *294*, 73–80.

[244] Leleux, P.; Johnson, C.; Strakosas, X.; Rivnay, J.; Hervé, T.; Owens, R. M.; Malliaras, G. G. Ionic liquid gel-assisted electrodes for long-term cutaneous recordings. *Adv. Healthc. Mater.* **2014**, *3*, 1377–1380.
[245] Murphy, B. B.; Mulcahey, P. J.; Driscoll, N.; Richardson, A. G.; Robbins, G. T.; Apollo, N. V.; Maleski, K.; Lucas, T. H.; Gogotsi, Y.; Dillingham, T. et al. A gel-free $Ti_3C_2T_x$-based electrode array for high-density, high-resolution surface electromyography. *Adv. Mater. Technol.* **2020**, *5*, 2000325.
[246] Stauffer, F.; Thielen, M.; Sauter, C.; Chardonnens, S.; Bachmann, S.; Tybrandt, K.; Peters, C.; Hierold, C.; Vörös, J. Skin conformal polymer electrodes for clinical ECG and EEG recordings. *Adv. Healthc. Mater.* **2018**, *7*, 1700994.
[247] Simić, M. Realization of digital LCR meter. In *Proceedings of 2014 International Conference and Exposition on Electrical and Power Engineering*, Iasi, Romania, 2014, pp 769–773.
[248] Zhang, C. C.; Li, M. J.; Xuan, X. W.; Zhou, B. Z.; Li, P. H.; Li, H. J. Nitrogen-doped multilayer graphene microtubes for high-density recording of occipital EEG signals. *Adv. Mater. Technol.* **2023**, *8*, 2201734.
[249] Roberts, T.; De Graaf, J. B.; Nicol, C.; Hervé, T.; Fiocchi, M.; Sanaur, S. Flexible inkjet-printed multielectrode arrays for neuromuscular cartography. *Adv. Healthc. Mater.* **2016**, *5*, 1462–1470.
[250] Theerthagiri, P. Chapter 1 - Genomics and neural networks in electrical load forecasting with computational intelligence. In *Data Science for Genomics*; Tyagi, A. K.; Abraham, A., Eds.; Academic Press: London, 2023; pp 1–10.
[251] Roubert Martinez, S.; Le Floch, P.; Liu, J.; Howe, R. D. Pure conducting polymer hydrogels increase signal-to-noise of cutaneous electrodes by lowering skin interface impedance. *Adv. Healthc. Mater.* **2023**, *12*, 2202661.
[252] Lundheim, L. On shannon and" shannon's formula". *Telektronikk* **2002**, *98*, 20–29.
[253] Singh, O. P.; Bocchino, A.; Guillerm, T.; O'Mahony, C. Design, fabrication and performance assessment of flexible, microneedle-based electrodes For ECG signal monitoring. In *Proceedings of the 2022 44th Annual International Conference of the IEEE Engineering in Medicine & Biology Society*, Glasgow, UK, 2022, pp 846–849.
[254] Kai, H.; Kumatani, A. A porous microneedle electrochemical glucose sensor fabricated on a scaffold of a polymer monolith. *J. Phys. Energy* **2021**, *3*, 024006.
[255] Zhang, B. L.; Yang, Y.; Zhao, Z. Q.; Guo, X. D. A gold nanoparticles deposited polymer microneedle enzymatic biosensor for glucose sensing. *Electrochim. Acta* **2020**, *358*, 136917.
[256] Sharma, S.; Huang, Z. Y.; Rogers, M.; Boutelle, M.; Cass, A. E. G. Evaluation of a minimally invasive glucose biosensor for continuous tissue monitoring. *Anal. Bioanal. Chem.* **2016**, *408*, 8427–8435.
[257] Yang, Y.; Chen, B. Z.; Zhang, X. P.; Zheng, H.; Li, Z.; Zhang, C. Y.; Guo, X. D. Conductive microneedle patch with electricity-triggered drug release performance for atopic dermatitis treatment. *ACS Appl. Mater. Interfaces* **2022**, *14*, 31645–31654.
[258] Jin, Q. C.; Chen, H. J.; Li, X. L.; Huang, X. S.; Wu, Q. N.; He, G.; Hang, T.; Yang, C. D.; Jiang, Z.; Li, E. L. et al. Reduced graphene oxide nanohybrid-assembled microneedles as mini-invasive electrodes for real-time transdermal biosensing. *Small* **2019**, *15*, 1804298.
[259] Hegarty, C.; McKillop, S.; McGlynn, R. J.; Smith, R. B.; Mathur, A.; Davis, J. Microneedle array sensors based on carbon nanoparticle composites: Interfacial chemistry and electroanalytical properties. *J. Mater. Sci.* **2019**, *54*, 10705–10714.
[260] Chatterjee, S.; Saxena, M.; Padmanabhan, D.; Jayachandra, M.; Pandya, H. J. Futuristic medical implants using bioresorbable materials and devices. *Biosens. Bioelectron.* **2019**, *142*, 111489.
[261] Bhattacharjee, S.; de Haan, L. H. J.; Evers, N. M.; Jiang, X.; Marcelis, A. T. M.; Zuilhof, H.; Rietjens, I. M. C. M.; Alink, G. M. Role of surface charge and oxidative stress in cytotoxicity of organic monolayer-coated silicon nanoparticles towards macrophage NR8383 cells. *Part. Fibre Toxicol.* **2010**, *7*, 25.
[262] Al-Shalawi, F. D.; Mohamed Ariff, A. H.; Jung, D. W.; Mohd Ariffin, M. K. A.; Seng Kim, C. L.; Brabazon, D.; Al-Osaimi, M. O. Biomaterials as implants in the orthopedic field for regenerative medicine: Metal versus synthetic polymers. *Polymers* **2023**, *15*, 2601.
[263] Kligman, S.; Ren, Z.; Chung, C. H.; Perillo, M. A.; Chang, Y. C.; Koo, H.; Zheng, Z.; Li, C. S. The impact of dental implant surface modifications on osseointegration and biofilm formation. *J. Clin. Med.* **2021**, *10*, 1641.
[264] Alcantar, N. A.; Aydil, E. S.; Israelachvili, J. N. Polyethylene glycol-coated biocompatible surfaces. *J. Biomed. Mater. Res.* **2000**, *51*, 343–351.
[265] Zheng, X. X.; Wang, Y. J.; Lan, Z. Y.; Lyu, Y. N.; Feng, G. K.; Zhang, Y. P.; Tagusari, S.; Kislauskis, E.; Robich, M. P.; McCarthy, S. et al. Improved biocompatibility of poly (lactic-co-glycolic acid) and poly-L-lactic acid blended with nanoparticulate amorphous calcium phosphate in vascular stent applications. *J. Biomed. Nanotechnol.* **2014**, *10*, 900–910.
[266] Marois, Y.; Guidoin, R. Biocompatibility of polyurethanes. In *Madame Curie Bioscience Database*. Bull, L., Ed.; Landes Bioscience: Austin, 2013.
[267] Alexandre, N.; Ribeiro, J.; Gärtner, A.; Pereira, T.; Amorim, I.; Fragoso, J.; Lopes, A.; Fernandes, J.; Costa, E.; Santos-Silva, A. et al. Biocompatibility and hemocompatibility of polyvinyl alcohol hydrogel used for vascular grafting—*In vitro* and *In vivo* studies. *J. Biomed. Mater. Res. Part A* **2014**, *102*, 4262–4275.
[268] Masmur, I.; Perangin-Angin, S.; Sembiring, H.; Tarigan, A. H.; Ginting, J.; Barus, D. A.; Ginting, M. Effect of different composition of polyethylene oxide-polypyrrole (PEO-PPy) nanofiber mats on antibacterial and biocompatibility properties. *ChemistrySelect* **2022**, *7*, e202201346.
[269] Amerian, M.; Amerian, M.; Sameti, M.; Seyedjafari, E. Improvement of PDMS surface biocompatibility is limited by the duration of oxygen plasma treatment. *J. Biomed. Mater. Res. Part A* **2019**, *107*, 2806–2813.
[270] Sultana, N.; Chang, H. C.; Jefferson, S.; Daniels, D. E. Application of conductive poly (3,4-ethylenedioxythiophene):Poly (styrenesulfonate)(PEDOT:PSS) polymers in potential biomedical engineering. *J. Pharm. Investig.* **2020**, *50*, 437–444.
[271] Peterson, R. C.; Wolffsohn, J. S.; Nick, J.; Winterton, L.; Lally, J. Clinical performance of daily disposable soft contact lenses using sustained release technology. *Cont. Lens Anterior Eye* **2006**, *29*, 127–134.
[272] Lü, J. M.; Wang, X. W.; Marin-Muller, C.; Wang, H.; Lin, P. H.; Yao, Q. Z.; Chen, C. Y. Current advances in research and clinical applications of PLGA-based nanotechnology. *Expert Rev. Mol. Diagn.* **2009**, *9*, 325–341.
[273] Zare, M.; Ghomi, E. R.; Venkatraman, P. D.; Ramakrishna, S. Silicone-based biomaterials for biomedical applications: Antimicrobial strategies and 3D printing technologies. *J. Appl. Polym. Sci.* **2021**, *138*, 50969.
[274] Khan, S.; Ul-Islam, M.; Ullah, M. W.; Israr, M.; Jang, J. H.; Park, J. K. Nano-gold assisted highly conducting and biocompatible bacterial cellulose-PEDOT:PSS films for biology-device interface applications. *Int. J. Biol. Macromol.* **2018**, *107*, 865–873.
[275] Ren, X. N.; Yang, M.; Yang, T. T.; Xu, C.; Ye, Y. Q.; Wu, X. N.; Zheng, X.; Wang, B.; Wan, Y.; Luo, Z. Q. Highly conductive PPY-PEDOT:PSS hybrid hydrogel with superior biocompatibility for bioelectronics application. *ACS Appl. Mater. Interfaces* **2021**, *13*, 25374–25382.
[276] Yang, T. T.; Yang, M.; Xu, C.; Yang, K.; Su, Y. M.; Ye, Y. Q.; Dou,

L. Y.; Yang, Q.; Ke, W. B.; Wang, B. et al. PEDOT:PSS hydrogels with high conductivity and biocompatibility for *in situ* cell sensing. *J. Mater. Chem. B* **2023**, *11*, 3226–3235.
[277] Lu, F.; Wang, C. S.; Zhao, R. J.; Du, L. D.; Fang, Z.; Guo, X. H.; Zhao, Z. Review of stratum corneum impedance measurement in non-invasive penetration application. *Biosensors* **2018**, *8*, 31.
[278] Yan, X. X.; Liu, J. Q.; Wang, L. F.; Yang, C. S.; Li, Y. G. Silicon-based microneedle array electrodes for biopotential measurement. *Key Eng. Mater.* **2011**, *483*, 443–446.
[279] Abu-Saude, M.; Consul-Pacareu, S.; Morshed, B. I. Feasibility of patterned vertical CNT for dry electrode sensing of physiological parameters. In *Proceedings of 2015 IEEE Topical Conference on Biomedical Wireless Technologies, Networks, and Sensing Systems*, San Diego, USA, 2015, pp 1–4.
[280] Peng, H. L.; Liu, J. Q.; Tian, H. C.; Xu, B.; Dong, Y. Z.; Yang, B.; Chen, X.; Yang, C. S. Flexible dry electrode based on carbon nanotube/polymer hybrid micropillars for biopotential recording. *Sens. Actuators A Phys.* **2015**, *235*, 48–56.
[281] Abu-Saude, M.; Morshed, B. I. Polypyrrole (PPy) conductive polymer coating of dry patterned vertical CNT (pvCNT) electrode to improve mechanical stability. In *Proceedings of 2016 IEEE Topical Conference on Biomedical Wireless Technologies, Networks, and Sensing Systems*, Austin, USA, 2016, pp 84–87.

This is an open access article under the terms of the Creative Commons Attribution 4.0 International License (CC BY 4.0, https://creativecommons.org/licenses/by/4.0/).

© The Author(s) 2025. Published by Tsinghua University Press.